PRODUCTION OF BIOMASS AND FILAMENTOUS HEMAGGLUTININ BY *BORDETELLA BRONCHISEPTICA*

by

SCOTT DAVID GUETTER

(Under the Direction of Mark A. Eiteman)

ABSTRACT

Traditional *Bordetella bronchiseptica* vaccine production utilizes batch fermentation and complex medium. Cultivation parameters and medium composition have a direct impact on growth rate, biomass generation, and virulence factor production, specifically filamentous hemagglutinin (FHA). A high yield controlled large scale production process is desirable for vaccine production. In this study, statistical modeling was used to investigate the impact of known virulence modulators, $MgSO_4$ and nicotinic acid. Lactate, succinate, citrate, and acetate were investigated as dual carbon sources in combination with glutamate to balance carbon:nitrogen in medium. Steady-state and fed-batch fermentation were explored as potential cultivation techniques to increase yield. Statistical modeling yielded two optimal Mg/SO_4/nicotinic acid concentration conditions: 1 mM/0.1 mM/32.5 μM and 0.1 mM/1.0 mM/32.5 μM. We also found the greatest yields from lactate-glutamate (commonly used in literature) and acetate-glutamate. However, acetate-glutamate generated greater FHA and 7 times the biomass. Steady-state and fed-batch fermentation proved to be undesirable fermentation techniques.

INDEX WORDS: *Bordetella bronchiseptica*, Filamentous hemagglutinin, Fermentation, Virulence factor, Chemostat, Fed-batch

PRODUCTION OF BIOMASS AND FILAMENTOUS HEMAGGLUTININ BY *BORDETELLA BRONCHISEPTICA*

by

SCOTT DAVID GUETTER

BSBE, The University of Georgia, 2003

A Thesis Submitted to the Graduate Faculty of The University of Georgia in Partial Fulfillment of the Requirements for the Degree

MASTER OF SCIENCE

ATHENS, GEORGIA

2012

PRODUCTION OF BIOMASS AND FILAMENTOUS HEMAGGLUTININ BY

BORDETELLA BRONCHISEPTICA

by

SCOTT DAVID GUETTER

Major Professor:	Mark A. Eiteman
Committee:	William Kisaalita Eric Lafontaine

Electronic Version Approved:

Maureen Grasso
Dean of the Graduate School
The University of Georgia
May 2012

DEDICATION

To my wife Megan and son Caleb. Thank you for all of your love and support.

ACKNOWLEDGMENTS

I would like to thank my major professor Dr. Mark A. Eiteman for his guidance and support during my undergraduate and graduate experience. He has had an instrumental part in my engineering education. Thank you, Merial Limited, for providing me with the financial, technical, and personal support to complete this project.

Special thanks to Brad Feilmeier, Troy Hughes, Brian Kern, Sarah Lee, Thasan Murugesu, Ernie Veal, and Michael Weinberg for your technical support and help.

Lastly, I would like to thank my family and friends for their continued support.

TABLE OF CONTENTS

LIST OF TABLES

Page

LIST OF FIGURES

Page

CHAPTER 1

INTRODUCTION & LITERATURE REVIEW

Introduction

The genus *Bordetella* encompasses nine species (summarized in Table 1): *B. pertussis*, *B. parapertussis*, *B. avium*, *B. holmesii, B. trematum, B. hinzii, B. petrii, B. ansorpii,* and *B. bronchiseptica* (Moot et al., 2007, see Table 1). *B. pertussis*, *B. parapertussis*, *B. avium*, and *B. bronchiseptica* are of primary medical and veterinary interest (Armstrong and Gross, 2007). *B. pertussis*, *B. parapertussis*, and *B. bronchiseptica* colonize the respiratory tracts of various mammalian species, while *B. avium* causes respiratory disease in birds (Parkhill, et al., 2003; Armstrong and Gross, 2007). These species form the classical *Bordetella* species, which are well characterized and studied (Fernandez, 2005). The genomes of *B. pertussis*, *B. parapertussis*, and *B. bronchiseptica* have recently been sequenced (Parkhill et al., 2003), and these species are closely related Gram-negative coccobacilli (Egberink et al., 2009). Based on sequence analysis, *B. pertussis* and *B. parapertussis* are independent derivatives of a *B. bronchiseptica*-like ancestor (Parkhill et al., 2003). The primary focus of many of these genomic studies has been on *B. pertussis*, which is the etiologic agent of whooping cough in humans. *B. bronchiseptica* causes chronic respiratory infections in many mammals including dogs, monkeys, cats, rabbits, ferrets, guinea pigs, mice, swine, foxes, rats, hedgehogs, horses, skunks, opossums, raccoons, koala bears, and occasionally humans (Goodnow, 1980).

The global economic impact due to *B. bronchiseptica* infections of mammals totals in the millions of dollars (Carbone et al., 1999). The primary economic loss occurs in swine, canine,

and laboratory animal industries, and is due to atrophic rhinitis and pneumonia in swine, infectious tracheobronchitis (commonly referred to as kennel cough) in dogs, and epizootic respiratory infections in laboratory animals (Goodnow, 1980). The financial expense is due to disfigured, slow growing, or stillborn swine, lost sales, medication costs, veterinary fees, and lost revenue in rearing and boarding facilities (Goodnow, 1980). *B. bronchiseptica* has been identified as a zoonotic disease, although infection in humans is rare and usually occurs in an immunocompromised host (Woolfrey and Moody, 1991).

Table 1: Species of genus *Bordetella*

Species	Host range/source	Disease	References
B. pertussis	Humans	Pertussis	Bordet and Gengou, 1906
B. parapertussis$_{HU}$	Humans	Pertussis	Eldering and Kendrick, 1938
B. parapertussis$_{OV}$	Sheep	Pneumonia	Cullinane et al., 1987; Porter et al., 1996
B. bronchiseptica	Many mammals	Respiratory disease	Ferry, 1912
B. holmesii	Humans	Septicemia, cough	Weyant et al., 1995
B. avium	Birds	Rhinotracheitis	Kersters et al., 1984
B. trematum	Humans	Wound infections, otitis media	Vandamme et al., 1996
B. hinzii	Poultry, Humans	Opportunistic infections in humans	Cookson et al., 1994
B. petrii	Environment, Humans	Opportunistic infections	Von Wintzingerode et al., 2001
B. ansorpii	Humans	Opportunistic infections	Ko et al., 2005

Adapted from Moot et al., 2007

Bordetella bronchiseptica

Ferry first identified *B. bronchiseptica* as *Bacillus bronchicanis* in 1910, since it was isolated from the respiratory tracts of dogs (Goodnow, 1980). The organism's nomenclature evolved in the following years: *Haemophilus bronchiseptica, Brucella bronchiseptica, Bacillus suisepticus, Alcaligenes bronchicanis,* and *Alcaligenes bronchisepticus* (Goodnow, 1980;

Woolfrey and Moody, 1991). The current name, *Bordetella bronchiseptica*, was given to the bacterium in 1952 when Moreno-Lopez described the genus *Bordetella,* in honor of Jules Bordet, who first isolated the organism causing pertussis (Sanden and Weyant, 2005).

Cellular Morphology

B. bronchiseptica is identified as a Gram-negative, non-sporeforming, coccobacilli. The bacterium usually ranges in size from 0.2-0.5 by 0.5-2.0 μm (Sanden and Weyant, 2005). Lacey showed that the *Bordetella* species alternate between at least three phenotypic phases depending on environmental conditions (Lacey, 1960). These were assigned as X (xanthic mode, mode of *Bordetella* species at high temperatures or in the presence of specific ions), C (cyanic mode, mode of growth at lower temperatures or in the presence of specific ions), and I (intermediate mode, mode of growth under conditions between mode X and C) (Lacey, 1960). The phenotypic modulation is controlled by the *Bordetella* virulence gene, *bvg,* regulon (Stibitz, 2007). The Bvg-plus (Bvg^+) phase is associated with virulence and corresponds with the X mode introduced by Lacey (Cotter and Miller, 1997). The Bvg-minus (Bvg^-) phase, associated with avirulence, corresponds to the C mode (Cotter and Miller, 1997). In 1997, Cotter and Miller also identified the Bvg-intermediate (Bvg^i) phenotype. Motility is a characteristic of the Bvg^- phase, delivered by peritrichous flagella (Cotter and Miller, 1994). Structural studies have shown that the cell wall and membranes are similar to other Gram-negative bacteria (Goodnow, 1980).

Colony Morphology

B. bronchiseptica isolates grown on agar produce both rough and smooth colonies. Initial research suggested that smooth colonies represented the virulent phase and the rough phase colonies as avirulent (Goodnow, 1980). Cotter and Miller (1997) showed the Bvg^+ phase

produced small, domed, hemolytic colonies, while the Bvg^- phase produced large, flat, non-hemolytic colonies.

BvgAS Regulation System

The BvgAS regulation system manages the infectious cycle of *Bordetella* species. The distinct phenotypic phases Bvg^+ and Bvg^- of *Bordetella* spp. are regulated by the BvgAS two-component signal transduction system (Yuk et al., 1998). A third phenotypic phase, Bvg^i, is a known intermediate state between Bvg^+ and Bvg^-. The exchange between different phenotypic phases ultimately defines different expression of distinct sets of gene products (Mishra and Deora, 2005). BvgA and BvgS belong to a family of bacterial proteins which regulate downstream gene expression based on environmental signals (Cotter and Miller, 1994). This two-component signal transduction system is commonly found in prokaryotes and lower eukaryotes (Yuk et al., 1998). BvgS is a transmembrane sensor protein which phosphorylates BvgA in response to environmental signals using a His-Asp-His-Asp phosphorelay (Cotter and Miller, 2000; Preston et al., 2003). The phosphorylated BvgA functions as an activator and repressor of separate gene classes. BvgAS then upregulates the expression of Bvg^+ phase proteins (Preston et al., 2003). Depending on the phase, different genes are repressed (*vrg*, virulence repressed genes) or expressed (*vag*, virulence activated genes) (Stibitz, 2007). The BvgAS regulation is shown in Figure 1. The infectious virulent phase, Bvg^+, is characterized by the expression of adhesins and toxins (Cotter and Miller, 1997). The non-infectious avirulent phase, Bvg^-, is primarily characterized by motility (Cotter and Miller, 1997). Under laboratory conditions, the phenotypic change from Bvg^+ to Bvg^- (or vice versa) is in response to environmental signals; specifically sulfate anion (commonly $MgSO_4$), nicotinic acid, growth at low temperatures, and nutrient limiting conditions (Akerley and Miller, 1993; Cotter and Miller,

1997). The BvgAS regulon is active in the absence of these specific environmental signals and in their presence the system becomes inactive (Stibitz, 2007). The Bvg^i phase is expressed as a result of genetic mutations in BvgS or by growth of wild-type strains in semimodulating conditions of environmental signals (Mishra and Deora, 2005). However, the actual environmental signal to which BvgAS responds in nature in not known (Stockbauer et al., 2001).

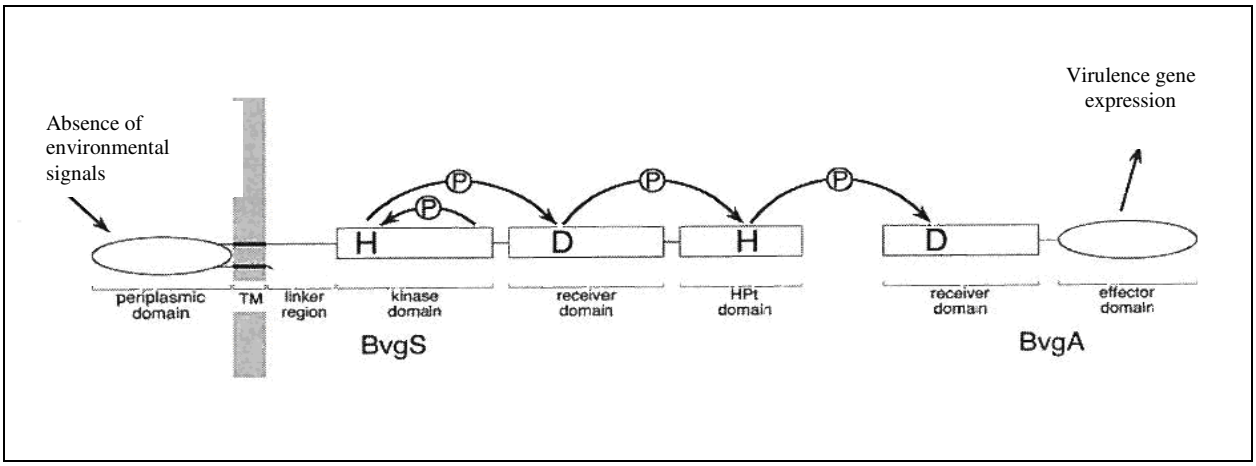

Figure 1: The BvgAS system: TM: transmembrane region; H: catalytic histidine; D: catalytic aspartic acid; P: phosphate (adapted from Stibitz, 2007). Note: The system becomes inactive in the presence of specific environmental signals.

While the BvgAS system is active, *Bordetella* are in the Bvg^+ phase. While in the Bvg^+ phase, the *vag* genes are expressed and *vrg* genes are repressed. The *vag* genes are characterized by the expression of the adhesins filamentous hemagglutinin (FHA), pili, fimbriae, and pertactin along with the toxins adenylate cyclase-hemolysin and dermonecrotic toxin (Akerley et al., 1992; Cotter and Miller, 1994). The virulence factors for *B. bronchiseptica* are listed in Table 2.

In the Bvg^- phase, the BvgAS system is inactive in response to environmental signals. The *vag* genes are downregulated, while the *vrg* genes are upregulated (Preston et al., 2003). In this phase the cell produces flagellar organelles for motility, and the hydroxamate siderophore alcaligin (Cotter and Miller, 1994). These Bvg phases are represented in Figure 2.

Table 2: *B. bronchiseptica* virulence factors

Virulence Factor	Molecular Mass (kDa)	Mechanism of Action	Protective Immunity	Location and other Features	Bvg Regulated
Agglutinogen2 / fimbria 2	22	Fim2 bindshepain; fimD binds heparin and integrin VLA-5	+	Located on fimbriae; confers protective immunity against serotypes 1 and 2	–
Agglutinin 3			+	Either a somatic or fimbrial antigen; confers protective immunity against serotypes 1 and 3	–
Fimbria 3	21.5	FimD binds to heparin and integrin VLA-5	+	Major fimbrial subunit	+
P:69 Pertactin	69	RGD motif, probably binds complement receptor 3	+	Somatic antigen	+
Filamentous hemagglutinin	220	Binds both the bacterium and macrophage complement receptor 3 to facilitate phagocytosis	+	Secreted	+
Adenylate cyclase / hemolysin	45	ATP hydrolysis with raised intracellular cAMP in macrophages and lymphocytes; induces apoptosis	–	Secreted by type I pathway requiring CyaB, D and E proteins; activated by eukaryotic calmodulin	+
Tracheal cytotoxin	921	DNA inhibition in ciliated epithelium	–	A muramyl peptide, derived from bacterial peptoglycan	–
Dermonecrotic toxin	102 with subunits of 30 and 24	Inhibition of Na^+ K^+ ATPase; vasoconstriction		Localized to the bacterial cytoplasm; part of molecule probably exposed at cell surface	
Lipopolysaccharide		Endotoxin-like effects; pyrogenic, sensitization to histamine		Two lipids, A and X; two different oligosaccharides, I and II	

Adapted from Cotter et al., 1998; Sanden and Weyant, 2005

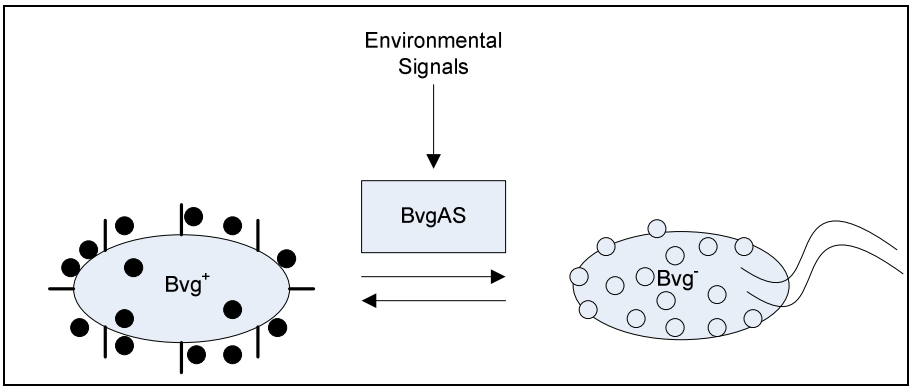

Figure 2: *B. bronchiseptica* phenotypic phases: The phase shift due to environmental signals controlled by BvgAS. In Bvg^+ phase, adhesins are represented by lines and toxins by solid circles. In Bvg^- phase, siderophore alcaligin are represented by open circles and flagella by curved lines. (Cotter and Miller, 1994).

Filamentous Hemagglutinin

Filamentous hemagglutinin (FHA) is a 220 kDa molecule which is expressed in the Bvg^+ phase of *B. bronchiseptica* and may be secreted or cell wall-associated (Cotter et al., 1998). This protein is considered the major adhesin of the genus *Bordetella*. FHA is used to facilitate adherence of cells to ciliated respiratory epithelial cells, an event which initiates the pathogenic cycle (Smith et al., 2001). FHA has a horseshoe nail shape comprising a 50 nm long and 4 nm wide monomer (Jacob-Dubuisson and Locht, 2007). The mature protein is synthesized from a 367 kDa precursor, FhaB, which is modified at the N terminus and cleaved at the C terminus to form the biologically active protein (Cotter et al., 1998).

FHA and the adhesins pertactin and fimbriae are immunogens and are primary components of acellular pertussis vaccines (Jacob-Dubuisson and Locht, 2007). All known virulence factors are expressed in the Bvg^+ phase in both *B. bronchiseptica* and *B. pertussis* (Cotter et al., 1998).

Metabolism

The metabolism of genus *Bordetella* is unique. Plotkin and Bemis (1998) investigated carbon and energy source utilization for *B. bronchiseptica* and confirmed that *B. bronchiseptica*

is asaccharolytic: growth was not supported on any carbohydrate or sugar alcohol tested including dextrose, mannose, galactose, maltose, mannitol, rhamnose, sorbitol, inositol, fructose, salicin, xylose, lactose, raffinose, and sucrose. Also, carbon and energy requirements could be met solely by any one of four amino acids (glutamate, glutamine, proline, or tyrosine) or any one of several organic acids such as succinate, citrate, α-ketoglutarate, acetate, fumarate, pyruvate, malate, lactate, or oxaloacetate (Plotkin and Bemis, 1998). This result is in contrast to the requirement for growth of *B. pertussis* for at least two amino acids for growth: glutamate or proline in addition to cystine or cysteine (Stainer and Scholte, 1971). Thalen et al. (1999) suggested cysteine serves only as a sulfur source, not an energy source. More recent genomic analysis supports experimental observations that *Bordetella* do not use sugars as a carbon source (Parkhill et al., 2003). Specifically, genes encoding glycolytic functions such as glucokinase, phosphofructokinase and fructose-1, 6-bisphosphatase are absent from the genome (Parkhill et al., 2003). The glycolytic and gluconeogenic pathways and citric acid cycle for *B. bronchiseptica* are shown in Figure 3.

In addition, all *Bordetella* species are missing the genes for several enzymes of the oxidative branch of the pentose phosphate pathway in which glucose-6-phosphate is oxidized to ribulose-5-phosphate. This section of the pathway is the location for the generation of nicotinamide adenine dinucleotide phosphate (NADPH). *Bordetella* must therefore generate the reducing power from other reactions since NADPH is the primary electron and hydrogen donor in cellular biosynthesis reactions (Armstrong and Gross, 2007).

Genome sequence predictions reveal *Bordetella* are capable of synthesizing most amino acids. *Bordetella* are also capable of using amino acids as a nitrogen source (Armstrong and Gross, 2007). Amino acid catabolism involves the removal of the amino group, resulting in an

α-keto acid which enters the citric acid cycle or is used for cellular reactions. The deamination produces ammonia. The assimilation of inorganic nitrogen into cellular components is only accomplished by the incorporation of ammonia as an amino group into glutamate and glutamine (Armstrong and Gross, 2007). When glutamate is provided as the primary carbon source, the ammonia generated is in excess, causing a carbon:nitrogen imbalance and alkalization in growth medium (Thalen et al. 1999).

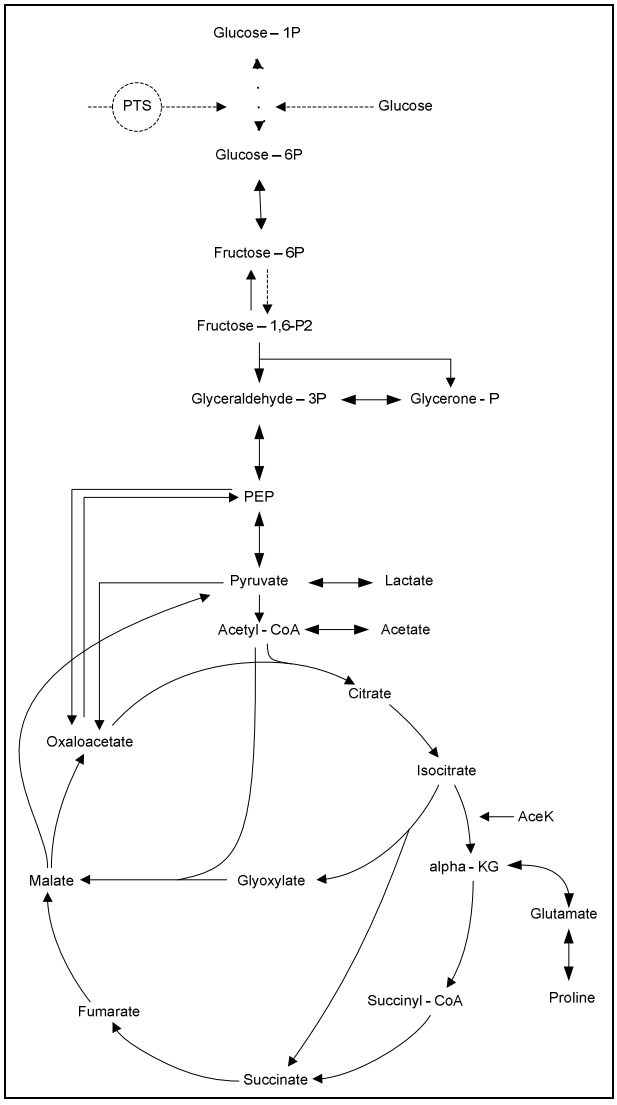

Figure 3: Glycolytic and gluconeogenetic pathways and citric acid cycle of *B. bronchiseptica.* Dashed arrows are absent reactions, Dot arrows represent enzymes which are functionally impaired (Armstrong and Gross, 2007).

Fermentation Design

There are two basic types of fermentation processes, batch and fed-batch. Traditionally, the antigen for the human whole-cell *Bordetella pertussis* vaccine is produced by batch fermentation. Whole-cell pertussis vaccines are suspensions of killed *B. pertussis*. The whole-cell vaccine frequently produced minor local reactions and less commonly severe systemic reactions. These reactions combined with public apprehension to whole-cell vaccines drove the need for a less reactogenic pertussis vaccine (Edwards and Decker, 2008). More recently, acellular *B. pertussis* vaccines have been developed to diminish adverse reactions which can occur after vaccination (Thalen et al., 2006). Even though acellular vaccines are commercially available, the whole-cell vaccine remains the most widely used globally, primarily due to cost (Edwards and Decker, 2008). The acellular *B. pertussis* vaccine requires 5-25 times the amount of the pertussis virulence factors to produce the same number of vaccine doses (Thalen et al., 2006), and thus more *B. pertussis* cells must be grown. To mitigate the demand for increased cultivation capacity and to target specific virulence factors, fed-batch fermentation approaches are being investigated. Optimized fed-batch cultures have the potential to produce higher cell densities and product formation. Table 3 summarizes some advantages and disadvantages of each fermentation method.

Table 3: Summary of advantages and disadvantages of batch and fed-batch fermentation

	Batch	Fed-Batch
Advantages	- Simplicity - Complete conversion of substrate possible - Lower contamination risk	- High cell density - greater control for batch reproducibility - Concentration of specific substrates controlled during the fermentation - Growth rate controlled - Production of by-products and catabolite repression controlled - Alternative mode of operation for fermentations leading with toxic substrates
Disadvantages	- Limited process control - Low cell density - Nutrients in the working volume become depleted - Limitation and depletion of substrate - Toxin formation - Growth subject to substrate inhibition, therefore lower initial substrate concentration - Growth rate not controlled	- Previous analysis of microorganism is required, including relationship between productivity and physiology - More complex set-up, process definition and development

By investigating the medium composition, growth rates, and limitation of specific nutrients the growth and metabolism of *B. bronchiseptica* can be controlled. The development of an optimized medium feed composition and feed rate regime for a fed-batch fermentation process for *B. bronchiseptica,* the fermentation process will produce a greater yield of biomass and expressed virulence factors necessary for vaccine production.

The objectives of this research are to: 1) define, simplify, and balance literature chemically defined medium for *B. bronchiseptica* 2) investigate the effect of different concentrations of known virulence modulators, $MgSO_4$ and nicotinic acid, on biomass generation and protein production 3) compare growth rates, biomass generation, and protein production of *B. bronchiseptica* on 4 different carbon source pairs; 4) under steady-state conditions compare growth rates, biomass production, protein production; 5) develop a fed-batch process for improved biomass and protein production.

CHAPTER 2

EFFECT OF Mg, SO_4, NICOTINIC ACID CONCENTRATIONS ON GROWTH AND FHA GENERATION BY BORDETELLA BRONCHISEPTICA

Introduction

Several studies have reported the effect of nicotinic acid and SO_4 (typically $MgSO_4$) on the antigenic state of *B. bronchiseptica* and *B. pertussis*. Usually, these experiments investigate the phenotypic state and/or expression of virulence factors after applying or removing these compounds. The concentrations of these compounds selected for these studies are typically relatively high, so that the impact of these factors on growth and expression of virulence factors is difficult to quantify. For example, the Bvg^- phase is reportedly induced by 50 mM $MgSO_4$, while the absence of $MgSO_4$ results in the Bvg^+ phase (Preston et al., 2003). Cotter and Miller (1994, 1997) reported that 40 mM $MgSO_4$ with 10 mM nicotinic acid, 20 mM $MgSO_4$ alone or 20 mM nicotinic acid alone resulted in the Bvg^- phase. Akerley et al. (1992) similarly noted that 40 mM $MgSO_4$ or 10 mM nicotinic acid produced cultures in Bvg^- phase.

Sulfur is a macronutrient which is required by all bacteria for cell synthesis. Sulfur is a necessary component due to its structural role in the synthesis of amino acids cysteine and methionine. It is also present in vitamins (biotin, thiamine, and lipoic acid) as well as several cofactors and coenzymes, such as glutathione and coenzyme A (Madigan et al., 2003). The KEGG pathway for sulfur metabolism in *B. bronchiseptica* is shown in Figure 4. A typical Gram negative bacterium, such as *Escherichia coli* contains less than 1% dry cell mass sulfur (Neidhardt et al., 1990). The synthesis of 1 g cells requires 3-10 mg of sulfur or about 0.3

mmoles (Fuchs, 1999). The original defined medium developed by Stainer and Scholte (1971) for large scale *B. pertussis* production and referred to as the SS medium contains 0.59 mM sulfur, and thus could result in about 2 g/L cells.

Most defined culture media for *Bordetella* contain cysteine or cystine and glutathione. These two components are important sources of sulfur for metabolic activity. Jebb and Tomlinson (1957) showed that neither methionine nor inorganic sulfate could serve as sulfur sources. Genomic analysis supports this observation. The *cys*C gene encoding adenosine phosphosulfate (APS) kinase (Figure 4: EC 2.7.1.25), is absent in *Bordetella*. This enzyme phosphorylates APS to produce phosphoadenosine phosphosulfate and is required for assimilation of inorganic sulfate into cellular building blocks (Armstrong and Gross, 2007).

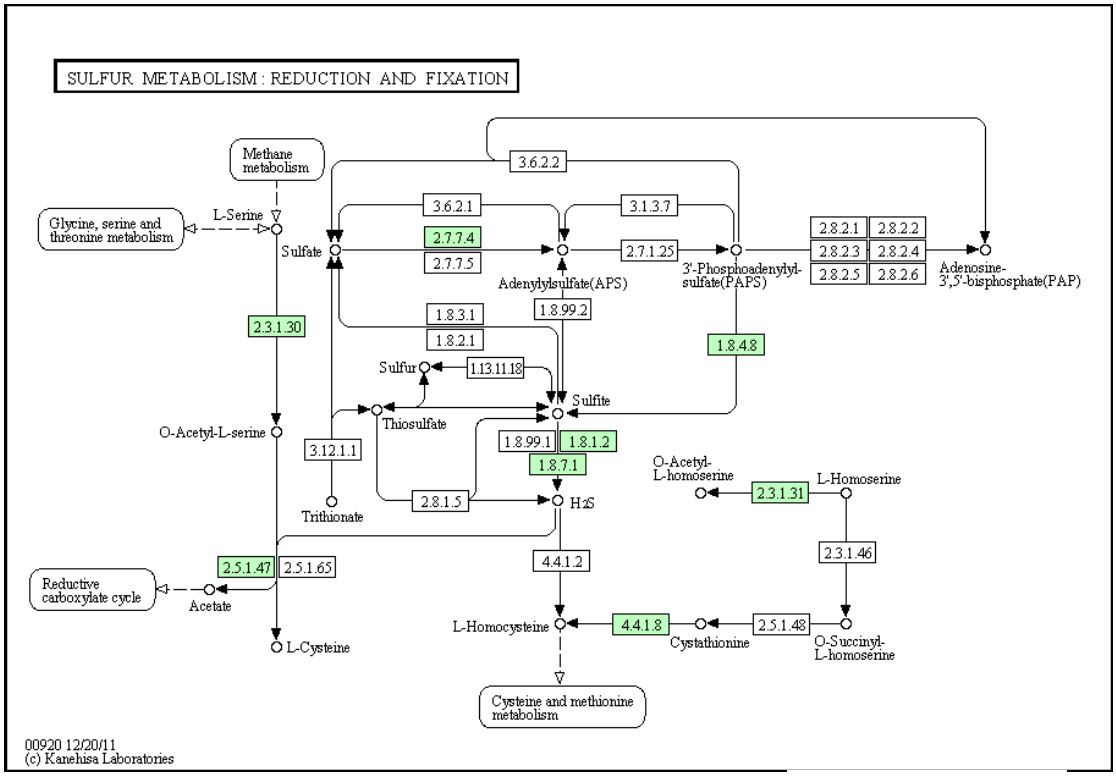

Figure 4: Metabolic pathway for sulfur in *Bordetella bronchiseptica* (Kanehisa et al., 2012)

Mg is another macronutrient required for cell synthesis. A typical bacterial cell contains 0.05% dry cell mass Mg (Neidhardt et al., 1990). A mass of 1 g cells therefore requires less than

1 mg Mg (0.04 mM). For comparison, a typical defined medium for bacterial growth may contain a final concentration of 0.8 mM Mg (Fuchs and Kröger, 1999). The *B. pertussis* SS medium contains 0.49 mM Mg (Stainer and Scholte, 1971), which would be sufficient to generate 12 g/L dry basis cells. Mg is required as a cofactor for enzymatic reactions, used as an inorganic cellular cation, and functions to stabilize ribosomes, cell membranes, and nucleic acids (Neidhardt et al., 1990; Madigan et al., 2003). Limited information is available on the utilization of Mg by *Bordetella*. Genomic analysis has identified two genes associated with Mg transport, the Mg transporter gene BB1811 and the Mg and Co efflux protein gene BB1354 (Armstrong and Gross, 2007; Caspi et al., 2009).

Jebb and Tomlinson (1955) reported *Bordetella* has an absolute requirement for nicotinic acid. Nicotinic acid is a precursor of NAD(P) and functions in electron transfer in oxidative-reduction reactions (Madigan et al., 2003; Armstrong and Gross, 2007). Vitamins are typically required in very small amounts, 10^{-6} to 10^{-7} M (Fuchs and Kröger, 1999). The *B. pertussis* SS medium contains 0.033 mM nicotinic acid (Stainer and Scholte, 1971). Thalen et al. (2006) investigated the replacement of nicotinic acid by the non-modulating compound anthranilic acid. They merely reported that anthranilic acid had no effect of pertussis toxin production or its association to the cell. Interestingly, the chemical modulators which have been identified, $MgSO_4$ and nicotinic acid, are not typically present in sufficient concentration in the host organism to influence virulence expression (Thalen et al., 2006b). Although these chemicals are known to modulate virulence gene expression under laboratory conditions, the actual environmental signals sensed by the organism *in vivo* remain unknown (Salyers and Whitt, 2002). Nevertheless, the concentrations of these modulators are crucial for vaccine production, and these compounds are commonly used in growth media.

In order to investigate the impact of Mg, SO_4, and nicotinic acid on growth and expression of virulence factors (specifically FHA) a series of batch fermentations were performed using a statistical design of experiments.

Materials and Methods

Batch Fermentation Media

The base chemically defined medium (CDM) used in batch processes is listed in Table 4. The medium is derived from two common *B. bronchiseptica* media (each detailed in Appendix B): the SS medium (Stainer and Scholte, 1971) and the CL medium (Imaizumi et al., 1983). In brief, compared to the SS medium, L-proline was removed; concentrations of NaCl, Tris, glutathione were reduced; L-cysteine concentration was increased; and β-cyclodextrin(heptakis(2,6-*O*-dimethyl)) was added. 26.4 mM lactic acid was used in this base medium to attain an initial C:N ratio of 6.24. (The secondary carbon source was further explored in subsequent experiments, see Chapter 3). The base CDM was supplemented with a low, medium, or high concentration of magnesium (Mg), sulfate (SO_4), and nicotinic acid. Specifically, CDM was supplemented with $MgCl_2 \cdot 6H_2O$ (Sigma-Aldrich M2670, Batch 028K00222), K_2SO_4 (Sigma P8541, Lot128K00992), and nicotinic acid (Sigma N0765, Batch 126K0693) to achieve three levels of Mg, SO_4, and nicotinic acid concentrations.

Table 4: Base CDM Formulation for Batch Fermentation Processes

Components	g/L
L-Glutamic Acid monosodium salt monohydrate (Aldrich 49621, Lot 0001380041)	10.700
L-Cysteine hydrochloride monohydrate (Sigma C-7880, Lot 32K0890)	0.500
L-Ascorbic Acid (Aldrich A92902, Batch 04308LC)	0.020
L-Glutathione, reduced (Sigma-Aldrich G4251, Lot 030M1775)	0.001
NaCl (Mallinckrodt 7532-20, Lot H50602)	1.040
KH_2PO_4 (Mallinckrodt 7096-06, Lot G43581)	0.500
KCl (Mallinckrodt 6838-06, Lot E48N94)	0.200
$CaCl_2$ (JT Baker 1311-01, Lot V45599)	0.020
Tris(hydroxymethyl)aminomethane (Sigma-Aldrich 252859, Batch 07705HH)	1.520
β-Cyclodextrin(heptakis(2,6-*O*-dimethyl)) (MP 157320, Lot 4318KA)	1.000
$FeSO_4 \cdot 7H_2O$ (JT Baker 2070-01, Lot C17H24)	0.010
Lactic Acid, 85% (JT Baker 0194-01, J11J03)	2.400

Batch Fermentation Process Conditions

For each batch experiment, one vial of X+9 frozen cell stock (1 mL; cell stock development located in Appendix A) was thawed at room temperature and used to inoculate 1.0 L CDM in the 2.0 L bioreactor with an AppliSens DO sensor, an AppliSens pH sensor, and a Pt100 temperature sensor using a ADI 1010 Biocontroller with the ADI 1025 Bioconsole (Applikon, Schiedam, Netherlands, see Figure 5 for schematic representation). Batch processes were carried out at 35°C, a of 500 RPM, and a pH of 6.9 controlled with 3 M lactic acid (JT Baker 0194-01) placed on a scale for mass measurement. Cells were aerated by sparged air at a constant rate of 400 mL/min controlled by mass flow controller (Aalborg, Orangeburg, SC, USA, model GFC17) which prevented oxygen limitation. Bioreactor process CDM contained 250 μL of a 20% antifoam solution per L (Biospumex 153K, Cognis, Batch S632610005). Temperature, pH, dissolved oxygen, RPM, and optical density were recorded using BioXpert Lite software.

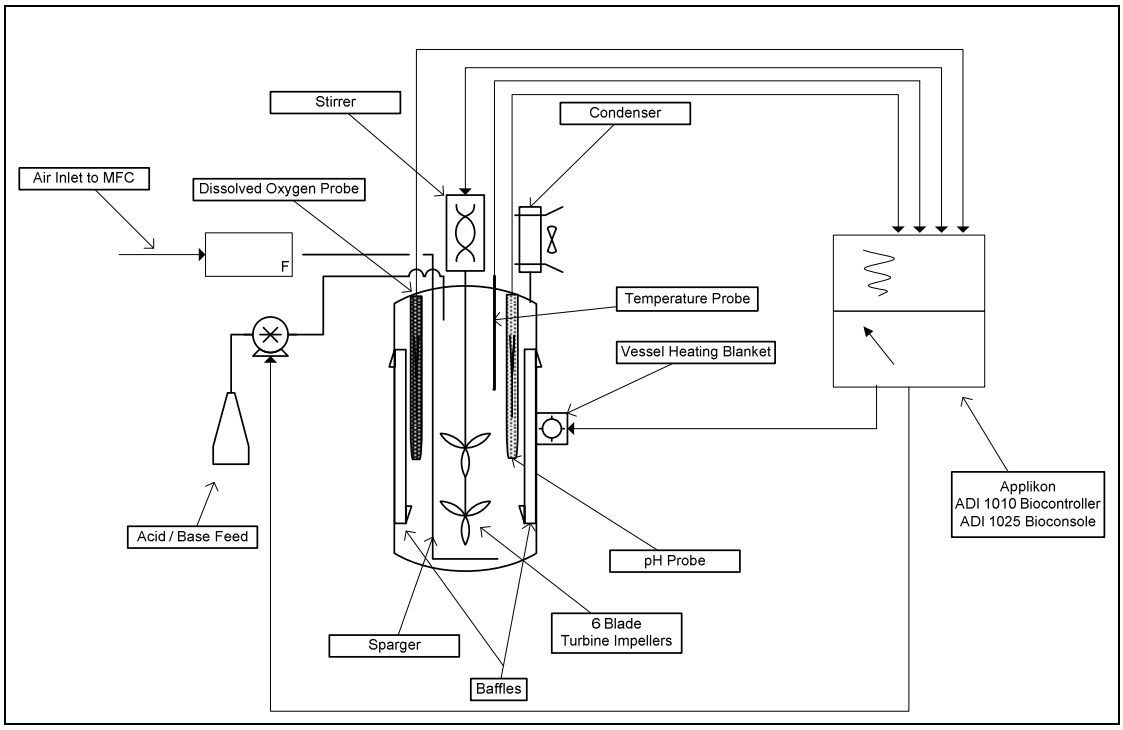

Figure 5: Schematic representation of batch fermentation

Statistical Design

Table 5 lists the Design of Experiments (DOE), where "-1" represents the low concentration level, "0" the medium concentration level, and "1" the high concentration level. For Mg and SO_4, the low (L), medium (M), and high (H) concentration levels were respectively 0.1 mM, 1 mM, and 10 mM. For nicotinic acid, L, M, and H were respectively 3.25 µM, 32.5 µM, and 325 µM. The specific medium formulation used was denoted by the three concentrations in order of Mg, SO_4, and nicotinic acid, so that for example, "LMH" refers to a medium containing 0.1 mM Mg, 1.0 mM SO_4, and 325 µM nicotinic acid. The data from the first 19 batch fermentations were inputed into statistical software for evaluation (Stat-Ease, Minneapolis, MN). A Box-Behnken DOE and response surface quadratic model was evaluated by stepwise regression. The response variables examined were FHA concentration (ng/mL) and specific FHA concentration (ng/OD unit). After modeling and selection, two additional

fermentations (Fermentation 19 and 20, LLM) were performed as a verification of statistical model.

Table 5: Design of Experiment: Investigation of Mg, SO_4, nicotinic acid concentration on *B. bronchiseptica* growth and FHA expression

Fermentation	Mg	SO_4	Nicotinic acid
0 - MMM	0	0	0
1 - MLM	0	-1	0
2 - MHM	0	1	0
3 - HMM	1	0	0
4 - MML	0	0	-1
5 - HMM	1	0	0
6 - MML	0	0	-1
7 - MHM	0	1	0
8 - MMH	0	0	1
9 - LMM	-1	0	0
10 - MMH	0	0	1
11 - MLM	0	-1	0
12 - LMM	-1	0	0
13 - LLH	-1	-1	1
14 - LLH	-1	-1	1
15 - LMH	-1	0	1
16 - MLH	0	-1	1
17 - MMM	0	0	0
18 - MMM	0	0	0
19 - LLM	-1	-1	0
20 - LLM	-1	-1	0

Analytical Methods

Optical Density

Optical density (OD_{600}) was measured at 600 nm using Beckman Coulter DU800 Spectrophotometer or Pharmacia LKB Ultrospec III, using 1 ml cuvettes. Dilutions were performed as needed.

FHA

The 11-14 h, 16-18 h, and 32-34 h sample for each fermentation were each analyzed by ELISA for FHA concentration. Maxisorp flat bottom plate was coated with the 100 µL per well of capture antibody, *B. pertussis* Anti-Sheep Serum 97/564 (NIBSC) at a dilution of 1:32000 in PBS (NaCl, 8.0 g/L; KCl, 0.2 g/L; Na_2HPO_4, 1.15 g/L; KH_2PO_4, 0.20 g/L). The plate was sealed and incubated static at 4°C overnight. The plate was washed three times with a wash buffer, PBS plus 0.05% v/v Tween 20, at 200 µL per well. 300 µL of blocking buffer (PBS plus 0.05% v/v Tween 20 and 0.15% v/v Odyssey blocking buffer) was added to each well. The plate was sealed and incubated at 37°C for 60 minutes shaking at 200 RPM. The plate was then washed three times with wash buffer at 300 µL per well. A non binding V-bottom transfer plate was used to prepare dilutions. 125 µL of blocking buffer was added to each well in the transfer plate. A known concentration of FHA was added to column 11 and 12 of row A. 125 µL of the samples for analysis was added to the remaining columns in row A. Samples were run in duplicate. The last row used as a blank. Two fold serial dilutions were performed down the plate, transferring 125 µL at a time. 100 µL per well was transferred to the test plate. The plate was sealed and incubated at 37°C for 60 minutes shaking at 200 RPM. The plate was then washed with 200 µL wash buffer per well, three times. 100 µL of the monoclonal antibody, anti-FHA monoclonal antibody 99/572 (NIBSC), at a 1:2000 dilution in blocking buffer, was added to each well. The plate was sealed and incubated at 37°C for 60 minutes shaking at 200 RPM. The plate was washed with 200 µL wash buffer per well, three times. 100 µL of the conjugate Goat anti-Mouse IgG (H+L) HRP (Jackson ImmunoResearch Labs) was added to each well at a 1:2000 dilution in blocking buffer. The plate was sealed and incubated at 37°C for 30 minutes shaking at 200 RPM. The plate was washed three times with 200 µL wash buffer per well. 100

µL of the substrate TMB Peroxidase Substrate one component (Moss, Inc) was added to each well. The plate was incubated at 37°C for 10 minutes shaking at 200 RPM. Substrate was stopped by adding 100 µL of 1M H_3PO_4 to each well. The plate was immediately read using a BioTek PowerWave Synergy HT plate reader at 450 nm and 630 nm and the ΔOD was calculated ($OD_{450} - OD_{630}$). Results were analyzed using BioTek's Gen5 data analysis software.

Analytes

Samples were evaluated for glutamate and glutamine using the Nova Biomedical Bioprofile Flex system (Nova Biomedical, Waltham, USA). Samples were centrifuged in Eppendorf tubes using a Fisher Scientific Micro Centrifuge, model 235C, for 1 minute for cell debris removal.

Morphology

Select samples were streaked on Bordet Gengou with 15% sheep's blood plates (BD BBL Prepared Plated Media, Catalog no. 297876) for morphology observation. Plates were incubated 48 h at 37°C.

Results and Discussion

Twenty-one batch fermentations summarized by the DOE (Table 5) were conducted to determine the effect of Mg, SO_4, and nicotinic acid on growth and FHA production. During the cultivations, samples were taken for OD, glutamate concentration, and glutamine concentration; and dissolved oxygen and acid addition were monitored throughout the process. Figures 6–9 show the results from the 21 conditions.

In general, cell growth was similar for all processes. All fermentations reached stationary phase between 12–14 h of growth (Figure 6). A correlation was apparent between nicotinic acid concentration and optical density achieved. For example, fermentation conditions MMH and

MLH achieved an OD of 3.9-4.2 after 34 h of growth, while the fermentation condition MML only attained an OD of only 0.8-1.3. The other experiments with a high level of nicotinic acid (LLH and LMH) reached OD values of 2.7-2.9, while those other conditions with low or medium nicotinic acid resulted in OD values of 1.6-2.1.

Figure 7 shows the dissolved oxygen (DO) profile generated during the 21 processes. No fermentation condition was oxygen limited during growth, although different DO profiles were generated by the different fermentation conditions. Thus, elevated biomass concentration resulted in an increased oxygen demand and consequent decrease in measured DO. The greatest oxygen demand were found in experiments LMH, MMH, and MLH, and then the LLH condition. Because such conditions yielded the greatest biomass concentration, not surprisingly, conditions with high nicotinic acid concentration required the most oxygen, while the MML condition required the least demand for oxygen. All other conditions had comparable dissolved oxygen demand.

Glutamate utilization by each fermentation condition is shown in Figure 8. Fermentation conditions MLH and MMH each depleted glutamate by the end of cultivation, consuming 53.3-56.1 mM. The next greatest consumption was achieved by LLH, LLM, and LMH conditions, with 14-17 mM remaining at the end of growth, consuming 36.2-42.8 mM. The condition which displayed the least consumption was MML, using about 14.5 mM. Glutamate utilization was similar for remaining conditions, consuming 23.6-28.2 mM glutamate. Increased glutamate utilization also corresponds to greater nicotinic acid and Mg concentrations, relating to increased biomass production.

A similar trend was observed with glutamine utilization (Figure 9), although three conditions consumed all available glutamine prior to end of cultivation. MMH condition

consumed all available glutamine (an average of 9.6 mM) by 17 h of growth. The greatest consumption of glutamine was observed in the LMH and MLH conditions, consuming 11.8 and 10.8 mM. Due to sampling time, the exact time of glutamine depletion was not captured, although depletion was most likely between 20-25 h. LMM and LLH consumed all available glutamine (an average of 9.3 and 6.9 mM, respectively) by 23 h. The least utilization of glutamine was observed by MML condition, using about 5.0 mM. Glutamine utilization was similar for remaining conditions, consuming on average 7.2-8.9 mM glutamine. Similar to glutamate utilization, increased glutamine consumption corresponds to greater nicotinic acid and Mg concentrations, relating to increased biomass production.

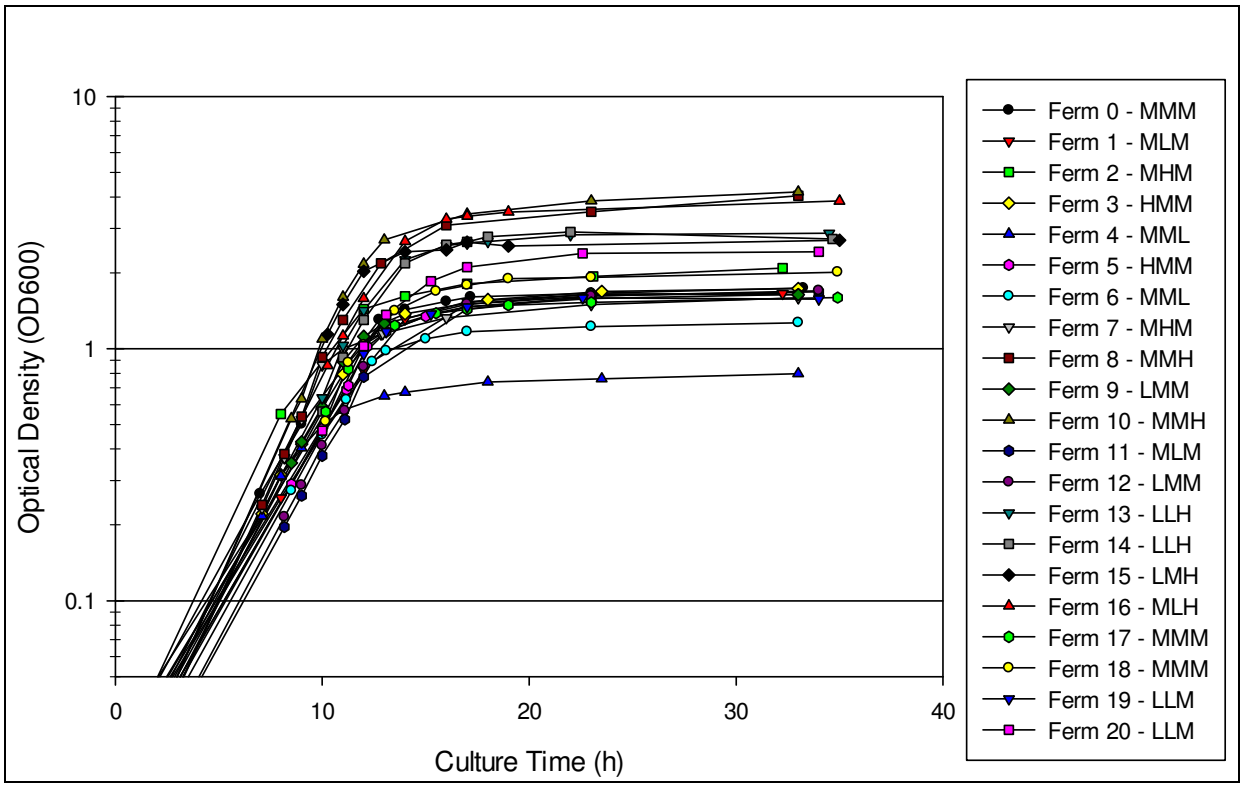

Figure 6: Growth curves for 21 batch fermentations at different concentration conditions of Mg/SO_4/nicotinic acid.

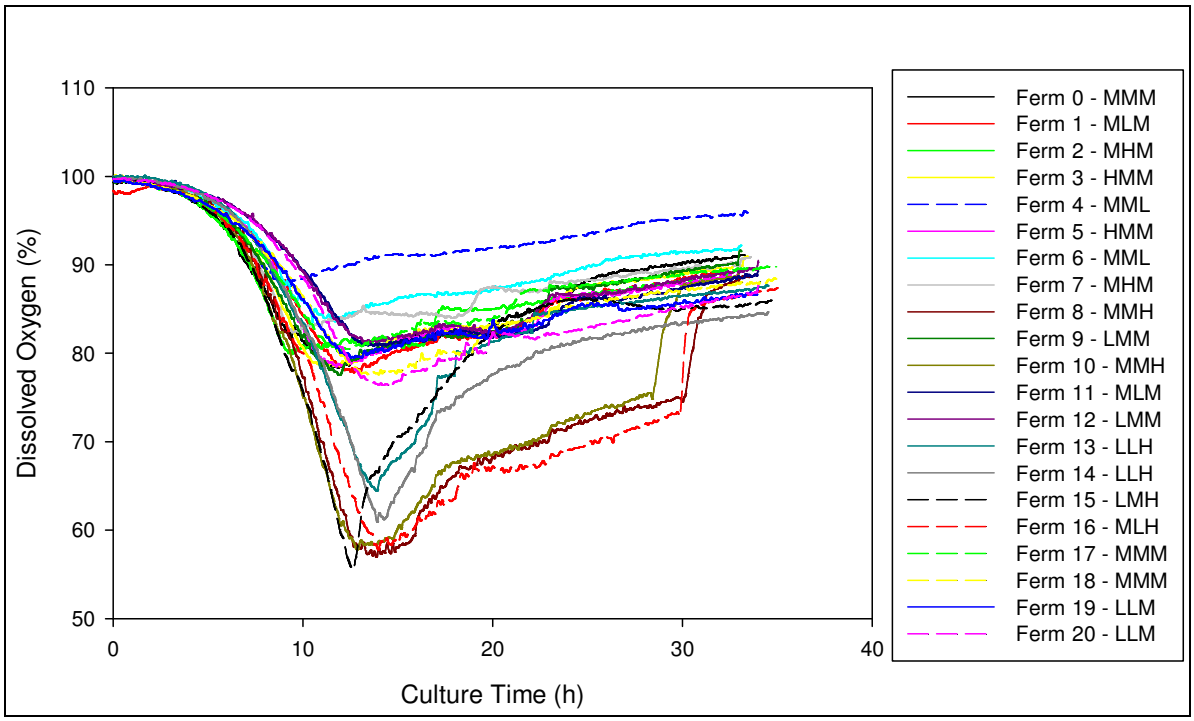

Figure 7: Dissolved oxygen profile for 21 batch fermentations at different concentration conditions of Mg/SO_4/nicotinic acid.

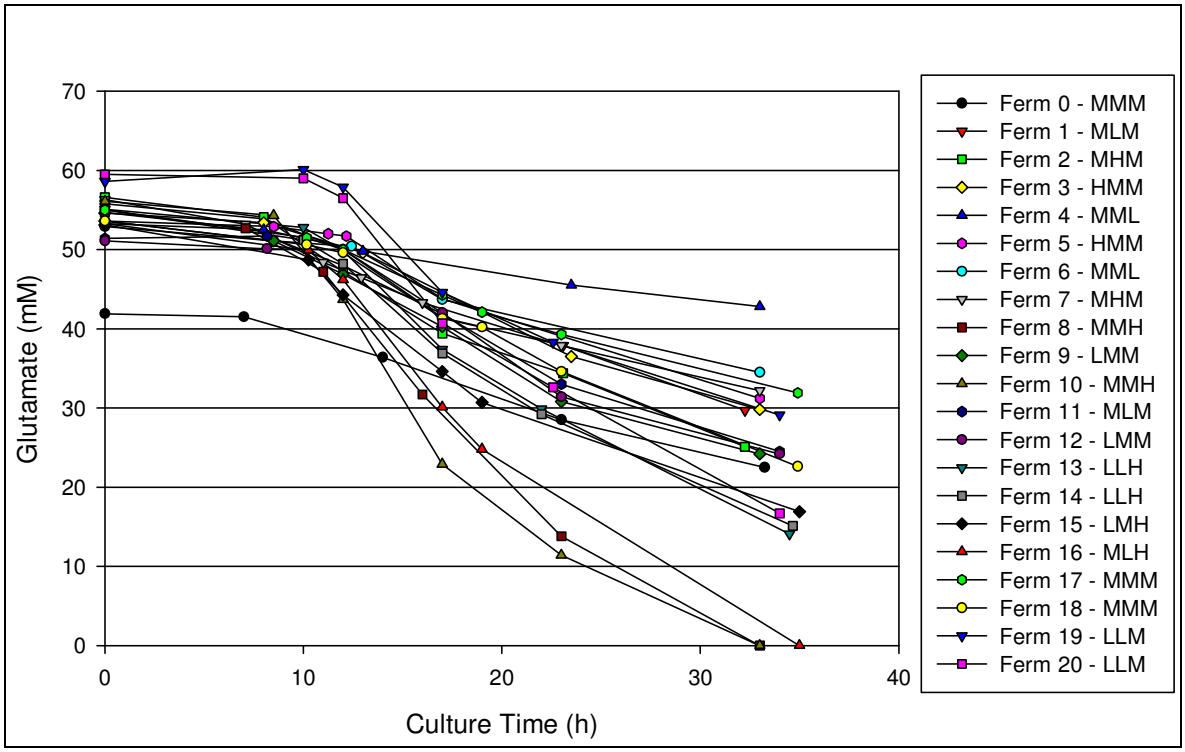

Figure 8: Glutamate utilization during 21 batch fermentations at different concentration conditions of Mg/SO_4/nicotinic acid.

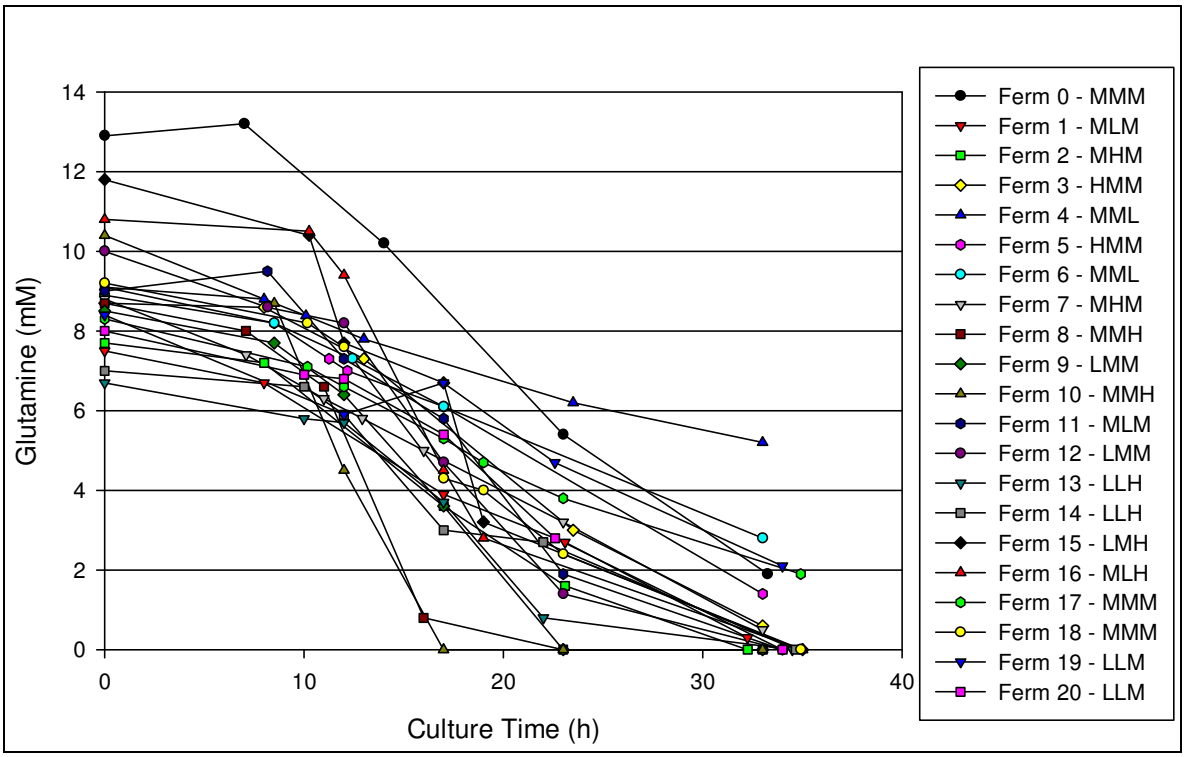

Figure 9: Glutamine utilization during 21 batch fermentations at different concentration conditions of Mg/SO_4/nicotinic acid.

Since fermentations with high nicotinic acid (325 µM) and medium Mg achieved an OD of about 4 while those using high nicotinic acid and low Mg (0.1 mM) achieved an OD of only 2.7-2.9, the processes with 0.1 mM may have been Mg limited. A growth limitation is supported by the observation that those fermentations with low Mg (e.g., LLH and LMH) showed an increase in DO compared to other conditions (Figure 7). The increased growth observed for the highest nicotinic acid concentration was correlated with greater oxygen consumption, glutamate depletion, increased lactic acid required to maintain the pH (data not shown), and early depletion of glutamine. Opposite effects were observed for low nicotinic acid concentration. Growth profiles and nutrient utilization were similar for other tested conditions.

FHA Production

In addition to growth characteristics and nutrient utilization, the 21 batch fermentations were evaluated for FHA production at 11-14 h, 16-18 h, and 32-34 h, corresponding to late

exponential growth, early stationary phase and late stationary phase. Table 6 shows the mean concentration of FHA for each condition. Generally, the greatest FHA concentrations were observed during the early stationary phase, with a decline in concentration by the end of culture, suggesting that FHA production was growth associated. FHA growth association can also be observed in the results for the specific FHA concentration (Table 7). A decline in FHA concentration was observed during the fermentation processes. This observation could be due to proteolytic activity, as proposed for toxin production in *B. pertussis* (Thalen et al., 2006b). Similar to the present results, proteolytic activity for pertussis toxin increased during exponential growth until early stationary phase, and a decrease in pertussis toxin was observed during stationary phase.

Table 6: Mean FHA concentration using different medium concentrations of Mg/SO_4/nicotinic acid during batch fermentations

Fermentation Condition	**11-14 h** (ng/ml)	**16-18 h** (ng/ml)	**32-34 h** (ng/ml)
LMM: 0.1 mM Mg/1 mM SO_4/32.5 µM Nicotinic acid	444	938	891
HMM: 10 mM Mg/1 mM SO_4/32.5 µM Nicotinic acid	373	363	310
MLM: 1 mM Mg/0.1 mM SO_4/32.5 µM Nicotinic acid	327	840	812
MHM: 1 mM Mg/10 mM SO_4/32.5 µM Nicotinic acid	0	0	0
MML: 1 mM Mg/1 mM SO_4/3.25 µM Nicotinic acid	295	300	358
MMH: 1 mM Mg/1 mM SO_4/325 µM Nicotinic acid	422	851	958
LLH: 0.1 mM Mg/0.1 mM SO_4/325 µM Nicotinic acid	488	653	346
LMH: 0.1 mM Mg/1 mM SO_4/325 µM Nicotinic acid	475	802	434
MLH: 1 mM Mg/0.1 mM SO_4/325 µM Nicotinic acid	547	1015	406
MMM: 1 mM Mg/1 mM SO_4/32.5 µM Nicotinic acid	431	222	204
LLM: 0.1 mM Mg/0.1 mM SO_4/32.5 µM Nicotinic acid	498	456	310

Table 7: Mean specific FHA concentration using different medium concentrations of Mg/SO_4/nicotinic acid during batch fermentations

Fermentation Condition	11-14 h (ng/OD_{600} unit)	16-18 h (ng/OD_{600} unit)	32-34 h (ng/OD_{600} unit)
LMM: 0.1 mM Mg/1 mM SO_4/32.5 µM Nicotinic acid	454	624	530
HMM: 10 mM Mg/1 mM SO_4/32.5 µM Nicotinic acid	347	239	183
MLM: 1 mM Mg/0.1 mM SO_4/32.5 µM Nicotinic acid	407	565	485
MHM: 1 mM Mg/10 mM SO_4/32.5 µM Nicotinic acid	0	0	0
MML: 1 mM Mg/1 mM SO_4/3.25 µM Nicotinic acid	384	298	337
MMH: 1 mM Mg/1 mM SO_4/325 µM Nicotinic acid	245	260	232
LLH: 0.1 mM Mg/0.1 mM SO_4/325 µM Nicotinic acid	359	247	124
LMH: 0.1 mM Mg/1 mM SO_4/325 µM Nicotinic acid	234	303	161
MLH: 1 mM Mg/0.1 mM SO_4/325 µM Nicotinic acid	345	302	105
MMM: 1 mM Mg/1 mM SO_4/32.5 µM Nicotinic acid	407	137	112
LLM: 0.1 mM Mg/0.1 mM SO_4/32.5 µM Nicotinic acid	505	257	160

The statistical analysis resulted in a model for ELISA and specific ELISA (Appendix C shows ANOVA Table). The model for FHA concentration resulted in the following equation:

$$\text{FHA} = 457.2 - 310.8(\text{A}) - 476.8(\text{B}) + 311.0(\text{C}) + 827.6(\text{A})(\text{C}) + 522.6(\text{B})(\text{C}) + 258.4(\text{A}^2) + 223.6(\text{C}^2)$$

where A = Mg, B = SO_4, and C = nicotinic acid. This model is significant at $p<0.0001$. FHA concentration was positively correlated with nicotinic acid concentration, and negatively correlated with Mg and SO_4 concentration. The negative correlation with SO_4 was stronger than the negative correlation with Mg. There was a positive interaction between nicotinic acid and Mg and between nicotinic acid and SO_4 concentration, and positive quadratic terms for both Mg and nicotinic acid. That is, Mg and SO_4 have a negative impact on FHA concentration as their concentration increase. However, the positive interactions for nicotinic acid and SO_4 or Mg, suggest that the effect of higher nicotinic acid concentration when combined with higher SO_4 or Mg concentration have a positive impact on FHA concentration.

The model for specific FHA concentration generated the equation:

$$\text{Specific FHA} = 344.3 - 145.1(\text{A}) - 295.5(\text{B}) - 93.3(\text{C}) + 256.6(\text{A})(\text{C}) + 216.7(\text{B})(\text{C}) + 148.2(\text{A}^2)$$

Specific FHA concentration was negatively correlated with Mg, SO_4, and nicotinic acid. The negative correlation with SO_4 was stronger than the negative correlation with Mg. Both SO_4 and Mg have a stronger negative correlation than nicotinic acid. There were positive interactions between Mg and nicotinic acid, and SO_4 and nicotinic acid. There was also a positive quadratic term for Mg. That is, Mg, SO_4, and nicotinic acid have a negative impact on specific FHA production as their concentration increase. However, the positive interactions for nicotinic acid and SO_4 or Mg, suggest that higher nicotinic acid concentration when combined with higher SO_4 or Mg concentration have a positive impact on FHA concentration. The model predicts optimal specific FHA concentration and FHA concentration should occur with medium conditions having medium to low nicotinic acid, and low to medium Mg and SO_4. For example, the model predicted:

- LLM condition: 1503 ng/mL and 933 ng/OD unit
- MLM condition: 934 ng/mL and 640 ng/OD unit
- LMM condition: 1026 ng/mL and 638 ng/OD unit

LLM is predicted to be the best optimum condition. Unfortunately, this was a condition which was not originally tested. However, MLM and LMM conditions were among the original test: MLM generated 840 ng FHA/mL or 565 ng FHA/OD unit, while LMM generated 938 ng FHA/mL or 624 ng FHA/OD unit (Table 6 and 7). Based on these conditions, the model seemed reasonable. Since the predicted optimal condition (LLM) was never tested, two additional batch fermentations were performed at this condition (results included in previous tables and figures). LLM did not match model predictions, resulting in concentrations of 498 ng FHA/mL and 505 ng FHA/OD unit.

Concluding Remarks

Based on the previous analysis two optimal conditions were selected for further investigation: 0.1 mM Mg/1 mM SO_4/32.5 μM nicotinic acid and 1 mM Mg/0.1 mM SO_4/32.5 μM nicotinic acid. These conditions were used to investigate the effect of carbon source on growth and FHA production (Chapter 3).

The original data set (of 19 fermentations) was updated with two additional batch fermentations, and the statistical analysis was repeated. Surprisingly, the model predictions changed. The models were significant at $p<0.0001$ and $p<0.0002$, respectively, and yielded the following equations (A=Mg, B=SO_4, and C=nicotinic acid):

$$\text{FHA} = 515.8 - 274.9(\text{A}) - 431.4(\text{B}) + 248.6(\text{C}) - 795.4(\text{A})(\text{B}) + 257.7(\text{A})(\text{C}) + 163.9(\text{A}^2)$$

$$\text{Specific FHA} = 440.1 - 128.1(\text{A}) - 287.3(\text{B}) - 109.6(\text{C}) - 172.5(\text{A})(\text{B}) - 152.8(\text{B}^2) - 87.3(\text{C}^2)$$

The principal difference between the original models and the revised models is the prediction that the optimum conditions will occur at high Mg rather than low to medium Mg. The second model predicted the optimal combination of medium components was HLM leading for an FHA concentration of 1632 FHA ng/mL and the HLL combination leading to a specific FHA concentration of 641 FHA ng/OD unit. The prediction for the two media selected for further study (MLM and LMM) were not substantially changed: about 950 FHA ng/mL and 570 ng FHA/OD unit. Ultimately, these conditions were selected since the previous conditions performed well with lactate-glutamate and data could subsequently be used for further investigation. However, this model could highlight the importance of Mg to growth and corresponding expression of *B. bronchiseptica*.

Medium composed of a high SO_4 concentration (10 mM) terminated FHA expression. Surprisingly, morphology analysis of these growing cultures revealed consistent Bvg^+ colonies (qualitative) when compared to the other conditions (Figure 10).

Figure 10: Bvg^+ phenotype observed using medium containing a high SO_4 condition (Fermentation 7, MHM). The concentration of FHA was found to be 0.0 ng FHA/mL based on ELISA.

As previously described, expression of virulence genes is activated by the BvgAS system. Cotter and Miller (1997) showed a distinct intermediate phase, Bvg^i. The RB50i strain was described as medium-sized, flattish, and slightly hemolytic. This phase is uniquely different from Bvg^+ phenotype, which produces small, domed, hemolytic colonies. It has been reported that adhesins, such as FHA, are expressed during the intermediate phase, while toxins are not expressed (Salyers and Whitt, 2002). Cotter and Miller (1997) reported FHA expression in RB50i; however the strain proved to have lower infectivity than wild-type RB50. Qualitative analysis suggests the non-FHA expressing culture was not fully in either the Bvg^i or Bvg^- phase. Perhaps, the loss of FHA expression while maintaining Bvg^+ phenotype in the presence of high SO_4 is a unique observation of another distinct phase of *Bordetella*. Although interesting, ultimately the presence of 10 mM SO_4 is detrimental to FHA expression and therefore unsuitable for vaccine production.

CHAPTER 3

EFFECT OF CARBON SOURCE ON GROWTH AND FHA GENERATION BY BORDETELLA BRONCHISEPTICA

Introduction

Members of the genus *Bordetella* do not have a functional glycolysis pathway. As a result, amino acids are typically used as both carbon and nitrogen sources during growth. The molar carbon:nitrogen (C:N) ratio of *B. pertussis* has been reported to be 6:1 (Thalen et al, 1999). Due to the close relationship of *B. bronchiseptica* to *B. pertussis*, a similar C:N composition can be assumed. Traditional *B. pertussis* CDM (SS medium) contains a C:N ratio of 5:1, using glutamate and proline as substrates (Thalen et al., 1999). Jebb and Tomlinson (1951) showed glutamate is easily oxidized by *B. pertussis*, and glutamate salts are inexpensive and readily available. Glutamate (as the sodium salt) is catabolized by the following reaction to produce energy (Frohlich et al., 1995):

$$Na^+ + Glu^- + \frac{9}{2}O_2 \rightarrow Na^+ + 5CO_2 + H_2O + NH_4^+ + 2OH^-$$

This reaction has several consequences commonly observed during *Bordetella* cultivation: 1) NH_4 accumulation; 2) Na accumulation; and 3) OH accumulation. Frohlich et al. (1995) observed growth rate deceleration followed by stationary phase, even though no nutrient limitation could be found. Further investigation found that NH_4 can inhibit growth at 350-400 mM; however, this was well above the typical concentration observed in culture (50-60 mM). Frohlich et al. (1995) also found that while Na inhibited growth, this cation was required for toxin production. Ultimately, a compromise between growth and expression needs to be made.

Initial batch fermentations (Chapter 2) were designed with 75 mM Na, considered optimal for growth rate, expression, and proteolytic activity for *B. pertussis* (Thalen et al., 2006b). Another consequence of the use of sodium glutamate was the systematic alkalinization of the media. These factors led to the use of a secondary organic acid for pH regulation, first suggested by Frohlich et al. (1995).

To balance the C:N ratio, a carbon source is needed that can be co-metabolized by *B. bronchiseptica* without generating excess ammonia. In a study of catabolic activity in *B. pertussis*, Jebb and Tomlinson (1951) found complete oxidation of glutamic acid, with similar rates of oxidation for lactate and succinate, with diminished rates of oxidation for α-ketoglutarate (50%) and pyruvate (15%). However, Thalen et al. (1999) suggested that amino acids which are degraded to pyruvate or α-ketoglutarate can be rapidly oxidized. Since *B. pertussis* is able to grow on glutamate and cysteine only; these two substrates allow the formation of amino acids, carbohydrates, fatty acids, and nucleotides (Thalen et al., 1999) with cysteine serving as a sulfur source. An investigation of various carbon sources at 10 mM (glutamate, α-ketoglutarate, malate, fumarate, succinate, lactate and pyruvate), only media containing glutamate or α-ketoglutarate were able to sustain growth, suggesting *B. pertussis* does not have a functional citric acid cycle (Thalen et al. 1999). Subsequent genomic analysis showed the presence of all citric acid cycle enzymes (Parkhill et al., 2003; Armstrong and Gross, 2007), although Thalen et al. (2006a) found that key enzymes are not expressed such as the gene *aceK* encoding isocitrate dehydrogenase kinase, where the DNA sequence is present, but has mutated to an inactive form via evolution. Armstrong and Gross (2007) suggest that this impaired pathway in *B. pertussis* is unique to this species, and *B. bronchiseptica* has a fully functional citric acid cycle.

Thalen et al. (1999) also investigated growth on dual carbon sources in shake flasks with limited control: 12.5 mM glutamate only, or a combination of 12.5 mM glutamate with another carbon source to achieve a final concentration of 100 mM: lactate, α-ketoglutarate, succinate, fumarate, or pyruvate. All carbon source combinations except pyruvate-glutamate at C:N ratios of 8:1 or 12:1 resulted in higher cell densities and less ammonium accumulation than cultures grown in glutamate only. Cultures with glutamate and acetate, ethanol, glycerol, citrate, α-, or β-glycerolphosphate resulted in growth curves and dry weights similar to glutamate-only cultures, although the C:N ratios used was not described (Thalen et al., 1999).

The goal of this study was to investigate the use of dual carbon sources on the growth and FHA generation in *B. bronchiseptica*. This work was built on previous work (Thalen et al. 1999) with *B. pertussis,* by using four organic acids (lactate, succinate, citrate, and acetate) combined with glutamate. Furthermore, these comparisons were made in controlled bioreactors.

Materials and Methods

In order to explore the effect of carbon source combinations on growth and FHA production by *B. bronchiseptica*, a series of batch fermentation experiments was conducted analogous to the procedure described in Chapter 2.

Batch Fermentation Process Conditions

Batch fermentation process conditions were previously described in Chapter 2.

Batch Fermentation Media

Based on previous results from the investigation of the effect of Mg, SO_4, nicotinic acid concentration, two optimal combinations were chosen for further study: 0.1 mM Mg/1 mM SO_4/32.5 μM nicotinic acid (LMM) and 1 mM Mg/0.1 mM SO_4/32.5 μM nicotinic acid (MLM) as described in Chapter 2. Four carbon source combinations were compared: lactate-glutamate

(studied previously in Chapter 2), succinate-glutamate, citrate-glutamate, and acetate-glutamate. Batch fermentation CDM was previously described (Table 4), except for specific Mg, SO_4, and nicotinic acid concentrations and a carbon source pair. Each organic acid had an initial concentration of 26.6 mM, which resulted in different initial C:N ratios: 6.24 for lactate, 6.68 for succinate, 7.56 for citrate, or 5.79 for acetate. Additional acid was added to any given batch fermentations on demand as necessary to control the pH. That is, for any given condition, the organic acid used for pH regulation corresponded to the carbon source organic acid used in the CDM. The acid concentration supplied for pH regulation was also different for each acid: 3 M lactic acid (JT Baker 0194-01, Batch H16508), 0.5 M succinic acid (JT Baker 0346-01, Batch H42599), 1 M citric acid (Sigma C1857, Batch 057K0090), or 1 M or 2 M acetic acid (JT Baker 9522-02, Batch H31806). Table 8 lists the experimental conditions which were investigated.

Table 8: Experimental conditions for the investigation of different carbon sources on growth and FHA generation

Fermentation	Carbon Source*	Mg (mM)	SO_4 (mM)	Nicotinic acid (μM)
9 – LMM**	Lactate	0.1	1.0	32.5
12 – LMM**	Lactate	0.1	1.0	32.5
1 – MLM**	Lactate	1.0	0.1	32.5
11 – MLM**	Lactate	1.0	0.1	32.5
21 – LLM	Succinate	0.1	1.0	32.5
22 – LLM	Succinate	0.1	1.0	32.5
23 – MLM	Succinate	1.0	0.1	32.5
24 – MLM	Succinate	1.0	0.1	32.5
25 – LMM	Citrate	0.1	1.0	32.5
26 – LMM	Citrate	0.1	1.0	32.5
27 – MLM	Citrate	1.0	0.1	32.5
28 - MLM	Citrate	1.0	0.1	32.5
29 – LMM	Acetate	0.1	1.0	32.5
30 – LMM	Acetate	0.1	1.0	32.5
31 – MLM	Acetate	1.0	0.1	32.5
32 - MLM	Acetate	1.0	0.1	32.5

* Initial organic acid concentration was 26.6 mM for each condition

** Previously performed in Chapter 2

Analytical Methods

Optical Density, FHA ELISA, Analytes, and Morphology

Samples throughout fermentation process were analyzed as previously described in Chapter 2.

Carbon Source

Samples were evaluated for carbon content by HPLC using a previous method (Eiteman and Chastain, 1997).

Results and Discussion

Growth Characteristics

Four different glutamate-organic acid combinations were examined at two combinations of Mg/SO_4/nicotinic acid (the lactate-glutamate runs were completed previously with results shown in Chapter 2). During cultivation, samples were taken for the measurement of OD, glutamate, glutamine, and organic acid concentration. Dissolved oxygen and pH acid addition were monitored throughout the process. Figures 11–22 show the results from the 16 fermentations (12 new conditions and 4 conditions described previously in Chapter 2). Figures 11 and 12 show growth curves (OD_{600}) for one of the replicates from each set of organic acid-glutamate experiments, for 1 mM/0.1 mM/32.5 μM and for 0.1 mM/1.0 mM/32.5 μM, respectively. Since replicates resulted in very similar growth, the one replicate generating the greater cell mass was consistently selected for graphical representation. Final cell densities were also similar for the two different Mg/SO_4/nicotinic acid concentrations for lactate-glutamate, succinate-glutamate, and citrate-glutamate: lactate-glutamate achieved an OD of 1.67, succinate-glutamate achieved an OD of 1.70, and citrate-glutamate achieved an OD of 0.78. The two medium compositions studied for the acetate-glutamate fermentations behaved considerably

differently from each other as well as from other three organic acid-glutamate combinations. For the LMM experiment, the OD reached 3.63, while for the MLM experiment, the OD reached 12.26. The difference in OD values between these two acetate-glutamate conditions suggests a nutrient limitation in the LMM fermentations. The only component in the medium that was lower in concentration in the LMM experiments, of course, was Mg. None of the other organic acids resulted in great enough culture OD to become Mg limited.

The growth kinetics were also similar for lactate-glutamate, succinate-glutamate and citrate-glutamate, with the former two reaching stationary phase after 12-14 h and citrate-glutamate reaching stationary phase at approximately 12 h. The acetate-glutamate/LMM and acetate-glutamate/MLM did not reach stationary phase until approximately 25 and 28 h, respectively. The maximum specific growth rate for each culture was calculated based on the following equation: $\mu_{\max} = \frac{(\ln(OD_2) - \ln(OD_1))}{(t_2 - t_1)}$. Where μ_{max} was maximum specific growth rate, OD_1 and OD_2 were optical density corresponding to timepoints, t_1 and t_2. The μ_{max} was similar for lactate-glutamate and succinate-glutamate runs with an average value of 0.32 h^{-1}. Citrate-glutamate had a mean maximum growth rate of 0.24 h^{-1}. Interestingly, acetate-glutamate runs similarly yielded a μ_{max} of 0.25 h^{-1}, even though acetate-glutamate cultures achieved remarkably high optical densities.

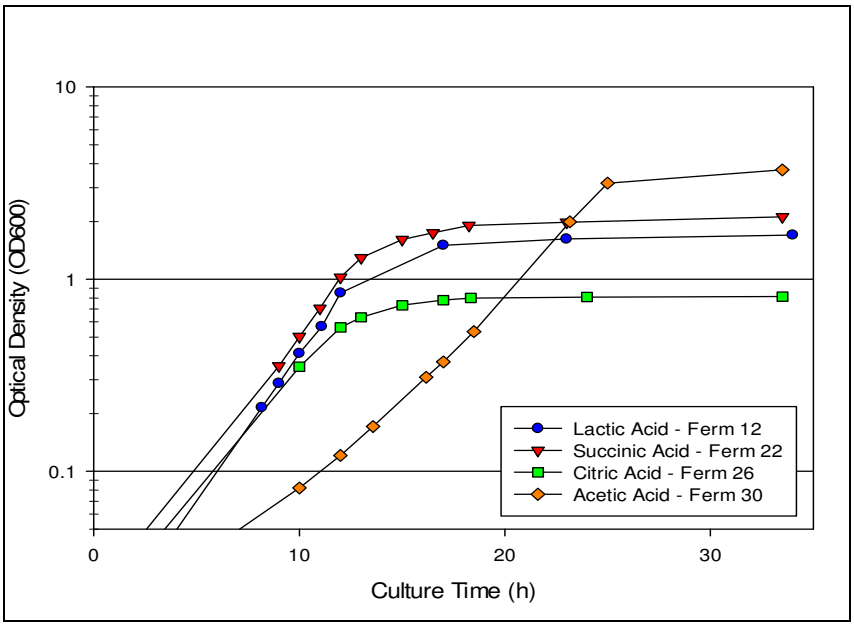

Figure 11: Growth curves for organic acid – glutamate carbon source combinations using medium concentrations of 0.1 mM Mg/1.0 mM SO_4/32.5 µM nicotinic acid.

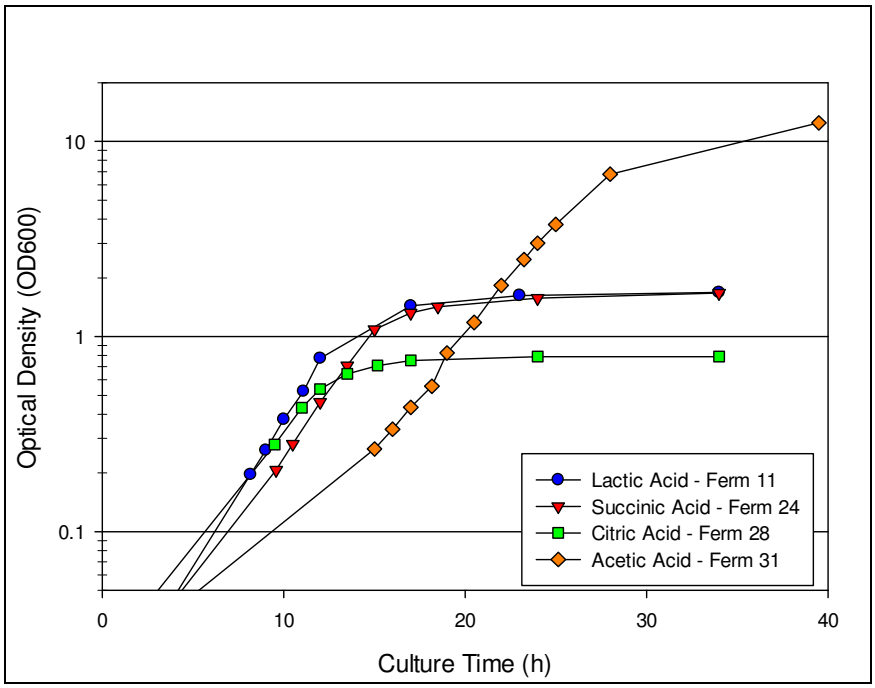

Figure 12: Growth curves for organic acid – glutamate carbon source combinations at using medium containing 1.0 mM Mg/0.1 mM SO_4/32.5 µM nicotinic acid.

Dissolved Oxygen

Figure 13 and 14 show dissolved oxygen profiles generated during fermentation processes. As previously noted, increased biomass concentration causes an increase in oxygen

demand and therefore a decrease in DO. No LMM fermentation, regardless of organic acid used, was oxygen limited during growth (Figure 13). The LMM fermentation condition which required the most oxygen was acetate-glutamate. Dissolved oxygen demand observed during cultivation was similar for succinate-glutamate and lactate-glutamate organic acid combinations, while citrate-glutamate required the least amount of oxygen. Observations confirm a correlation between increased biomass (OD) and increased oxygen demand.

Figure 14 shows the DO profiles for each MLM organic acid-glutamate combination. The citrate-, lactate-, succinate- combinations for MLM were similar to the experiments using LMM: citrate-glutamate experiments required the least oxygen, and lactate-glutamate and succinate-glutamate fermentations again were similar to each other. However, the acetate-glutamate/MLM DO profile behaved differently from acetate-glutamate/LMM. Specifically, the acetate-glutamate/MLM experiments became oxygen limited at 27 h. Other processes were performed using constant air aeration (400 mL/min) and agitation (500 RPM). For the acetate-glutamate/MLM experiment, when the DO reached 0% DO (27 h) the agitation was increased from 500 to 700 RPM, which increased aeration and hence the value of DO measured (Figure 14). The culture then continued to consume oxygen at a progressively greater rate (as measured by the slow decrease in DO) until 29.5 h, at which time the measured DO increased suddenly. This DO increase at 29.5 h correlated with the maximum OD, and is consistent with the exhaustion of a required nutrient.

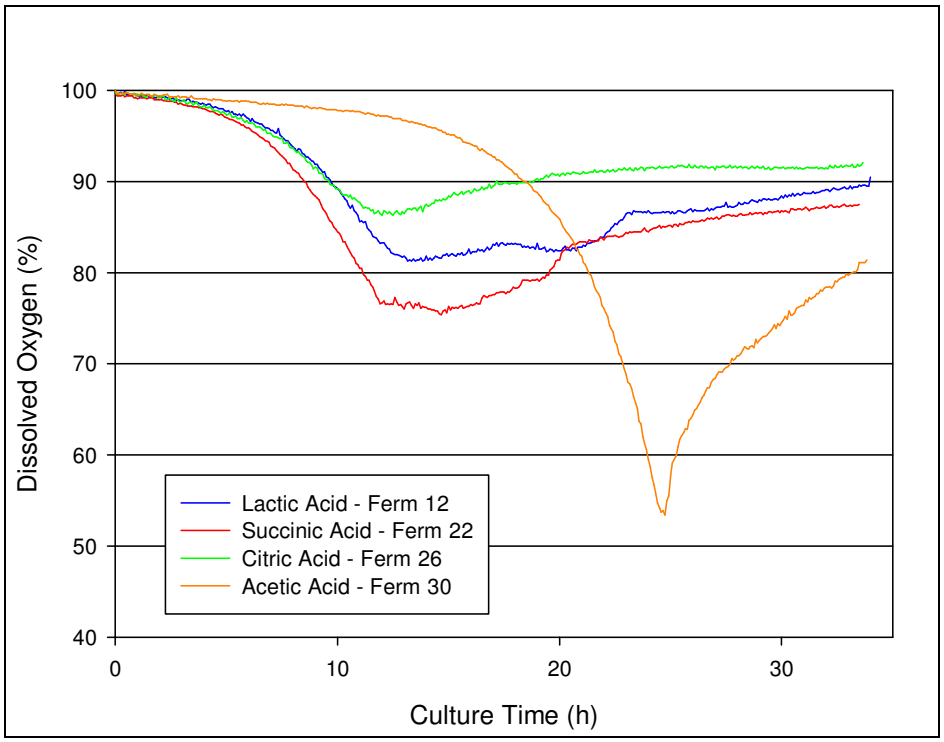

Figure 13: Dissolved oxygen for organic acid–glutamate carbon source combinations using medium containing 0.1 mM Mg/1.0 mM SO_4/32.5 µM nicotinic acid.

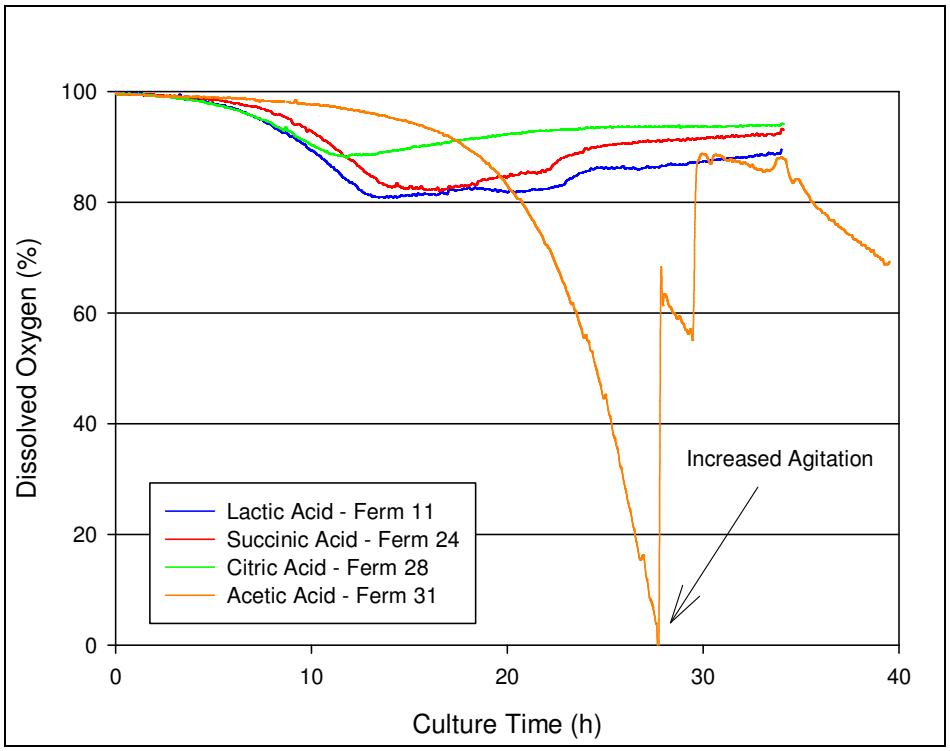

Figure 14: Dissolved oxygen for organic acid–glutamate carbon source combinations using medium containing 1.0 mM Mg/0.1 mM SO_4/32.5 µM nicotinic acid.

Substrate Utilization

Figures 15 and 16 show glutamate utilization during the fermentation processes. Lactate-glutamate and succinate-glutamate each consumed glutamate similarly, regardless of Mg/SO_4/nicotinic acid concentrations. In both cases slightly less glutamate was consumed for MLM (mean 25 mM) compared to LMM (28 mM). The least amount of glutamate (mean of 10 mM) was consumed for the citrate-glutamate experiments. Acetate-glutamate/LMM utilized about 28 mM acetate, a similar amount to lactate and succinate. This result is unexpected considering the difference in biomass generated between these three conditions: acetate (OD 3.63); lactate (OD 1.67), succinate (OD 1.71). In other words for the same amount of glutamate consumed, growth on acetate led to twice as much biomass compared to growth on either lactate or succinate. *B. bronchiseptica* may have an affinity for acetate utilization over lactate and succinate for biomass generation while glutamate is being consumed. All glutamate was depleted during the acetate-glutamate/MLM experiments. Although the glutamate concentration was measured to be 0 mM at 39.5 h, this compound was likely depleted by 30 h, consistent with the increase in DO observed at approximately this time (Figure 14).

Figure 17 and 18 show glutamine concentration during cultivation. Lactate-glutamate and succinate-glutamate consumed similar amounts of glutamine regardless of Mg/SO_4/nicotinic acid concentrations. For these conditions glutamine depletion most likely occurred around 25 h. Citrate-glutamate used the least amount of glutamine, consuming approximately one-third the amount. Acetate-glutamate/LMM consumed a similar amount of glutamine as the lactate- and succinate- experiments although in these cases over 1 mM remained at the end of the cultivations. Similar to glutamate utilization, this suggests *B. bronchiseptica* may have an affinity for acetate utilization for biomass generation, over lactate and succinate. Acetate-

glutamate/MLM consumed all available glutamine by 28 h. Thus, at the time the DO increased (about 29 h), both glutamate and glutamine were depleted.

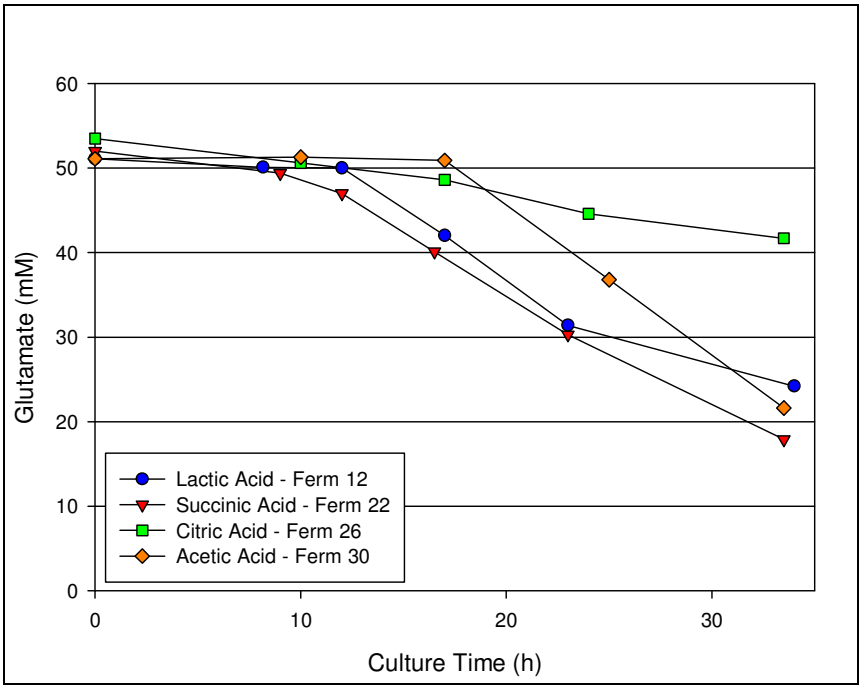

Figure 15: Glutamate concentration for organic acid–glutamate carbon source combinations using medium containing 0.1 mM Mg/1.0 mM SO_4/32.5 µM nicotinic acid.

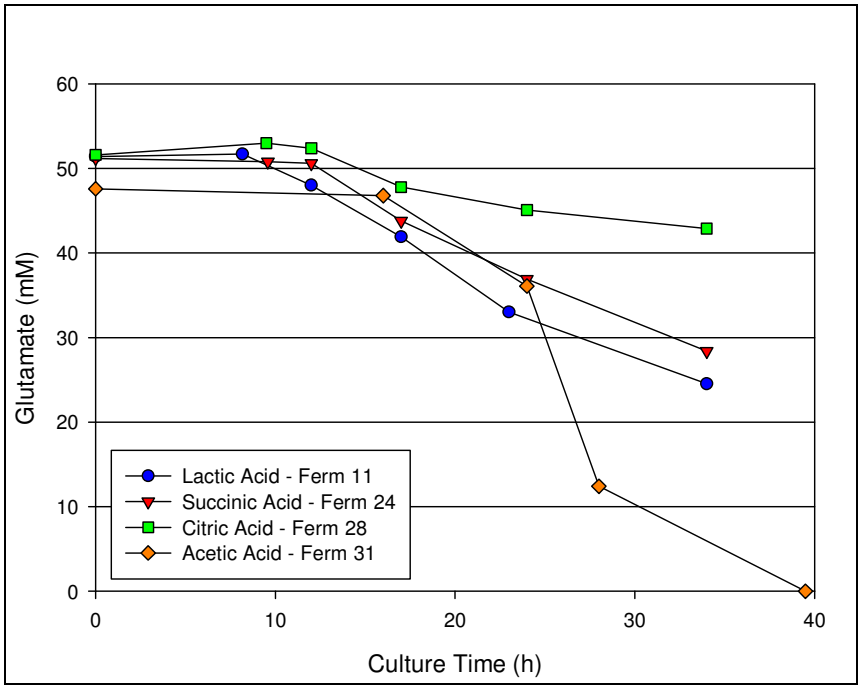

Figure 16: Glutamate concentration for organic acid–glutamate carbon source combinations using medium containing 1.0 mM Mg/0.1 mM SO_4/32.5 µM nicotinic acid.

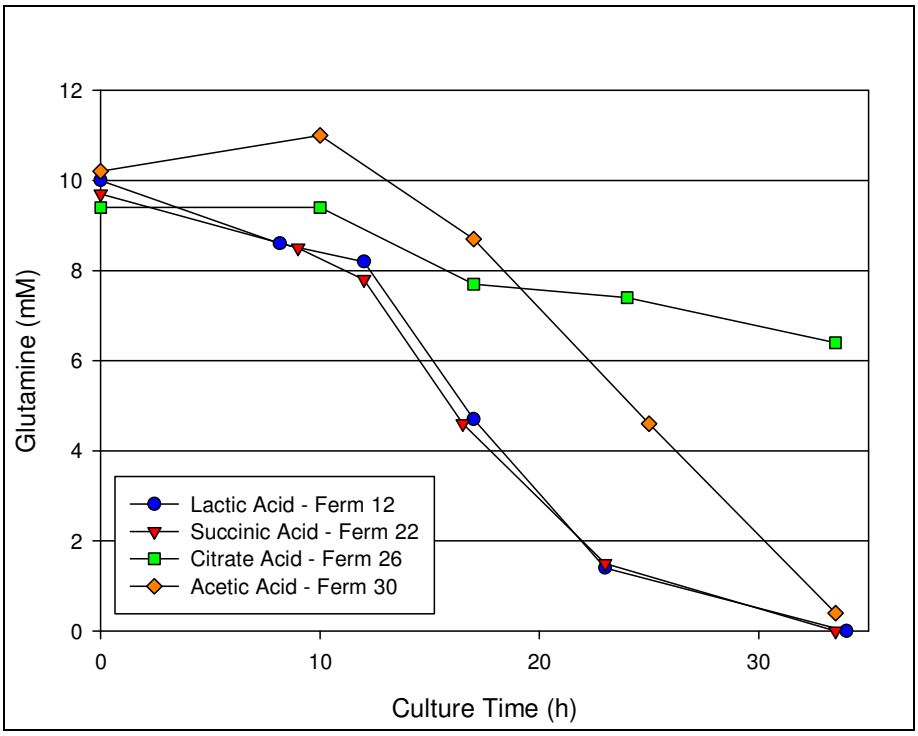

Figure 17: Glutamine utilization for selected organic acid–glutamate carbon source combination at 0.1 mM Mg/1.0 mM SO_4/32.5 µM nicotinic acid concentrations

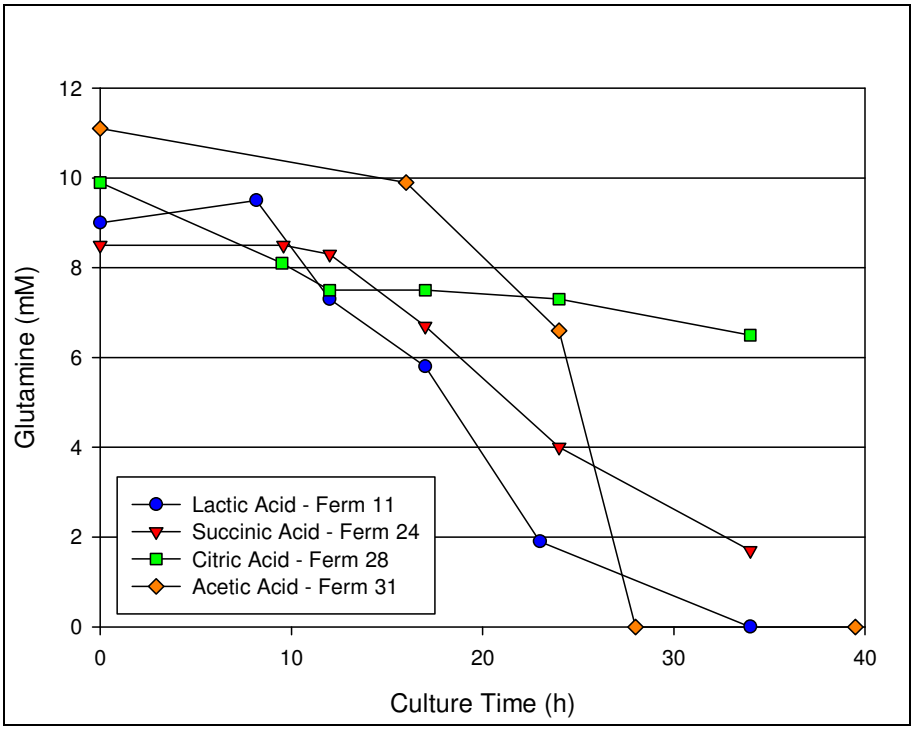

Figure 18: Glutamine utilization for selected organic acid–glutamate carbon source combination at 1.0 mM Mg/0.1 mM SO_4/32.5 µM nicotinic acid concentrations

Organic Acid Utilization

In addition to growth characteristics, organic acids used in each experimental condition were evaluated for utilization, as well as their impact on the C:N balance in the medium. Figures 19-22 display the residual concentration of organic acid in CDM (closed symbols) as well as the total amount of organic acid added (open symbols) for selected fermentation conditions. Since the fermentations were supplemented with additional organic acid by pH regulation, the feed was dependent on the pH control loop and the demand for acid.

Figure 19 represents one replicate of each lactate-glutamate condition. On average, lactate-glutamate consumed 4.8 g (LMM) and 5.1 g (MLM) lactate over the entire fermentation. The greatest rate of pH feed occurred during exponential growth, while greatest consumption of lactate occurred during stationary phase. Lactate utilization was similar for the two Mg/SO_4/nicotinic acid conditions. Figure 20 is an example of succinate-glutamate process condition. Succinate utilization was similar to lactate; consuming 5.3 g (LMM) and 4.8 g (MLM) succinate. Again, the greatest rate of pH feed occurred during exponential growth, with greatest consumption during stationary phase. The least utilization of an organic acid was found in the citrate-glutamate experiments (Figure 21), with only about 1.5 g citrate consumed in all cases. Acetate-glutamate/LMM also consumed very little organic acid, 1.3 g, while the acetate-glutamate/MLM batches consumed 7.1 g acetate (Figure 22).

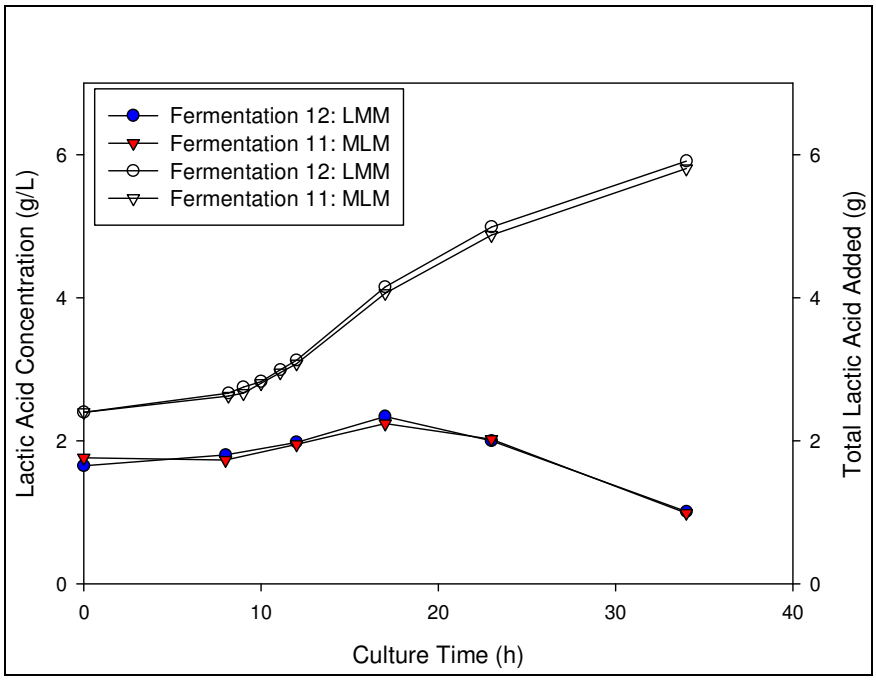

Figure 19: Total lactate added and residual lactate detected for lactate–glutamate carbon source combination at LMM and MLM Mg/SO_4/nicotinic acid concentrations.

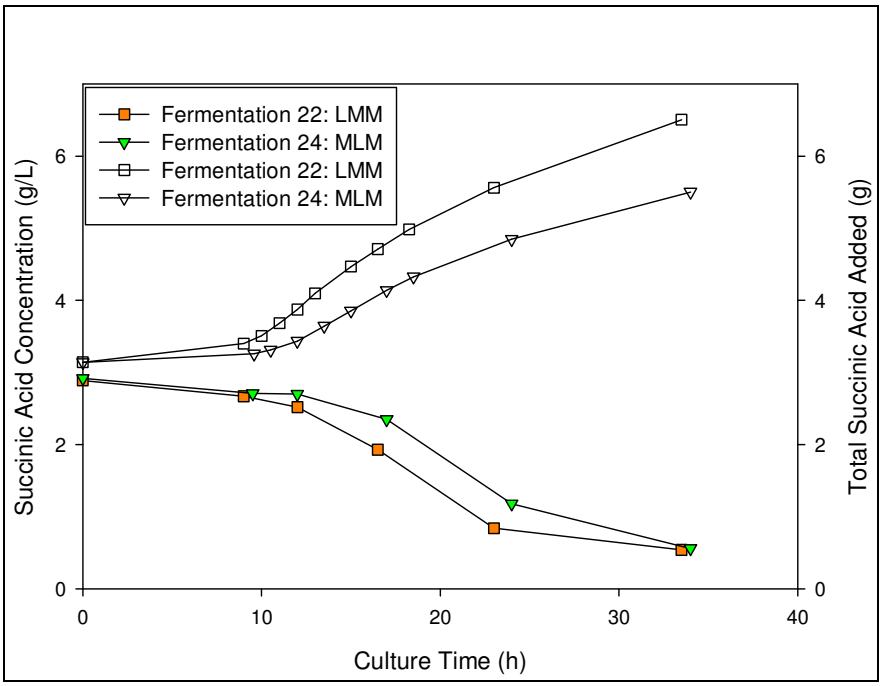

Figure 20: Total succinate added and residual succinate detected for succinate–glutamate carbon source combination at LMM and MLM Mg/SO_4/nicotinic acid concentrations.

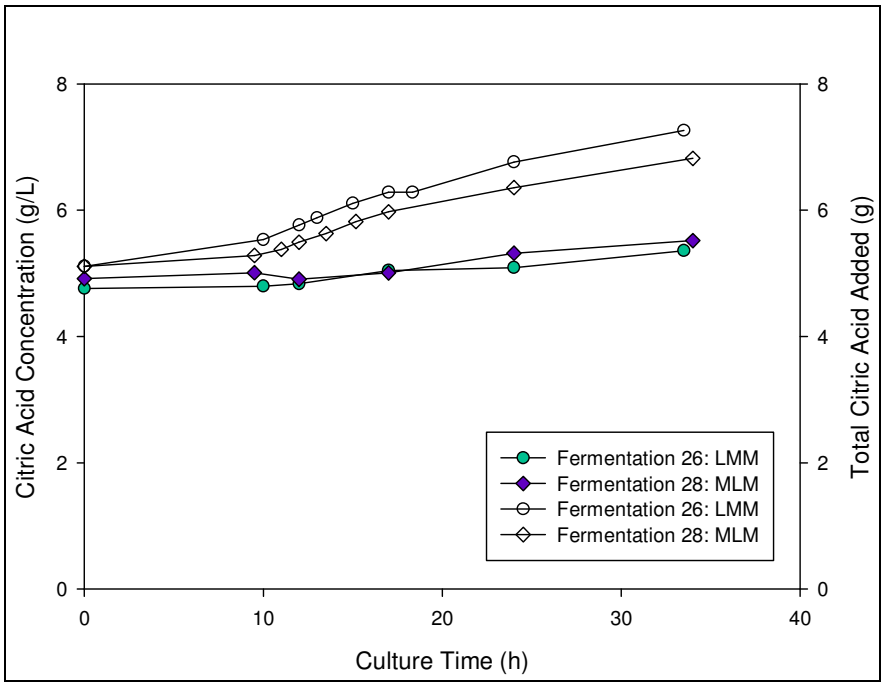

Figure 21: Total citrate added and residual citrate detected for citrate-glutamate carbon source combination at LMM and MLM Mg/SO_4/nicotinic acid concentrations.

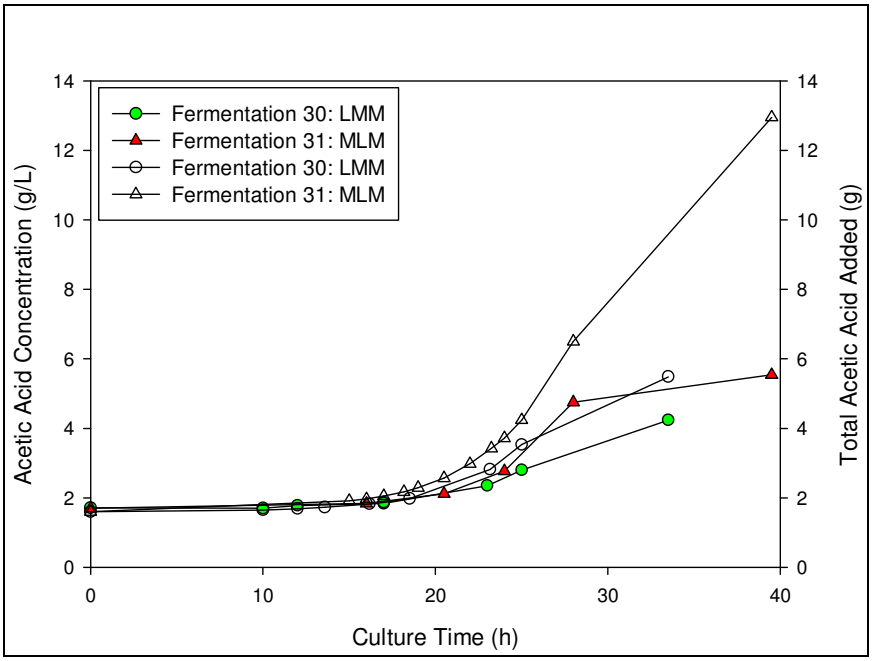

Figure 22: Total acetate added and residual acetate detected for acetate–glutamate carbon source combination at LMM and MLM Mg/SO_4/nicotinic acid concentrations.

Table 9 lists the C:N ratios based on total secondary organic acid added by pH regulation over the entire fermentation. All fermentations achieved C:N ratio of nearly 8 with the exception

of acetate-glutamate/MLM condition which achieved a ratio of ~12. These were similar C:N values explored by Thalen et al. (1999).

Table 9: End of cultivation C:N ratio for 0.1 mM Mg/1.0 mM SO_4/32.5 μM nicotinic acid and 1.0 mM Mg/0.1 mM SO_4/32.5 μM nicotinic acid conditions for each organic acid.

Secondary Carbon Source	C:N Ratio: LMM Condition	C:N Ratio: MLM Condition
Lactate	8.00 - 8.18	8.12 – 8.43
Succinate	7.95 – 8.58	8.01 – 8.02
Citrate	8.54 – 8.68	8.45 – 8.55
Acetate	7.78 – 7.95	11.84 – 12.10

Table 10 lists the total amount of secondary organic acid consumed over the entire fermentation. Lactate-glutamate and succinate-glutamate conditions consumed similar amounts of primary carbon (glutamate) as well as secondary carbon source. Both conditions had similar growth kinetics. Not surprising, citrate-glutamate consumed the least amount of carbon, while acetate-glutamate/MLM consumed the greatest amount. Acetate-glutamate/LMM may have consumed a greater amount of acetate if not for Mg limitation.

Table 10: Concentration of organic acid consumed for 0.1 mM Mg/1.0 mM SO_4/32.5 μM nicotinic acid and 1.0 mM Mg/0.1 mM SO_4/32.5 μM nicotinic acid conditions for each organic acid.

Secondary Carbon Source	mmol Consumed LMM Condition	mmol Consumed MLM Condition
Lactate	45.6 – 47.6	47.8 – 64.9
Succinate	39.0 – 50.9	39.1 – 41.5
Citrate	7.2 – 9.7	6.9 – 8.3
Acetate	21.3 – 23.1	111.4 – 124.2

FHA Production

In addition to growth characteristics and nutrient utilization, the 12 new batch fermentations were evaluated for FHA production and compared with lactate-glutamate conditions previously tested. For each experiment, five samples were analyzed for total FHA and specific FHA concentrations. The five samples were evaluated: 8-10 h, 12 h, 16-17 h, 23-24 h, and 32-34 h for lactate-glutamate, succinate-glutamate, and citrate-glutamate. Acetate-

glutamate/LMM was sampled at 12, 17, 23, 25, and 33.5 h, while acetate-glutamate/MLM was sampled at 16, 20.5, 24, 28, 39.5 h. Sample times correspond to early exponential growth, late exponential growth, early stationary phase, middle stationary phase, and end of culture late stationary phase. Figure 23 shows average FHA concentration for each fermentation condition. Generally, the greatest FHA concentrations were observed at early stationary phase, with a decline in concentration by the end of culture. This result suggests that FHA production was growth associated, and confirmed a similar trend observed in FHA production in previous experiments. By investigating specific FHA production, on a per OD unit basis (Figure 24), a decline in FHA concentration was observed during the fermentation process, supporting previous experiment observations and possibly due to proteolytic activity previously discussed in Chapter 2.

Succinate-glutamate and lactate-glutamate conditions produced similar amounts of FHA: 652 ng/mL (MLM) and 695 ng/mL (LMM) for lactate-glutamate; 593 ng/mL (MLM) and 717 ng/mL (LMM) for succinate-glutamate. Citrate-glutamate generated the least FHA at 410 ng/mL (MLM) and 340 ng/mL (LMM). Acetate-glutamate produced the greatest overall amount at 1,170 ng/mL (MLM) and 1,010 ng/mL (LMM). The greatest values were generated during exponential growth or early stationary phase.

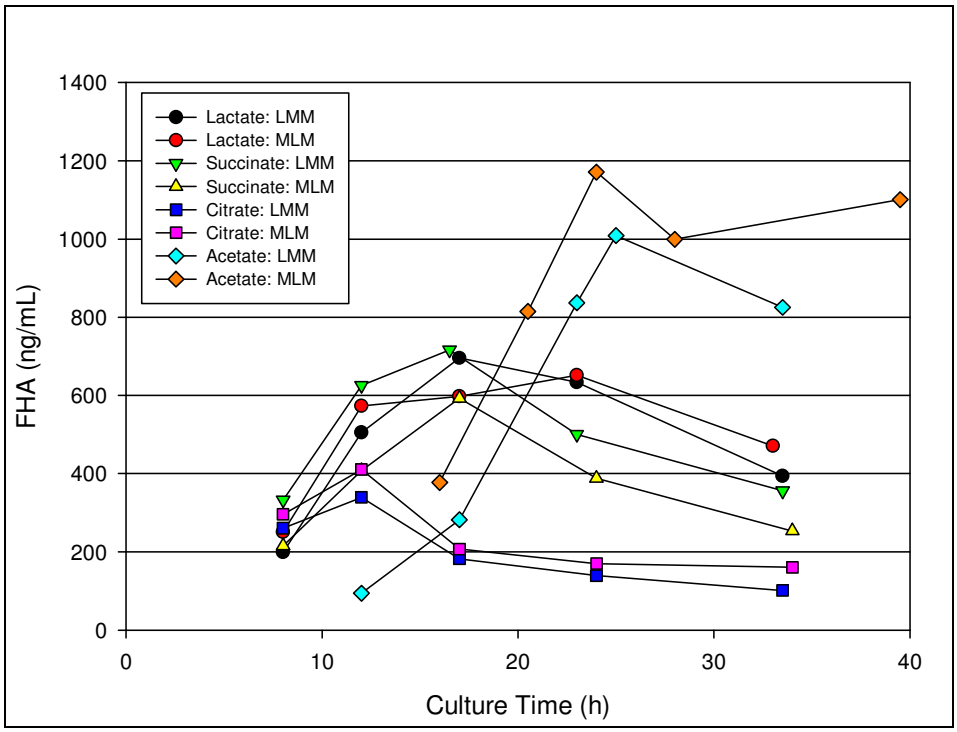

Figure 23: Average FHA production for selected organic acid–glutamate carbon source combination at LMM and MLM Mg/SO_4/nicotinic acid concentrations

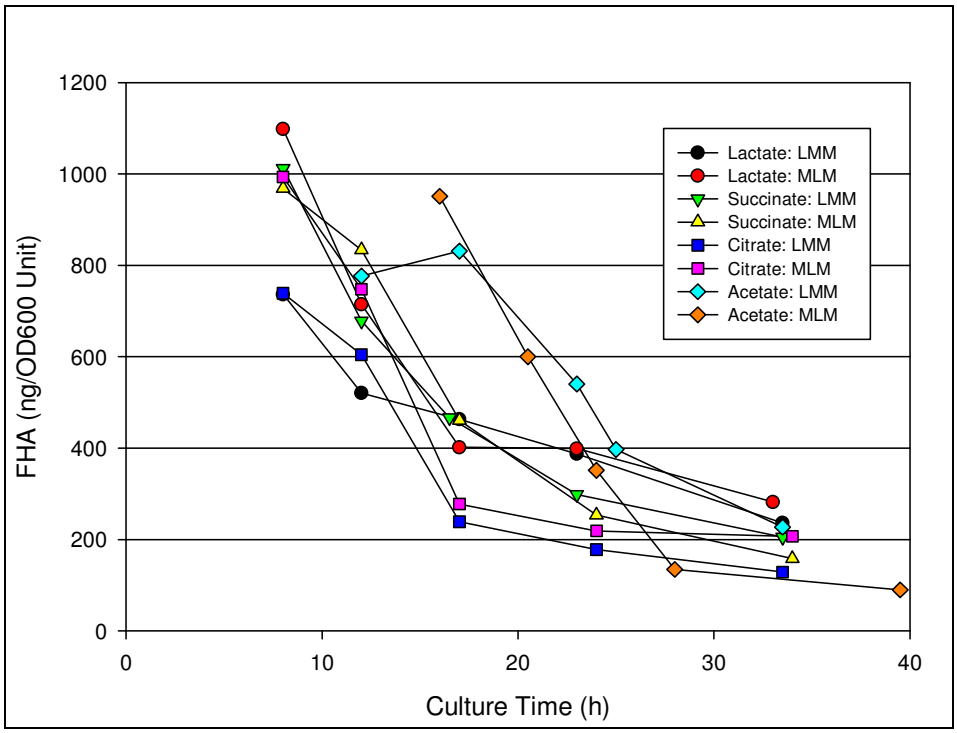

Figure 24: Average specific FHA production for selected organic acid–glutamate carbon source combination at LMM and MLM Mg/SO_4/nicotinic acid concentrations**.** Normalized per OD_{600} unit

Concluding Remarks

FHA expression

Similar to the results described in Chapter 2, we observed a decline in FHA expression after measuring greatest concentration during early stationary phase. Primary reasons for decreased FHA expression could be: 1) cell decreases expression levels in response to culture conditions; 2) protein secretion adversely affected by culture conditions; or 3) protein degradation due to proteolytic activity. Culture conditions, in respect to known modulators, should not affect expression levels only later in growth. This seems reasonable considering our observation that 10 mM SO_4 was detrimental to FHA expression throughout the entire fermentation. Protein secretion due to changing ionic concentrations was also an unlikely explanation. Frohlich et al. (1995) found that specific toxin yields did not correlate with medium's ionic concentration; therefore this does not explain decreased toxin production. Proteolytic activity was likely responsible for decreased FHA during stationary phase. Several studies have investigated the formation and degradation of pertussis toxin during cultivation (Thalen et al., 2006a, Thalen et al., 2006b, Peppler et al., 1985). Thalen et al. (2006a) showed that pertussis toxin was growth associated. However, they found that toxin production terminated before growth concluded. They suggest this may be a consequence of regulatory mechanism rather than a result of medium composition or metabolism. The decreased FHA concentration may also be due to natural protein degradation and unfolding during stationary growth. A gradual decline in concentration is observed in all conditions during stationary phase, that is protein may be degraded at 35 °C over 15-20 h.

Interestingly, acetate-glutamate condition displayed a shift to Bvg^- colonies (qualitative) when compared to other conditions (Figure 25). The 39.5 h plate for the acetate-glutamate/MLM

showed the greatest amount of Bvg^- colonies. An O_2 limitation may have impacted the Bvg phase presented. Cotter and Miller (1994, 1997) reported that environmental stress can cause a shift in phenotype.

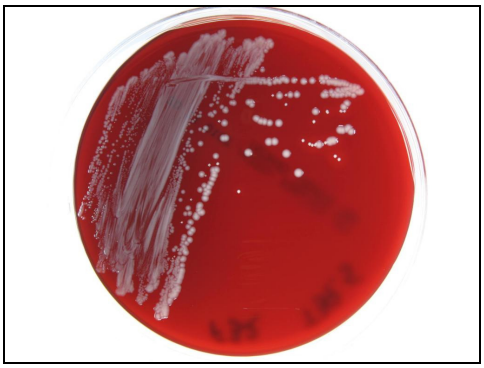

Figure 25: Fermentation 32 - MLM: Example of Bvg^- phenotype using acetate as the secondary carbon source

Growth Characteristics

A gradual deceleration in growth rate until stationary phase was observed between 12 and 16 h for lactate-glutamate, succinate-glutamate, and citrate-glutamate conditions. A similar growth characteristic was observed for *B. pertussis* by Frohlich et al. (1995). Growth rate deceleration was not observed for acetate-glutamate/MLM condition. After confirming no nutrient limitation, major protein inhibition or ammonium inhibition, Frohlich et al. (1995) discovered higher salt concentration had an effect on cell growth rate, but only in later stages of batch growth and did not affect the initial growth rate. Although salt concentration could be a reason for decreased growth in our experiments, the medium used was designed for and considered optimal for growth rate, expression, and proteolytic activity. A minor byproduct may have been autoinhibitory in *Bordetella* cultivation. Frohlich et al. (1996) explored this possibility and found that free fatty acids, specifically palmitic, palmitoleic, and stearic acids, caused autoinhibition in *B. pertussis*. Although not tested, it is possible we are seeing a similar effect in *B. bronchiseptica*.

Organic Acid Utilization

Thalen et al. (1999) found that acetate-glutamate and citrate-glutamate carbon source combinations were not metabolized by *B. pertussis*. This was concluded by comparing growth curves and DCW between glutamate only and acetate-glutamate or citrate-glutamate. The growth data was not provided, however, they observed biomass yields of ~20 IOU (1 OD_{590} = 20 IOU) with glutamate only. Additionally, they reported lactate-glutamate and succinate-glutamate achieved IOU of ~30 and 25, respectively. Although we did not test glutamate alone, the present experiments did show growth in the presence of either citrate or more significantly in the presence of acetate. Thalen et al. (1999) also found that pyruvate (19.4 and 25 mM), when combined with glutamate, was detrimental to the cell. They suggest that this concentration interferes with normal cellular metabolism. Interestingly, we observed a decrease in growth rate and biomass with citrate-glutamate conditions. It is possible we are seeing a similar effect with citrate. Citrate is in effect toxic to the cell.

Other potential explanations for decreased citrate utilization could be limited diffusion into the cell or *B. bronchiseptica* metabolizes the 6 carbon organic acid at a slower rate than the others tested. Generally, we see organic acid utilization increases as the total number of carbon atoms decrease. For MLM condition, the mM of organic acid consumed from greatest to least are: acetate (2 C organic acid), lactate (3 C), succinate (4 C), and then citrate (6 C). Another question one must ask is, Is *B. bronchiseptica* unable to utilize citrate like impaired *B. pertussis*? From an evolutionary stand point this is plausible, since *B. pertussis* lineage in derived from a *B. bronchiseptica*-like ancestor (Parkhill et al., 2003). Though these observations are interesting, it was considered outside the scope of this work and we concluded citrate was not a suitable organic acid carbon source.

Another interesting observation was acetate-glutamate/LMM did not consume acetate during the stationary phase. All other acid-glutamate combinations continued to consume organic acid at a greater rate during stationary phase. As this was the only condition during which nutrient limitation was suspected, perhaps the nutrient limitation was critical to organic acid transport and metabolism. Both acetate-glutamate conditions, revealed an unknown byproduct during HPLC analysis. The HPLC method quantifies a range of acids including acetic, butyric, citric, formic, fumaric, isobutyric, α-ketoglutaric, lactic, malic, propionic, pyruvic, succinic, and uric acids (Eiteman and Chastain, 1997). The unknown peak eluted at 11.0 min and generated an area greater than 161,000 for acetate, whereas lactate, succinate, and citrate experiments resulted in areas less than 10,000.

Thalen et al. (1999) selected lactate-glutamate because they observed a 30% higher cell yield over succinate, α-ketoglutarate, or fumarate. In contrast, our results indicate succinate-glutamate yielded very similar growth and FHA to lactate-glutamate. Also, lactate-glutamate resulted in no metabolite excretion when present at 1.6:1 molar ratio, and there was a net consumption of NH_4 instead of accumulation and possible inhibitory effects (Thalen et al., 1995). *B. pertussis* was able to redistribute NH_4 from glutamate to other cellular compounds synthesized from lactate. Even though we found similar results between lactate and succinate, we chose lactate-glutamate for further investigation because this has been literature's primary focus. Acetate-glutamate was also selected for further investigation as this condition yielded the greatest FHA production and biomass generation.

CHAPTER 4

STEADY-STATE CULTURE OF BORDETELLA BRONCHISEPTICA

Introduction

The traditional approach for studying microbial physiology, metabolism, and expression of virulence factors has been in batch type cultures. Batch cultures can be accomplished by a variety of sizes, techniques, and may include regulating pH, dissolved oxygen, temperature, aeration, and mixing. A disadvantage of the batch culture is the microbial environment is continuously changing. Growth, product formation, and substrate utilization terminate after some time period. These obstacles may be overcome through the use of a continuous flow stirred tank reactor (CSTR). In a continuous culture, fresh nutrient medium is supplied to a well-mixed culture, while cells, products, and unutilized nutrients are concurrently withdrawn. A specific type of CSTR which is commonly used is the chemostat or "chemically static" process.

The key variable which constrains and defines a chemostat system is the dilution rate. The dilution rate, D, is described by the equation: $D = \frac{F}{V} = \mu$. Here, F is nutrient feed rate, V is constant volume of culture, and μ is growth rate. From this equation, growth rate can be easily controlled by changing the nutrient feed rate. Cell density will be determined by the feed concentration of a limiting nutrient. At steady state, cell, product, and substrate concentrations remain constant. By using a chemostat, effects of different growth limiting conditions on fermentation parameters (e.g., product accumulation) may be determined. Several studies have used steady-state conditions to investigate *B. pertussis* (Licari et al., 1991 and Frohlich et al., 1995). No investigations have been reported using chemostats to investigate *B. bronchiseptica*.

Our focus was to utilize this technique to investigate the effect of different growth rates, secondary carbon source, and nutrient limiting conditions (specifically Mg and S limitation) on biomass production and FHA expression.

Materials and Methods

Steady State Culture Process Conditions

Continuous fermentations of 1.0 L volume operated as chemostats were initiated in batch mode in a 2.0 L bioreactor (Applikon, Schiedam, Netherlands, see Figure 26 for schematic representation). Chemostat operation was performed with the same pH, DO, temperature, and aeration parameters described for batch fermentation with the exception of the Fe-limitation chemostat, which was performed at pH of 7.6 with 3 N HCl and temperature of 36°C. Two carbon source combinations, lactate-glutamate and acetate-glutamate, were selected for study. The specific dilution rate used is noted in Appendix E, either 0.1 or 0.075 h^{-1}. A steady-state condition was assumed after five residence times, and confirmed by observing stable oxygen and carbon dioxide concentrations in the effluent gas. The intended limiting nutrient for all chemostats were confirmed by spiking the culture at steady-state with 3-4X culture concentration of limiting nutrient. Any changes in OD, O_2 % and CO_2 % effluent were then monitored to assess nutrient limitation.

Batch Fermentation Media

A comparison of the chemostat media composition is shown in Table 11.

Analytical Methods

Optical Density, FHA ELISA, Carbon source, Morphology, and Analytes

Samples throughout fermentation process were analyzed as previously described in Chapter 2 and 3.

Dry cell weight

For DCW measurement, 40 mL of cell culture was centrifuged for 15 min at 10000 × g (9500 RPM in a Beckman Coulter J-model centrifuge with JA-20 fixed angle rotor), the supernatant decanted, the pellet washed with DI water and the tube centrifuged again at 15 min at 10000 × g (repeated one additional time). The pellet was resuspended in a small amount of water and poured into a (pre-weighed) weighing boat, making sure all the cells are added to the boat. The boat was dried at 60°C for 24 hours and re-weighed.

Effluent gas analysis

Effluent gas was analyzed for O_2 and CO_2 concentrations using an ABB Gas Analyzer Advance Optima, with the Uras 14 CO_2 module and Magnos 106 O_2 module (ABB, Cary, USA).

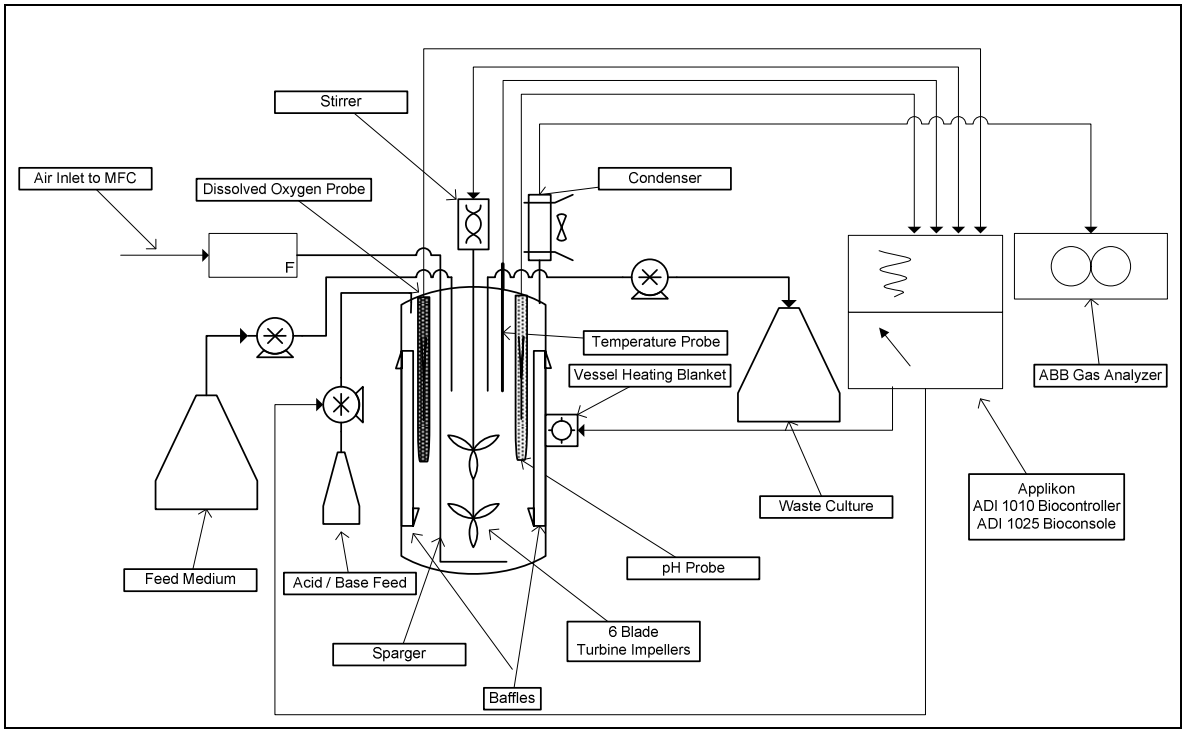

Figure 26: Schematic representation of chemostat fermentation

Table 11: Steady-state continuous culture CDM formulation

Components	Mg-Limited lactate-glutamate	S-Limited* lactate-glutamate	Mg-Limited acetate-glutamate	Modified S-Limited lactate-glutamate	Fe-Limited Licari et al. (1991)
	g/L	**g/L**	**g/L**	**g/L**	**g/L**
L-Glutamic Acid monosodium salt monohydrate (Aldrich 49621, Lot 0001380041)	10.700	10.700	10.700	10.700	17.000
L-Cysteine hydrochloride monohydrate (Sigma C-7880, Lot 32K0890)	0.500	0.053	0.500	0.018	0.040
L-Ascorbic Acid (Aldrich A92902, Batch 04308LC)	0.020	0.020	0.020	0.020	0.400
L-Glutathione, reduced (Sigma-Aldrich G4251, Lot 030M1775)	0.001	0.001	0.001	0.001	0.150
NaCl (Mallinckrodt 7532-20, Lot H50602)	1.040	1.040	1.040	1.040	2.500
KH_2PO_4 (Mallinckrodt 7096-06, Lot G43581)	0.500	0.500	0.500	0.500	-
KCl (Mallinckrodt 6838-06, Lot E48N94)	0.200	0.200	0.200	0.200	0.500
$CaCl_2$ (JT Baker 1311-01, Lot V45599)	0.020	0.020	0.020	0.020	0.020
Tris(hydroxymethyl)aminomethane (Sigma-Aldrich 252859, Batch 07705HH)	1.520	1.520	1.520	1.520	6.100
$FeSO_4 \cdot 7H_2O$ (JT Baker 2070-01, Lot C17H24)	0.010	0.010	0.010	0.010	0.001
$MgCl_2 \cdot 6H_20$ (Sigma-Aldrich M2670, Batch 028K00222)	0.008	0.020	0.008	0.020	0.100
K_2SO_4 (Sigma P8541, Lot 128K00992)	0.168	0.011	0.168	0.000	-
Nicotinic Acid (Sigma N0765, Batch 126K0693)	0.004	0.004	0.004	0.004	0.004
Lactic Acid, 85 % (JT Baker 0194-01, J11J03)	5.405	5.405	-	5.405	-
Acetic Acid (JT Baker 9522-02, Batch H31806)	-	-	3.603	-	-
Casamino Acids (BD 223050 Lot 0221441)	-	-	-	-	3.000
L-Proline (Sigma P5607-25G Batch 077K0009)	-	-	-	-	0.240

* Chemostat S-limitation was not valid. The sulfur concentration was amended for the Modified S-Limitation chemostat

Results and Discussion

A series of continuous cultures were performed using a variety of conditions to investigate the effect of different growth rates, secondary carbon source, and nutrient limiting conditions (specifically Mg and S limitation) on biomass production and FHA expression.

Mg and S Limited Chemostats

Two initial chemostats were performed using lactate as the secondary carbon source testing for Mg or S limitation. The lactate-Mg limited chemostat with a steady-state Mg concentration of 0.04 mM was demonstrated to be Mg-limited by spiking the culture with Mg, which increased the OD from 1.14 to 1.38, the effluent O_2 decreased from 20.60% to 20.31%, and the effluent CO_2 increase from 0.28% to 0.60% over 3 h. An initial lactate-S limited chemostat with a feed S concentration of 0.4 mM proved not to be S-limited after spiking the system with a cysteine/K_2SO_4 mixture: no change in OD, CO_2 or O_2 was observed. When the S concentration in the feed medium was modified to a concentration of 0.14 mM, the process was demonstrated to be S-limited after an increase in the feed S concentration increased the OD from 5.35 to 5.75, decreased the effluent O_2 from 19.98% to 19.29%, and increased the effluent CO_2 from 0.78% to 1.55% over 4 h.

Unexpectedly, FHA expression was lost over the course of each chemostat operation. An acetate-glutamate Mg-limited chemostat was performed to investigate an alternate secondary carbon source effect on FHA production. This chemostat also failed to produce FHA.

Fe-Limited Chemostat

Previous studies using *B. pertussis* showed that pertussis toxin production was growth associated, and a continuous culture had greater productivity than batch cultures (Licari et al., 1991). This chemostat experimental design was repeated using the RB50 strain of *B.*

bronchiseptica as a Fe-limited process with a few modifications: 1) heptakis (2,6-di-*O*-methyl)-β-cyclodextrin and kanamycin sulfate were removed from the medium, and 2) pH was controlled (at 7.6) with HCl instead of with H_2SO_4 to avoid known SO_4 phenotype shift. The chemostat was operated at 0.075 h^{-1}. Samples were taken at every residence time (13.3 h) for FHA analysis (Table 12).

Table 12: FHA expression during the unsteady-state portion of a continuous culture in Licari medium. (RT = residence time of 13.3 h)

Chemostat Phase	End of Batch Growth	RT 1	RT 2	RT 3	RT 5 (Steady State)
FHA (ng/mL)	485	733	0	0	0

FHA expression was lost between the first and second dilutions. These results were supported qualitatively by morphology observations: a phenotypic shift occurred to Bvg^- colonies at the second residence time. Brickman et al. (2011) have recently investigated the role of Fe limitation and its effect on virulence gene expression. They reported that Fe starvation is not related to increased expression of Bvg-dependent virulence genes; however iron limitation may be an important host environmental signal which triggers mechanisms to obtain essential Fe and informs the organism of host arrival and subsequent virulence factor expression. Although the Fe spike to chemostat culture caused a slight increase in OD, it is possible the culture was not Fe limited, since glassware was not acid rinsed prior to use.

Irie et al. (2004) and Kuchma et al. (2005) suggest quorum sensing may impact virulence phase and gene expression in *Bordetella* spp. However, the focus is primarily on biofilm formation and its link to pathogenesis regulation. Perhaps this phenomenon is impacting FHA expression.

These chemostat results were compared with Frohlich et al. (1995) and Licari et al. (1991) who both reported on *B. pertussis* chemostat experiments. Frohlich reported steady-state cell concentrations were no higher than 6 to 8 OD_{530} corresponding to 2.0-2.7 g/L DCW, higher than observed presently for *B. bronchiseptica* (OD_{600} between 1.14 and 5.32 and DCW of 0.63-1.78 g/L). Licari reported a specific substrate utilization rate (Q_E, g glutamate/g DCW·h for glutamate as a function of specific growth (μ, h^{-1}) rate for *B. pertussis* as:

$$Q_E = 0.01 + 4.65(\mu)$$

Based on Licari's experimental data, *B. pertussis* had specific glutamate utilization rate of 0.36 g glutamate (g DCW·h)$^{-1}$ at a specific growth rate of 0.075 h^{-1}. Fe-limited *B. bronchiseptica* chemostat had a specific glutamate utilization rate of 0.14 g glutamate (g DCW·h)$^{-1}$. Licari also reported the true growth yield of cells on glutamate as 0.22 g DCW/g glutamate for *B. pertussis* with a maintenance requirement of 0.01 g glutamate/g DCW·h. Fe-limited *B. bronchiseptica* chemostat had an observed growth yield of cells on glutamate of 0.54 g DCW/g glutamate.

It is important to note that both Licari and Frohlich used a mutant strain of *B. pertussis*, SK101 mod(-). They used this strain based on its resistance to antigenic modulation. The phenotypic shift, as previously described, results in a loss of virulence factors. Cotter and Miller (1994, 1997) investigated nutrient limitation using the *B. bronchiseptica* RB50 strain. They showed the organism's ability to survive under nutrient limiting conditions, however, wild-type *B. bronchiseptica* shifts to the Bvg^- phase while under stress. They also showed the genetically modified, for Bvg^+ phase, strain had the ability to spontaneously form Bvg^- phase mutants under nutrient limitation. Typically, the modulation occurred within two days (Cotter and Miller 1994). This phenomenon is likely occurring in the present chemostat experiments, since nutrient limitation is a requirement. The use of a wild-type *B. bronchiseptica* RB50 has demonstrated a

shift to avirulent Bvg$^-$ phase resulting in a complete loss of expression of FHA protein. As a result, chemostat technique for culture analysis was not a useful tool for further investigation. Further chemostat experimentation would require the use of a mutant or genetically modified strain of *B. bronchiseptica*.

CHAPTER 5

FED-BATCH FERMENTATION INVESTIGATION

Introduction

The development of acellular *B. pertussis* vaccines has resulted in the need for higher virulence factor yield per fermentation. Virulence factors associated with acellular vaccines are required in greater concentration than whole cell vaccines. Acellular *B. pertussis* vaccines require 5-25 times pertussis toxin and 2-3 times FHA, pertactin, and fimbriae (Thalen et al., 2006a). In order to increase fermentation capacity, to offset the increase yield demand, fed-batch cultivation of *B. pertussis* has been investigated as a potential solution (Thalen et al., 2006a). This logic could also be applied to traditional batch fermentation for whole cell vaccine production. By implementing and optimizing fed-batch fermentation for *B. bronchiseptica*, higher cell densities and product concentrations may be achieved.

Thalen et al. (2006a) completed a study investigating the feed composition and feed rate to increase yield in fed-batch fermentation for *B. pertussis.* They investigated a feed medium of 0.51 M glutamate and 0.855 M lactic acid fed simultaneously at the same volumetric rate, either 10 mmol C $L^{-1}h^{-1}$ or 45 mmol C $L^{-1}h^{-1}$. They observed cell density yields of 8.2 OD_{590} for low feed rate versus 3.3 OD_{590} for the high feed rate. Both feed rates generated greater biomass compared to batch cultures (typically OD_{590} = 2.0). However, this low feed rate fermentation only produced a 30% higher pertussis toxin yield, suggesting the toxin produced is not directly related to the amount of biomass.

Thalen et al. (2006a) also investigated the use of exponential feed rate fed-batch fermentation. They investigated three growth rates, μ=0.11, 0.09, and 0.07 h^{-1}. The corresponding OD_{590} achieved were 7.3, 5.9, and 13.6, respectively. Interestingly, cultures grown at 0.11 h^{-1} contained unused substrates in the medium throughout the fermentation, even though the culture did not grow at the maximum growth rate of 0.16 h^{-1}. Substrates were also observed after 25 h of growth for 0.09 h^{-1} growth rate condition. They concluded 0.11 and 0.09 h^{-1} growth rates were too high to maintain fed-batch fermentation. A possible explanation proposed was increased Na concentration due to the Na-glutamate feed. An additional study reported the maximum growth rate of *B. pertussis* depended on Na concentrations (Thalen et al., 2006b).

Materials and Methods

Two fed-batch fermentations were performed. The first utilized a dual feed by taking advantage of pH control loop in addition to a constant rate feed. A 1 M acetate/1 M HCl solution was used to maintain pH, where a 400 mM Na glutamate/1.4 mM $MgCl_2 \cdot 6H_2O$/1 mM K_2SO_4 mixture was fed at a constant rate of 5 mL/h after 20 h of batch growth. The constant feed rate of Na-glutamate corresponds to the low feed rate regime of 10 mmol C $L^{-1}h^{-1}$ used by Thalen et al. (2006a), but does not include the additional carbon from acetate in the pH-control feed. The second fed-batch fermentation utilized only the pH control loop to supply 1 M acetate,/400 mM L-glutamic acid (Sigma G-8415, Batch 50K0335)/1.5 mM $MgCl_2 \cdot 6H_2O$, for a pH control feed slurry.

Fed-Batch Process Conditions

Constant feed rate fed-batch fermentation was initiated with 1.0 L medium in a 2.0 L bioreactor (Applikon, Schiedam, Netherlands, see Figure 27 for schematic representation) in

batch mode for approximately 20 h. Then, fed-batch operation was commenced by feeding a nutrient solution at a constant flow rate of 5 mL/h. The feed contained 400 mM Na glutamate, 1.4 mM $MgCl_2 \cdot 6H_2O$, and 1 mM K_2SO_4, and used a 50:50 mixture of 1 M acetate and 1 M HCl for pH regulation. A subsequent pH loop controlled fed-batch used 1 M acetate, 400 mM L-glutamic acid (Sigma G-8415, Batch 50K0335), and 1.5 mM $MgCl_2 \cdot 6H_2O$ for a pH control feed slurry.

The fed-batch process was carried out at 35°C, a pH of 6.9, a constant agitation of 500 RPM, and DO was regulated at greater than 30%. An AppliSens DO sensor (Applikon, Schiedam, Netherlands) measures the dissolved oxygen in the medium and an AppliSens pH sensor (Applikon, Schiedam, Netherlands) measures pH. Temperature was measured with a Pt100 temperature sensor (Applikon, Schiedam, Netherlands). Cells were aerated by constant sparged air at a constant 400 mL/min controlled by mass flow controller (Aalborg, Orangeburg, USA, model GFC17) and supplemented with pure O_2, utilizing DO control loop, to prevent oxygen limited growth. All sensors were connected to an ADI 1010 Biocontroller with ADI 1025 Bioconsole (Applikon, Schiedam, Netherlands). The temperature, pH, DO, and RPM were recorded in BioXpert Lite software.

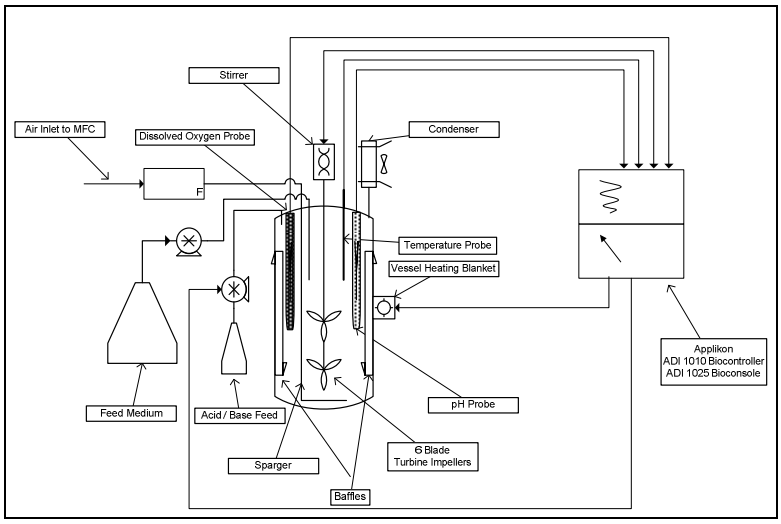

Figure 27: Schematic representation of fed-batch fermentation

Fed-Batch Fermentation Medium

The fed-batch medium is shown in Table 13.

Table 13: Fed-batch CDM composition

Components	Constant Rate Fed-batch Fermentation	pH Control Loop Fed-batch Fermentations
	g/L	**g/L**
L-Glutamic Acid monosodium salt monohydrate (Aldrich 49621, Lot 0001380041)	10.700	10.700
L-Cysteine hydrochloride monohydrate (Sigma C-7880, Lot 32K0890)	0.500	0.500
L-Ascorbic Acid (Aldrich A92902, Batch 04308LC)	0.020	0.020
L-Glutathione, reduced (Sigma-Aldrich G4251, Lot 030M1775)	0.001	0.001
NaCl (Mallinckrodt 7532-20, Lot H50602)	1.040	-
KH_2PO_4 (Mallinckrodt 7096-06, Lot G43581)	0.500	0.500
KCl (Mallinckrodt 6838-06, Lot E48N94)	0.200	0.200
$CaCl_2$ (JT Baker 1311-01, Lot V45599)	0.020	0.020
Tris(hydroxymethyl)aminomethane (Sigma-Aldrich 252859, Batch 07705HH)	1.520	-
$FeSO_4 \cdot 7H_2O$ (JT Baker 2070-01, Lot C17H24)	0.010	0.010
$MgCl_2 \cdot 6H_20$ (Sigma-Aldrich M2670, Batch 028K00222)	0.020	0.020
K_2SO_4 (Sigma P8541, Lot 128K00992)	0.168	0.168
Nicotinic Acid (Sigma N0765, Batch 126K0693)	0.004	0.004
Acetic Acid (JT Baker 9522-02, Batch H31806)	1.598	1.598

Results and Discussion

Two fed-batch fermentations were performed. One strategy used a dual feed with a 1 M acetate/1 M HCl solution used to maintain pH, and fed a 400 mM Na-glutamate/1.4 mM $MgCl_2 \cdot 6H_2O$/1 mM K_2SO_4 mixture at constant rate of 5 mL/h after 20 h of batch growth. A second strategy involved a fed-batch fermentation using 1 M acetate/400 mM L-glutamic acid/1.5 mM $MgCl_2 \cdot 6H_2O$ utilizing the pH control loop for feed.

Constant Feed Rate Fed-Batch Fermentation

A comparison is valuable between the fed-batch condition with fermentations acetate-glutamate/LMM in batch experiments conducted previously (Chapter 3, compiled in Figures 30

and 31). The only differences between acetate-glutamate/LMM batch and fed-batch fermentation were:

- Fed-batch medium contained no heptakis (2,6-di-*O*-methyl)-β-cyclodextrin instead of 1 g/L.
- Fed-batch used 1 M HCl in addition to 1 M acetate for pH regulation instead of 1 M acetate.
- Fed-batch used a constant nutrient feed of 5 mL/h containing 400 mM Na-glutamate, 1.4 mM $MgCl_2 \cdot 6H_2O$, 1 mM K_2SO_4 between 20 and 40 h culture time whereas the batch had no feed.

Figures 28 and 29 compare biomass generation, FHA production, and substrate utilization during fed-batch. On a biomass basis, the fed-batch process yielded an average OD of 6.89 at 40 h compared to 3.63 for batch process at 33.5 h. Acetate-glutamate/LMM batch process stopped generating biomass at ~25 h, most likely due to Mg limitation in the medium. Fed-batch showed a dramatic decrease in growth rate at 25 h; however, the biomass continued to increase until 40 h.

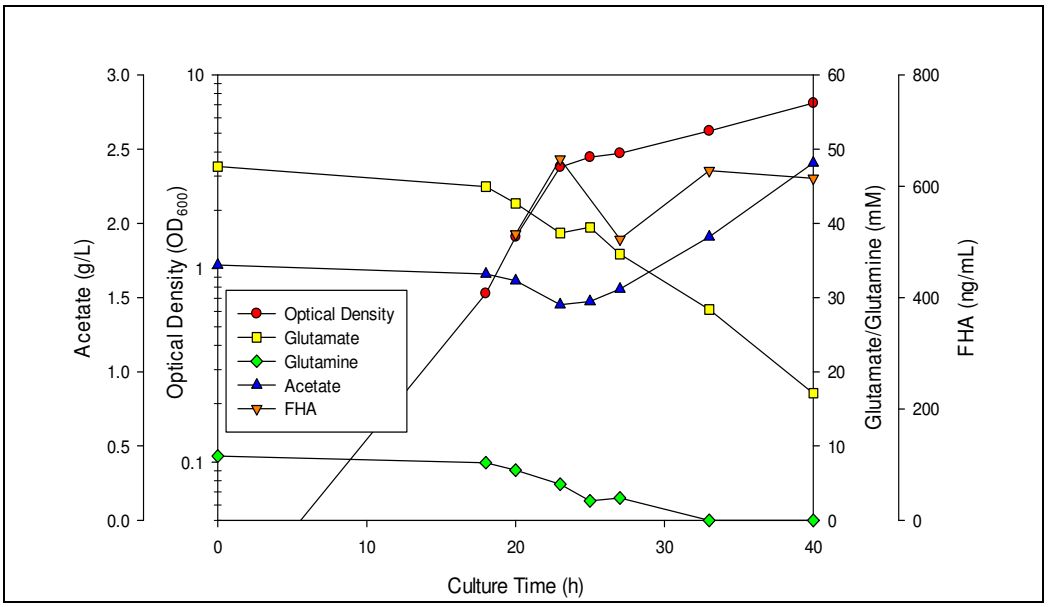

Figure 28: Comparison of biomass generation, FHA production, and substrate utilization under constant feed rate fed-batch conditions, replicate 1.

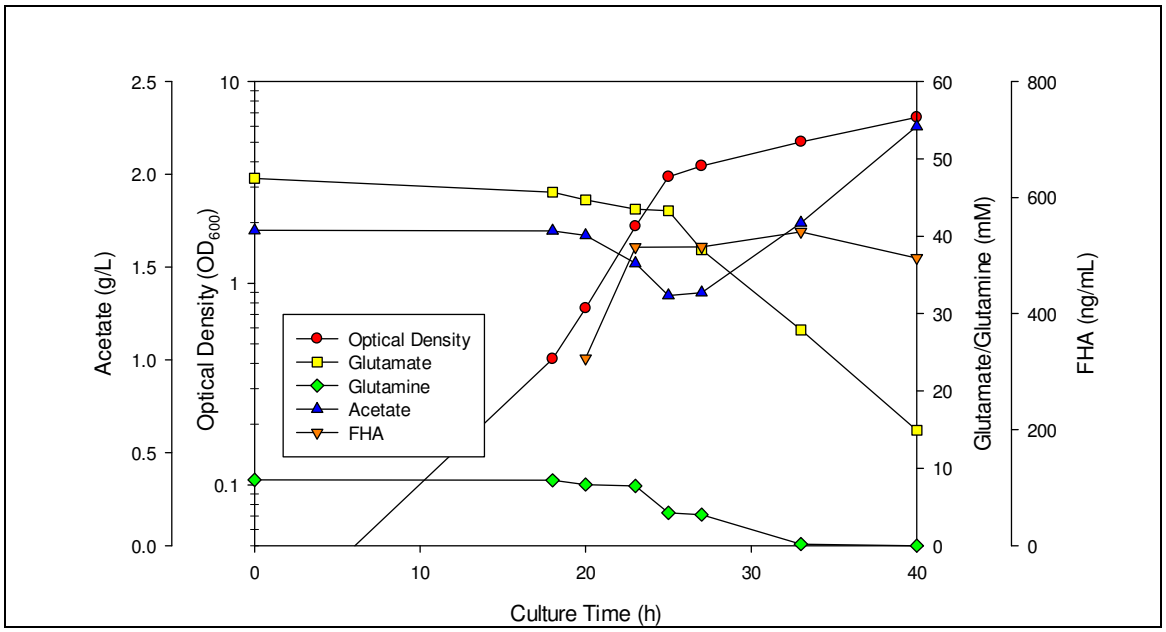

Figure 29: Comparison of biomass generation, FHA production, and substrate utilization under constant feed rate fed-batch conditions, replicate 2.

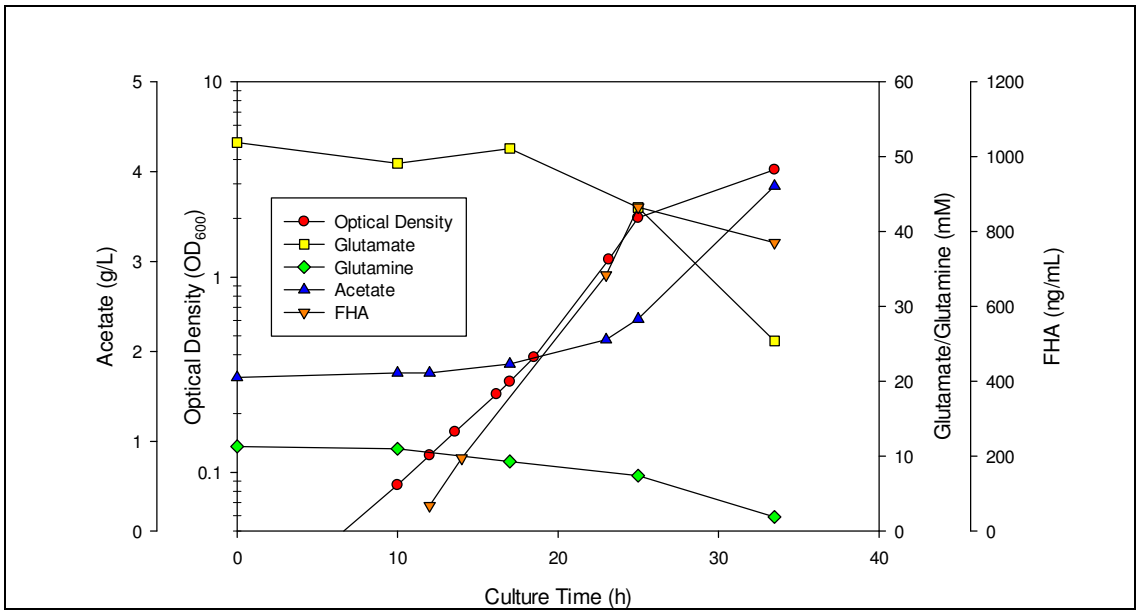

Figure 30: Batch Fermentation for Acetate-Glutamate - 0.1 mM Mg/1.0 mM SO_4/32.5 µM nicotinic acid condition, replicate 1.

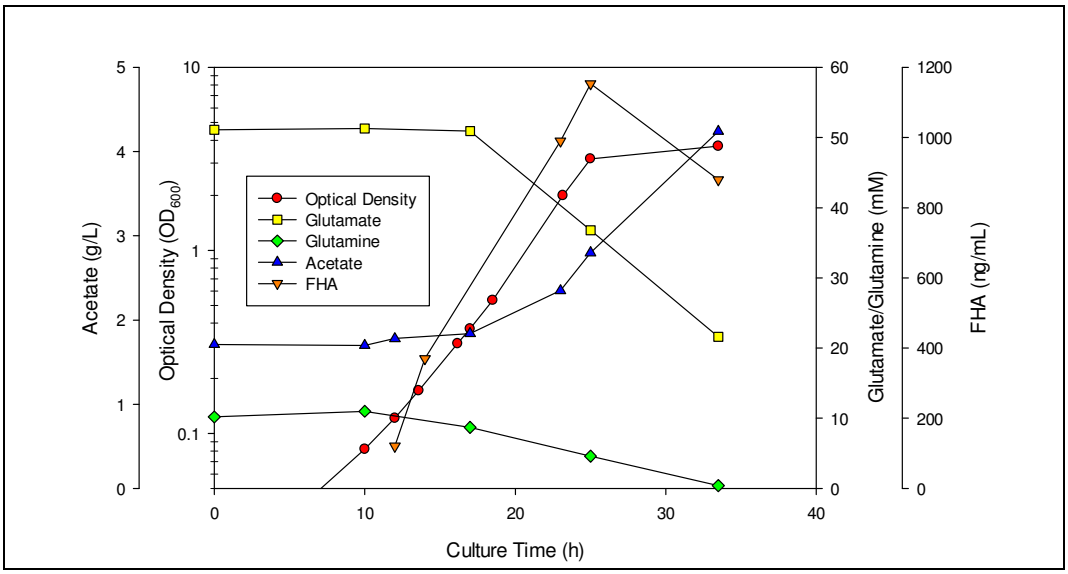

Figure 31: Batch Fermentation for Acetate-Glutamate - 0.1 mM Mg/1.0 mM SO_4/32.5 µM nicotinic acid condition, replicate 2.

Based on pH control loop feed volume and HPLC analysis, the total amount of acetate added for batch process was on average 5.45 g, where 1.45 g were consumed through the process. These values compare to 6.15 g acetate added and 3.85 g consumed during the fed-batch process. Unfortunately, FHA expression did not increase with biomass. The yield of FHA for fed-batch process decreased by nearly half, compared to the batch process.

Figure 32 compares the morphology between a batch and fed-batch process on blood agar plates. There was a clear shift to Bvg^- phase during batch process, whereas the fed-batch fermentation does not seem to shift from Bvg^+ phenotype. This result is surprising since the FHA concentrations (measured by ELISA) showed a decrease in expression, when compared to batch process. The phenotype shift in batch fermentation may be due to Mg limitation as discussed previously.

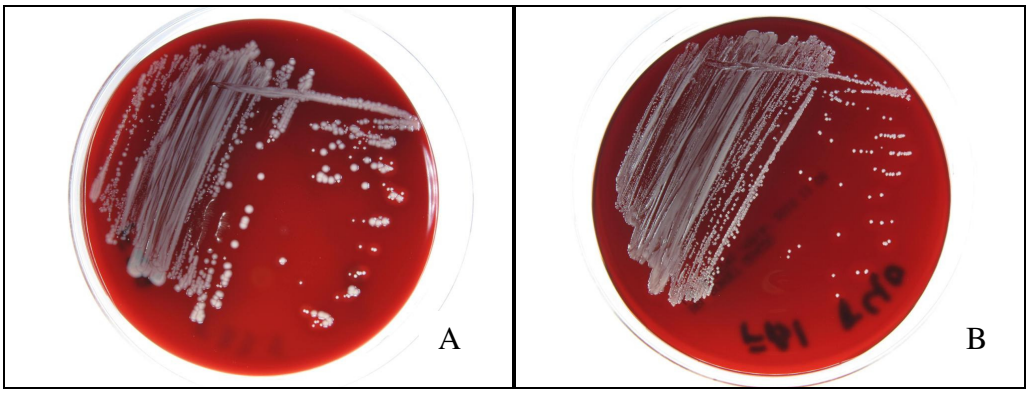

Figure 32: Phenotype observation between batch and constant feed rate fed-batch process: (A) Batch fermentation at 33.5 h (B) Fed-batch fermentation at 40 h

A possible explanation for decreased growth rate and expression during the course of the fed-batch is the increase in Na concentration. This phenomenon was explored by Thalen et al. (2006a, 2006b). They observed maximum optical density for cultures with 50 mM Na was 80% greater than cultures with 175 mM Na. The batch fermentations were designed with a Na concentration of 75 mM, considered optimal for growth rate, expression, and proteolytic activity for *B pertussis.* By implementing a constant feed strategy, however, which included Na glutamate, the Na concentration increased from 75 mM to 115 mM over the course of fed-batch fermentation.

Another explanation could be degradation of FHA during fermentation. Studies with *B. pertussis* showed pertussis toxin is formed and degraded during cultivation (Thalen et al., 2006a, Thalen et al., 2006b, Peppler et al., 1985). Thalen et al. (2006b) reported the Phe-Asp sequence that is recognized by *B. pertussis* protease occurs seven times in FHA and once in the pertussis toxin. They also reported a maximum proteolytic activity for *B. pertussis* between 100 and 125 mM Na. If *B. bronchiseptica* behaves in a similar manner, FHA could be degraded during the fermentation process. The degradation may have been exacerbated during the fed-batch due to the increase in Na concentration to 115 mM.

Frohlich et al. (1995) reported the total ionic concentration directly affects the growth rate and productivities of *B. pertussis*. They observed stationary phase at half cell concentration in the presence of 120 mM NaCl, casamino acids, or NH_4Cl. Since our fed-batch process used 1 M HCl in addition to acetate for pH control, ~75 mM Cl was added over the fermentation. Coupled with the addition of 40 mM Na from the constant nutrient feed, a similar concentration as observed by Frohlich was added during fed-batch. The increase in ionic strength of the solution may explain decreased growth rate observed after feeding regime was initiated.

pH Control Loop Fed-Batch Fermentation

Frohlich et al. (1995) and Thalen et al.(2006a) both suggested the addition of glutamic acid instead of the commonly used Na-glutamate. Frohlich et al. also suggested removing unnecessary salts from the medium and eliminating HCl for pH control. Based on their observations, a similar experiment was attempted. NaCl and tris were removed from the medium. The pH control feed consisted of 1M acetate, 400 mM L-glutamic acid , and 1.5 mM $MgCl_2 \cdot 6H_2O$ (Figures 33 and 34).

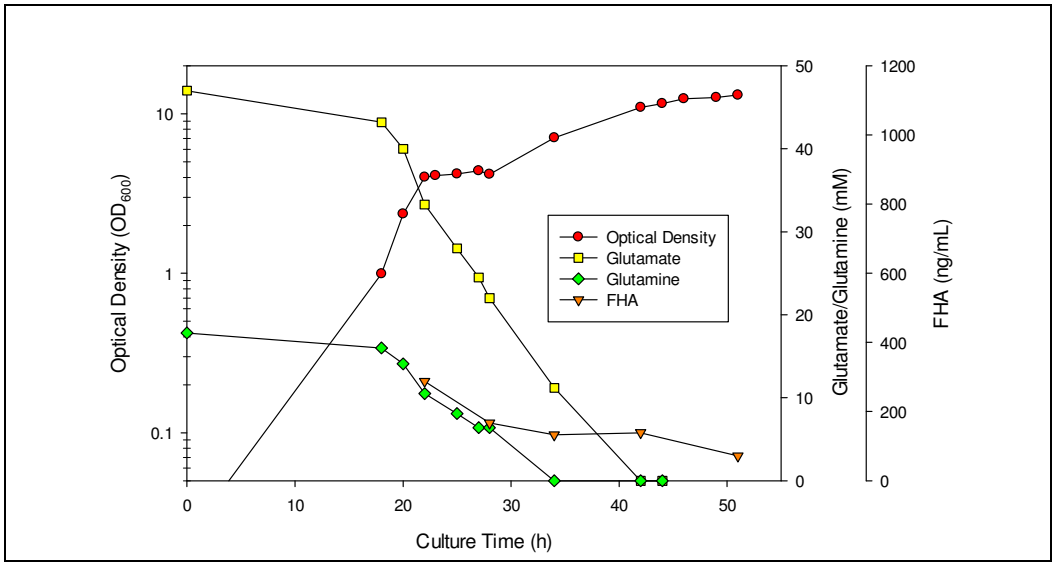

Figure 33: Comparison of biomass generation, FHA production, and substrate utilization under quasi fed-batch conditions in low salt medium with acetate/glutamic acid/$MgCl_2$ pH feed, replicate 1.

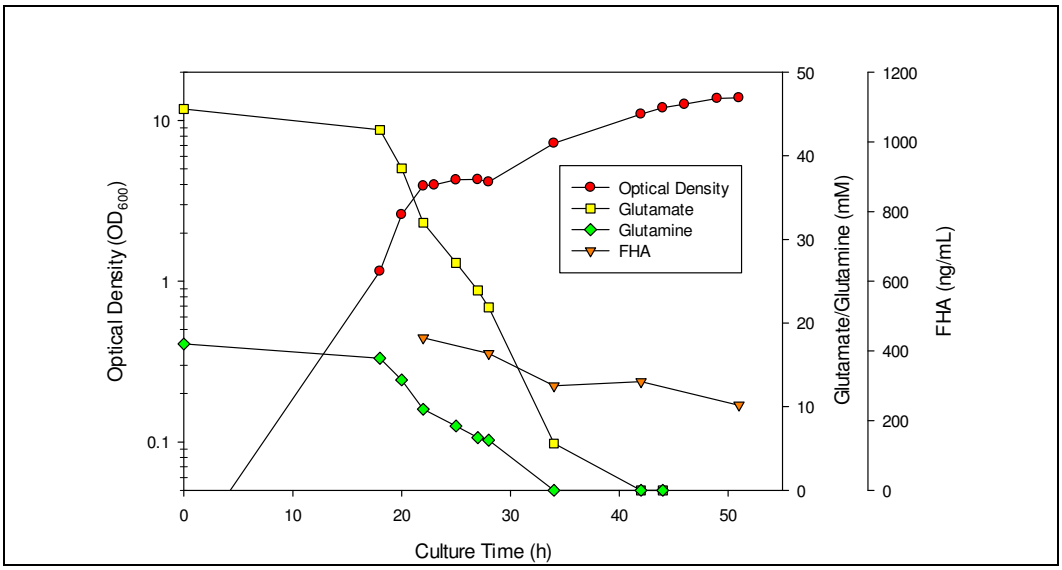

Figure 34: Comparison of biomass generation, FHA production, and substrate utilization under quasi fed-batch conditions in low salt medium with acetate/glutamic acid/$MgCl_2$ pH feed, replicate 2.

Since glutamic acid is not soluble, the feed used for pH control was a slurry continuously mixed using a magnetic stir plate. This method proved to be unreliable since the pH feed pump was too slow to draw the solid glutamic acid through pH feed tubing (evident in Figures 33 and 34 as glutamate was depleted by 42 h). Therefore, the concentration of glutamic acid added to the fermentation remains unknown. Smaller tubing diameter was tried, which resulted in blockage by the solid glutamic acid. Despite the failure of glutamic acid pH feed, the growth rate decreased at 22 h at an OD of ~4. This decrease was followed by a stationary phase of 6 h and then growth resumes at a slower growth rate until a final OD of 13-14 was reached at the end of cultivation. Even though the glutamate concentration was zero, the culture continued to grow, suggesting some dissolved glutamic acid continued to be fed via pH control or the culture adapted and continues to grow with acetate as the primary carbon source. Unfortunately, expression of FHA was less than 400 ng/mL in all samples tested.

REFERENCES

Akerley, B. J., D. M. Monack, S. Falkow, and J. F. Miller. 1992. The bvgAS locus negatively controls motility and the synthesis of flagella in *Bordetella bronchiseptica*. J. Bacteriol. 174: 980-990.

Akerley, B. J., J. F. Miller. 1993. Flagellin gene transcription in *Bordetella bronchiseptica* is regulated by the BvgAS virulence control system. J. Bacteriol. 175: 3468–3479.

Armstrong, S. K. and R. Gross. 2007. *In* C. Locht (Ed.), *Bordetella*: Molecular Microbiology (pp. 165-190). Wymondham, Norfolk, U.K.: Horizon Bioscience.

Brickman, T. J., C. A. Cummings, S. Liew, D. A. Relman, and S. K. Armstrong. 2011. Transcriptional Profiling of the Iron Starvation Response in *Bordetella pertussis* Provides New Insights into Siderophore Utilization and Virulence Gene Expression. Journal of Bacteriology. 193: 4798-4812.

Carbone, M., M. T. Fera, M. G. Pennisi, M. Masucci, A. De Sarro, C. Macri. 1999. Activity of nine fluoroquinolones against strains of *Bordetella bronchiseptica*. International Journal of Antimicrobial Agents. 12: 355-358.

Caspi R., T. Altman, J. M. Dale, K. Dreher, C. A. Fulcher, F. Gilham, P. Kaipa, A. S. Karthikeyan, A. Kothari, M. Krummenacker, M. Latendresse, L. A. Mueller, S. Paley, L. Popescu, A. Pujar, A. G. Shearer, P. Zhang, and P. D. Karp. 2009. The MetaCyc database of metabolic pathways and enzymes and the BioCyc collection of pathway/genome databases. Nucleic Acids Research. 38: D473-9.

Cotter, P. A., and J. F. Miller. 1994. BvgAS-mediated signal transduction: Analysis of phase locked regulatory mutants of *Bordetella bronchiseptica* in a rabbit model. Infect. Immun. 62: 3381–3390.

Cotter, P. A., and J. F. Miller. 1997. A mutation in the *Bordetella bronchiseptica* bvgS gene results in reduced virulence and increased resistance to starvation, and identifies a new class of Bvg-regulated antigens. Mol. Microbiol. 24: 671–685.

Cotter, P. A., and J. F. Miller. 2000. Genetic analysis of the *Bordetella* infectious cycle. Immunopharmacology. 48: 253-255.

Cotter, P. A., M. H. Yuk, S. Mattoo, B. J. Akerley, J. Boschwitz, D. A. Relman, J. F. Miller. 1998. Filamentous hemagglutinin of *Bordetella bronchiseptica* is required for efficient establishment of tracheal colonization. Infect. Immun. 66: 5921–5929.

Edwards, K. M. and M. D. Decker. 2008. Pertussis vaccines. In S. A. Plotkin, W. A. Orenstein, and P. A. Offit (Eds.) *Vaccines*, 5th Ed. Elsevier, China, pp. 467-517.

Egberink, H., D. Addie, S. Belák, C. Boucraut-Baralon, T. Frymus, T. Gruffydd-Jones, K. Hartmann, M. J. Hosie, A. Lloret, H. Lutz, F. Marsilio, M. G. Pennisi, A. D. Radford, E. Thiry, U. Truyen, and M. C. Horzinek. 2009. *Bordetella bronchiseptica* infection in cats: ABCD guidelines on prevention and management. Journal of Feline Medicine and Surgery. 11: 610-614.

Eiteman, M. A. and M. J. Chastain. 1997. Optimization of the ion-exchange analysis of organic acids from fermentation. Anal. Chim. Acta 338:69-75.

Fernández, J., F. Sisti, D. Bottero, M. E. Gaillard, D. Hozbor. 2005. Constitutive expression of bvgR-repressed factors is not detrimental to the Bordetella bronchiseptica–host interaction. Research in Microbiology. 156: 843–850.

Frohlich, B. T., E. R. De Bernardez Clark, G. R. Siber, R. W. Swartz. 1995. Improved pertussis toxin production by Bordetella pertussis through adjusting the growth medium's ionic composition. Journal of Biotechnology. 39: 205-219.

Frohlich, B. T., M. d'Alarcao, R. S. Feldberg, M. L. Nicholson, G. R. Siber, R. W. Swartz. 1996. Formation and cell-medium partitioning of autoinhibitory free fatty acids and cyclodextrin's effect in the cultivation of *Bordetella pertussis*. Journal of Biotechnology. 45: 137-148.

Fuchs, G. and A. Kröger. 1999. *In* J. W. Lengeler, G. Drews, and H. G. Schlegel (Ed.), Biology of Prokaryotes (pp. 88-109). New York, U.S.A: Blackwell Science.

Fuchs, G. 1999. *In* J. W. Lengeler, G. Drews, and H. G. Schlegel (Ed.), Biology of Prokaryotes (pp. 110-162). New York, U.S.A: Blackwell Science.

Goodnow, R. A. 1980. Biology of Bordetella bronchiseptica. Microbiol. Rev. 44: 722-738.

Imaizumi, A., Y. Suzuki, S. Ono, H. Sato, Y. Sato. 1983. Effect of Heptakis(2,6-*O*-Dimethyl)β-Cyclodextrin on the Production of Pertussis Toxin by *Bordetella pertussis*. Infection and Immunity. 41: 1138-1143.

Irie, Y., S. Mattoo, and M. H. Yuk. 2004. The Bvg Virulence Control System Regulates Biofilm Formation in *Bordetella bronchiseptica*. Journal of Bacteriology. 186: 5692-5698.

Jacob-Dubuisson, F. and C. Locht. 2007. *In* C. Locht (Ed.), Bordetella: Molecular Microbiology (pp. 69-96). Wymondham, Norfolk, U.K.: Horizon Bioscience.

Jebb, W. H. H. and A. H. Tomlinson. 1951. The Catabolic Activity of Washed Suspensions of *Haemophilus pertussis*. J. gen. Microbiology. 5: 951-965.

Jebb, W. H. H. and A. H. Tomlinson. 1955. The Nutritional Requirements of *Haemophilus pertussis*. J. gen. Microbiology. 13: 1-8.

Jebb, W. H. H. and A. H. Tomlinson. 1957. The Minimal Amino Acid Requirements of *Haemophilus pertussis*. J. gen. Microbiol. 17: 59-68.

Kanehisa, M., S. Goto, Y. Sato, M. Furumichi, and M. Tanabe. 2012. KEGG for integration and interpretation of large-scale molecular datasets. Nucleic Acids Res. 40: D109-D114.

Kuchma, S. L., S. P. Connolly, and G. A. O'Toole. 2004. A Three-Component Regulatory System Regulates Biofilm Maturation and Type III Secretion in *Pseudomonas aeruginosa*. Journal of Bacteriology. 187: 1441-1454.

Lacey, B. W. 1960. Antigenic modulation of Bordetella pertussis. J. Hyg. 58: 57-93.

Licari, P., G. R. Siber, and R. Swartz. 1991. Production of cell mass and pertussis toxin by *Bordetella pertussis*. Journal of Biotechnology. 20: 117-130.

Madigan, M. T., J. M. Martinko, and J. Parker. 2003. Brock Biology of Microorganisms. Upper Saddle River, NJ: Prentice Hall.

Mishra, M. and R. Deora. 2005. Mode of Action of the *Bordetella* BvgA Protein: transcriptional Activation and Repression of the *Bordetella bronchiseptica bipA* Promoter. Journal of Bacteriology. 187: 6290-6299.

Mooi, F. R., O. He, and N. Guiso. 2007. *In* C. Locht (Ed.), Bordetella: Molecular Microbiology (pp. 17-46). Wymondham, Norfolk, U.K.: Horizon Bioscience.

Neidhardt, F. C., J. L. Ingraham, and M. Schaechter. 1990. Physiology of the Bacterial Cell. Sunderland, Massachusetts: Sinauer Associates, Inc.

Parkhill J., M. Sebaihia, A. Preston, L. D. Murphy, N. Thomson, D. E. Harris, M. T. Holden, C. M. Churcher, S. D. Bentley, K.L.Mungall, A. M. Cerdeno-Tarraga, L. Temple, K. James, B. Harris, M. A. Quail, M. Achtman, R. Atkin, S. Baker, J. Basham, D. Bason, N. Cherevach, I. Chillingworth, T. Collins, M. Cronin, A. Davis, P. Doggett, T. Feltwell, A. Goble, N. Hamlin, H. Hauser, S. Holroyd, K. Jagels, S. Leather, S. Moule, H. Norberczak, S. O'Neil, D. Ormond, C. Price, E. Rabbinowitsch, S. Rutter, M. Sanders, D. Saunders, K. Seeger, S. Sharp, M. Simmonds, J. Skelton, R. Squares, S. Squares, K. Stevens, L. Unwin, S. Whitehead, B. G. Barrell, D. J. Maskell. 2003. Comparative analysis of the genome sequences of *Bordetella pertussis*, *Bordetella parapertussis* and *Bordetella bronchiseptica*. Nat. Genet. 35: 32–40.

Peppler, M.S., R. C. Judd, and J. J. Munoz. 1985. Effect of proteolytic enzymes, storage and reduction on the structure and biological activity of pertussisigen, a toxin from *Bordetella pertussis*. Dev Biol Stand. 61:75-87.

Plotkin, B. J. and D. A. Bemis. 1998. Carbon source utilisation by *Bordetella bronchiseptica*. J. Med. Microbiology. 47: 761-765.

Preston, A., E. Maxim, E. Toland, E. J. Pishko, E. T. Harvill, M. Caroff and D. J. Maskell. 2003. *Bordetella bronchiseptica* PagP is a Bvg-regulated lipid A palmitoyl transferase that is required for persistent colonization of the mouse respiratory tract. Molecular Microbiology. 48: 725–736.

Salyers, A. A. and D. D. Whitt. 2002. Bacterial Pathogenesis: A Molecular Approach. Washington D.C.: ASM Press.

Sanden, G. and R. S. Weyant. 2005. Genus III. Bordetella Moreno - Lopez 1952, 178^{AL}. In Brenner, Krieg, and Staley (Editors), *Bergey's Manual of Systematic Bacteriology*, 2nd Ed., Vol. 2C, Springer, New York, pp. 662-671.

Smith, A. M., C. A. Guzmán, M. J. Walker. 2001. The virulence factors of *Bordetella pertussis*: a matter of control. FEMS Microbiology Reviews. 25: 309-333.

Stainer, D. W. and M. J. Scholte. 1971. A Simple Chemically Defined Medium for the Production of Phase I *Bordetella pertussis*. Journal of General Microbiology. 63: 211-220.

Stibitz, S. 2007. *In* C. Locht (Ed.), Bordetella: Molecular Microbiology (pp. 47-68). Wymondham, Norfolk, U.K.: Horizon Bioscience.

Stockbauer, K. E., B. Fuchslocher, J. F. Miller, and P. A. Cotter. 2001. Identification and characterization of BipA, a *Bordetella* Bvg-intermediate phase protein. Molecular Microbiology. 39: 65-78.

Sukumar, N., C. F. Love, M. S. Conover, N. D. Kock, P. Dubey, and R. Deora. 2009. Active and Passive Immunizations with *Bordetella* Colonization Factor A Protect Mice against Respiratory Challenge with *Bordetella bronchiseptica*. Infection and Immunity. 77: 885-895.

Thalen, M., J. van den Ijssel, W. Jiskoot, B. Zomer, P. Roholl, C. de Gooijer, C. Beuvery, and J. Tramper. 1999. Rational medium design for *Bordetella pertussis*: basic metabolism. Journal of Biotechnology. 75: 147-159.

Thalen, M., M. Venema, A. Dekker, L. Berwald, J. van den Ijssel, B. Zomer, C. Beuvery, D. Martens, and J. Tramper. 2006(a). Fed-batch cultivation of *Bordetella pertussis*: Metabolism and Pertussis Toxin production. Biologicals. 34: 289-297.

Thalen, M., M. Venema, J. van den Ijssel, L. Berwald, C. Beuvery, D. Martens, and J. Tramper. 2006(b). Effect of relevant culture parameters on Pertussis Toxin expression by *Bordetella pertussis*. Biologicals. 34: 213-220.

Woolfrey, B. F., and J. A. Moody. 1991. Human infections associated with *Bordetella bronchiseptica*. Clin. Microbiol. Rev. 4: 243-255.

Yuk, M. H., E. T. Harvill, and J. F. Miller. 1998. The bvgAS virulence control system regulates type III secretion in *Bordetella bronchiseptica*. Mol. Microbiol. 28: 945–959.

APPENDIX A

BACTERIAL CELL STOCK DEVELOPMENT

Bacterial cell stocks

Cell stocks were generated using Bacto Tryptic Soy Broth (TSB, BD, Franklin Lakes, NJ). TSB was prepared at 30 g/L and autoclaved for 30 minutes. 60% (v/v) aqueous glycerin (Glycerin, U.S.P., Mallinckrodt Baker, Inc, Phillipsburg, NJ Cat. No. 2143-01) solution was filter (0.2 μm) sterilized for preparation of frozen stock aliquots.

X+1

The freeze dried strain *Bordetella bronchiseptica* ATCC® BAA-588 (X) was resuspended in 0.5 mL TSB. This material was then added to 100 mL TSB in a 500 mL polycarbonate baffled shake flask with a 0.22 μm vented cap (Triforest Labware, Irvine, CA, part # FPC0500S). The initial OD_{600} was 0.045. Flask was agitated on an orbital shaker at 180 RPM at 37°C (VWR orbital shaker model DS2-500E-1, 25 mm orbit) for 18.5 h, at which time OD_{600} was 4.26.

X+2

After 18.5 h of X+1 growth, a second flask (100 mL TSB in 500 ml baffled flask) was inoculated to an initial OD_{600} of about 0.1. The X+2 culture was grown under the same conditions as X+1, and samples were taken periodically for OD_{600} measurements. At an OD_{600} of 1.1, 25 mL of 60% glycerin was added to 75 mL of X+2 culture (final concentration 15% glycerin), and culture was allowed to shake for a few minutes to allow proper mixing. The culture was then divided into 1 mL aliquots in 2 mL cryovials and stored at -70°C. A Gram stain

was performed for purity, observed Gram-negative rods. Limited mobility was observed under phase contrast microscopy.

X+3

A frozen vial of the X+2 cell stock, stored at -70°C was thawed at room temperature and streaked onto a Bordet Gengou with 15% sheep's blood plate (BD BBL, Franklin Lakes, NJ, product number 297876) for colonies isolation. Plates were incubated at 37°C for 48 hours.

X+4

A single colony was selected from each *Bordetella* morphology (assuming Bvg^+ and Bvg^-) and individually streaked on Bordet Gengou with 15% sheep's blood plates. (two Bvg^+ and two Bvg^-). Plates were incubated at 37°C for 48 h. An API® 20 NE (bioMérieux, Marcy I'Etoile, France) identification test was performed on each colony morphology. The Bvg^+ plate was identified as *Bordetella bronchiseptica* (% ID = 97.3). The Bvg^- plate was identified as *Bordetella bronchiseptica* (% ID = 94.8).

X+5

A single colony was selected from the Bvg^+ *Bordetella* morphology and streaked on a Bordet Gengou with 15% sheep's blood plate. The plate was incubated at 37°C for 48 h.

X+6

The X+5 plate was harvested and resuspended in Phosphate Buffered Saline (PBS, NaCl, 8 g/L; KCl, 0.2 g/L; Na_2HPO_4, 1.15 g/L, KH_2PO_4, 0.2 g/L; pH 7.2) to an OD_{600} of 5.45. 917 µL of the resuspended X+5 was used to inoculate a shake flask (100 mL CDM-I (Table 14) in 500 mL baffled flask) was inoculated to an initial OD_{600} of about 0.05. The X+6 culture was grown under the same conditions as X+1, and samples were taken periodically for OD_{600} measurements. At an OD_{600} of 1.0, 25 mL of 60% glycerin was added to 75 mL of X+6 culture (final

concentration 15% glycerin), and the culture was allowed to shake for a few minutes to allow proper mixing. The culture was then divided into 1 mL aliquots in 2 mL cryovials and stored at -70°C.

The CDM-I used in the seed production was formulated as follows (Imaizumi, et al. 1983; Thalen, et al. 2006a, 2006b), and the pH adjusted to 6.9 with 3 M KOH (Sigma-Aldrich P5958, Batch 028K07551).

Table 14: Bacterial Seed CDM-I Formulation

Components	g/L
L-Glutamic Acid monosodium salt monohydrate (Aldrich 49621, Lot 0001380041)	10.700
L-Cysteine hydrochloride monohydrate (Sigma C-7880, Lot 32K0890)	0.500
L-Ascorbic Acid (Aldrich A92902, Batch 04308LC)	0.020
L-Glutathione, reduced (Sigma-Aldrich G4251, Lot 030M1775)	0.001
NaCl (Mallinckrodt 7532-20, Lot H50602)	1.040
KH_2PO_4 (Mallinckrodt 7096-06, Lot G43581)	0.500
KCl (Mallinckrodt 6838-06, Lot E48N94)	0.200
$CaCl_2$ (JT Baker 1311-01, Lot V45599)	0.020
Tris(hydroxymethyl)aminomethane (Sigma-Aldrich 252859, Batch 07705HH)	1.520
β-Cyclodextrin(heptakis(2,6-*O*-dimethyl)) (MP 157320, Lot 4318KA)	1.000
$FeSO_4 \cdot 7H_2O$ (JT Baker 2070-01, Lot C17H24)	0.010
Lactic Acid, 85% (JT Baker 0194-01, J11J03)	2.400
$MgCl_2 \cdot 6H_20$ (Sigma-Aldrich M2670, Batch 028K00222)	0.100
Nicotinic Acid (Sigma N0765, Batch 126K0693)	0.004

X+7

A frozen vial of the X+6 cell stock, stored at -70°C was thawed at room temperature and streaked onto a Bordet Gengou with 15% sheep's blood plate for colonies isolation. The plates were incubated at 37°C for 48 hours.

X+8

A single colony from the X+7 plate was selected from the Bvg$^+$ *Bordetella* morphology and streaked on a Bordet Gengou with 15% sheep's blood plate. The plate was incubated at 37°C for 48 hours.

X+9

The X+8 plate was used to inoculate 1.0 L of CDM-I in a 2.0 L bioreactor with an AppliSens DO sensor, an AppliSens pH sensor, and a Pt100 temperature sensor and a ADI 1010 Biocontroller with the ADI 1025 Bioconsole (Applikon, Schiedam, Netherlands, see Figure 5 for schematic representation). Batch process was carried out at 37°C, a pH of 6.9 (controlled with 3 M HCl) and a constant agitation of 500 RPM. HCl addition bottle was placed on a scale for mass measurement. Cells were aerated by sparged air at a constant rate of 400 mL/min controlled by mass flow controller (Aalborg, Orangeburg, USA, model GFC17) which prevented oxygen limitation. Optical density (OD_{600}) was measured at 600 nm using Pharmacia LKB Ultrospec III, using 3 mL cuvettes. Dilutions were performed as needed. Temperature, pH, dissolved oxygen, RPM, and optical density were recorded using BioXpert Lite software (Figure 35).

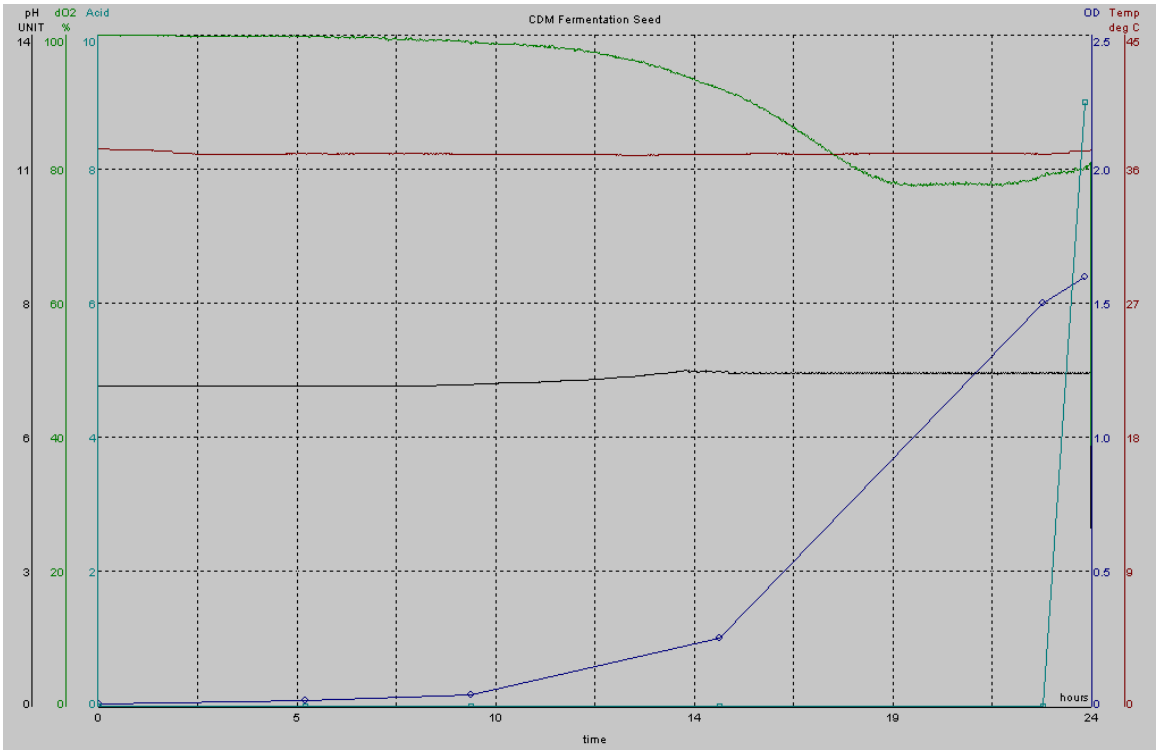

Figure 35: BioXpert generated X+9 CDM Fermentation Chart

After 24 h, the bioreactor was harvested at an OD_{600} of 1.6. Cells were pelleted (Beckman Coulter J-model centrifuge with JA-10 fixed angle rotor at 4420 x g (5000 RPM) for 15 min), then resuspended in 75 mL CDM-I and 25 mL 60% glycerin added (final concentration 15% glycerin). This solution was mixed, then culture divided into 1 mL aliquots in 2 mL cryovials and stored at -70°C.

APPENDIX B

PRELIMINARY INVESTIGATION

A vial of the frozen X+2 working cell stock was thawed by hand and plated onto blood agar plates and incubated at 37°C for 38 h. After observing a homogeneous lawn of cells, the plates were harvested into 2 mL of sterile PBS to an $OD_{600\ nm}$ ~1. Serial dilution was performed from 10^{-1} to 10^{-10} (0.5 mL to 4.5 mL PBS). 100 µL of the 10^{-6} to 10^{-9} dilutions were spread on plates for Colony Forming Unit (CFU), performed in triplicate. The third plate contained 50 µg/mL streptomycin to determine antibiotic resistance. Plates were incubated until colony formation. Calculated CFUs were 6.0×10^9 and 7.2×10^9 for RB50-1 and RB50-2, respectively. Observed plates appeared to be in Bvg^- phase, colonies appeared wide and flat. Figure 36 is an example of one of the 10^{-6} dilution plates. Antibiotic treatment was negligible.

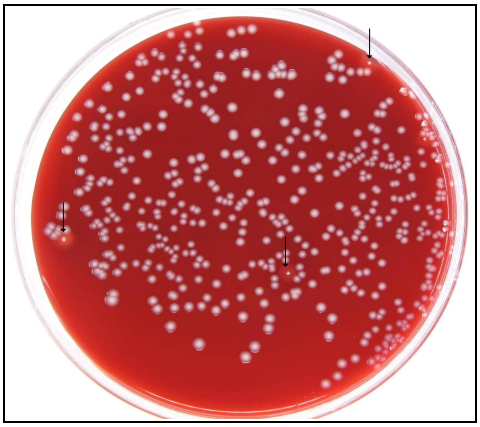

Figure 36: Example of CFU 10^{-6} dilution plate, Bvg^-. Colonies appear wide and flat with no hemolysis. The arrows point to a few small colonies with hemolysis (assumed Bvg^+). Incubation at 37°C for 48 hours.

Four small hemolytic colonies were chosen from 10^{-7} dilution plates and restreaked for isolation blood plates. One large, flat non hemolytic colony was restreaked as a control. Figure

37 is an example of restreaked plates. Large colony plates did not exhibit hemolysis and were assumed Bvg^-. All small colony plates colonies appeared small, pinpoint, and hemolytic, assumed Bvg^+. Another RB50 X+2 working seed was thawed for confirmation, and exhibited morphology similar to Figure 36. X+2 working seed was primarily in the Bvg^- phase.

Figure 37: Large and Small Colony Isolation for *B. bronchiseptica*. Incubation 37°C for 48 hours.

Four small colony isolation plates were restreaked on plates for a lawn of cells and aliquot of a Bvg^+ working seed. Plates were harvested into 20 mL sterile PBS, $OD_{600} = 4$. The resuspension was further diluted to 64 mL with PBS. 21.3 mL of a 60% glycerin solution was added for a final 15% glycerin concentration. The final $OD_{600} = 0.87$. Stocks were aliquoted at 1 ml and frozen at -70°C. This cell stock was the X+6 passage.

Prior to freezing, the X+6 cell stock was streaked for isolation, plates are shown in Figure 38. Plates appeared to contain both small hemolytic colonies (Bvg^+) and large non-hemolytic colonies (Bvg^-).

Figure 38: Pre-freeze X+6 cell stock streak for isolation. Incubation 37°C for 48 hours.

Post freeze X+6 cell stock was also streaked for isolation, plates are shown in Figure 39. Plates appeared to contain both small hemolytic colonies (Bvg^+) and large non-hemolytic colonies (Bvg^-).

Figure 39: Post-freeze X+6 cell stock streak for isolation. Incubation 37°C for 48 hours.

Serial dilutions were performed in triplicate from 10^{-1} to 10^{-8} (100 µL to 900 µL) from a newly thawed vial of X+6 cell stock to investigate the percentage of Bvg^+ to Bvg^- colonies. Figure 40 displays the 10^{-6} serial dilution plates. The colony counts and CFU data for each phase are shown in Table 15. Frozen X+6 cell stock contains 72.5 % Bvg^+ phase organisms. Selection of an individual colony from a mixed phase population was able to be propagated to a homogeneous plate.

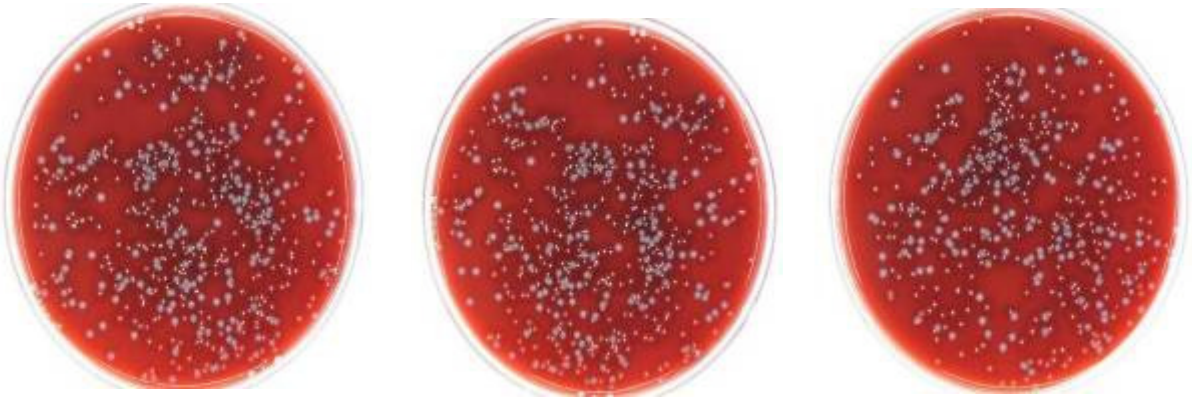

Figure 40: Serial dilution (10^{-6}) plates of X+6 cell stock. Incubation 37°C for 48 hours

Table 15: CFU count by Bvg phase for X+6 cell stock

Dilution	10^{-6}	10^{-7}	CFU	% of Total
Bvg^- Colony	162, 148, 164	9, 20, 15	1.52×10^9	27.5 %
Bvg^+ Colony	389, 330, 410	50, 46, 31	4.00×10^9	72.5 %
Total Colony	551, 478, 574	59, 66, 46	5.52×10^9	

Several shake flask trial experiments were performed using a chemically defined media based on the study by Plotkin and Bemis (1998). Initially these studies produced growth to an OD_{600} of ~0.3 using glutamate as the carbon source. It was observed that the pH increased from 7.2 to greater than 8, while generating glutamine and NH_4. Several more studies were performed using different buffering strength and starting pH. The more buffered medium allowed the pH to remain between 6.9 and 7.5 for ~28 h of growth. The culture only produced an OD_{600} of 0.366 at 27.5 h and 0.466 at 46 h with a final pH of 7.8. Although this was considered poor growth, the specific growth rate was 0.199 h^{-1} with a mean generation time (MGT) of 3.47. These values are similar to the work performed by Plotkin and Bemis. An initial study similar to the effect of Mg, SO_4, nicotinic acid concentration batch fermentation DOE(Chapter 2) was performed using a modified Plotkin and Bemis medium, listed in Table 16. The first eight shake flask scenarios

were performed using a seed shake flask for inoculation, instead of direct inoculation from frozen seed vial. This was explored to possibly reduce the lag time observed in initial shake flask screening and have a CDM adapted inoculum.

Table 16: Plotkin and Bemis CDM base

10X/100X/1000X Magnesium Stock Solution	
$MgCl_2 \cdot 6H_2O$ (Sigma M-0250, Batch 71K0033)	2.0351 g
H_2O	100 ml
10X/100X/1000X Sulfate Stock Solution	
K_2SO_4 (Sigma P8541, Batch 128K00992	1.7419 g
H_2O	100 ml
10X/100X/1000X Nicotinic acid Stock Solution	
Nicotinic acid (Sigma N0765, Batch 126K0693)	6.2 mg
H_2O	100 ml
PNC stock Solution	
K_2HPO_4 (JT Baker 3252-05 Lot C47155)	2.0 g
KH_2PO_4 (Mallinckrodt 7096-06 Lot E10630)	4.0 g
Glutamic Acid (Sigma G-8415, Batch 50K0335)	2.94 g
H_2O	100 ml
10X Vitamin Solution	
Biotin (Sigma B4501, Batch 019K1769)	20.0 µg
D-Pantothenic Acid Hemicalcium Salt (Sigma P2250, Batch 097K10504)	4.0 mg
Folic Acid (Sigma F7876, Batch 098K0082)	20.0 µg
Myo-Inositol (Sigma I5125, Batch 117K0666)	20.0 mg
4-Aminobenzoic Acid (Sigma A9878, Batch 099K1610)	2.0 mg
Pyridoxine Hydrochloride (Sigma P9755, Batch 039K1637)	4.0 mg
Riboflavin (Sigma R4500, Batch 069K1585)	2.0 mg
Thiamine Hydrochloride (Sigma T4625, Batch 118K0122)	4.0 mg
H_2O	1000 ml
10X Trace Element Solution	
H_3BO_3 (Sigma B0394, Batch 035K0222)	5.0 mg
$CuSO_4 \cdot 5H_2O$ (Sigma C7631, Batch 10828PH)	0.4 mg
KI (Sigma P2963, Batch 079K0118)	1.0 mg
$FeCl_3 \cdot 6H_2O$ (JT Baker 2000-01, Lot T30636)	2.0 mg
$MnSO_4 \cdot 1H_2O$ (Sigma M-7634, Batch 127H0549)	4.0 mg
$Na_2MoO_4 \cdot 2H_2O$ (Sigma S-6646, Batch 41K0265)	2.0 mg
$ZnSO_4 \cdot 7H_2O$ (Sigma 221376, Batch 08014AD)	4.0 mg
NaCl (Mallinckrodt 7532-20, Lot G31623)	1.0 g
$CaCl_2 \cdot 2H_2O$ (Sigma C8106, Batch 037K0085)	1.0 g
H_2O	1000 ml

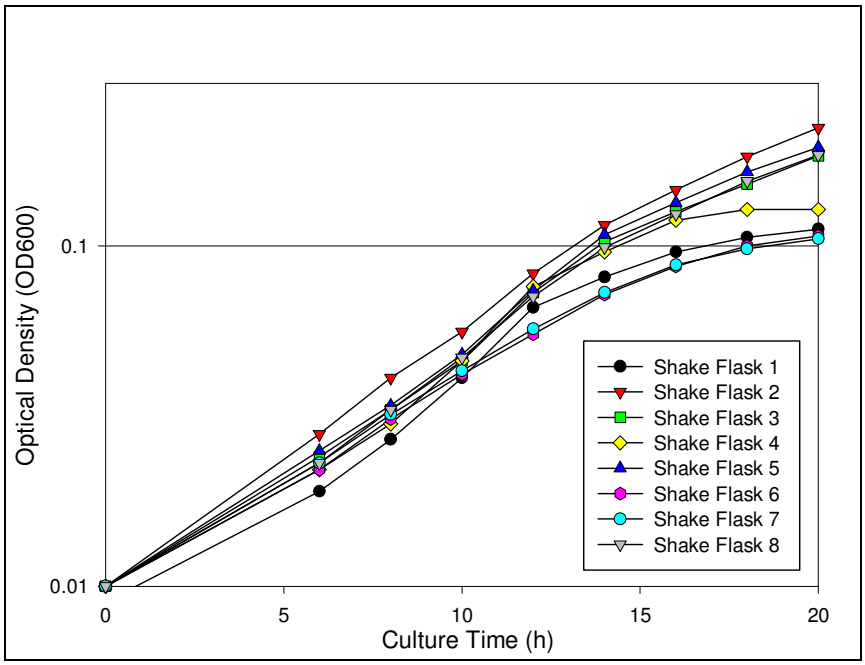

Figure 41: Plotkin and Bemis CDM shake flask growth curves

Figure 41 presents the OD_{600} values over the 20 hours of growth. The experiment yielded poor OD results with growth rates ranging from 0.14 - 0.20 h^{-1}. The MGT and growth rates were again similar to the literature values from Plotkin and Bemis. Samples were taken and analyzed for FHA by ELISA. The cultures produced no detectable FHA ELISA values.

Due to the failure of this initial experiment, further investigation was made into the medium. A shake flask test was performed using an alternate carbon source, succinate, in the modified Plotkin and Bemis (P&B) medium. For comparison a *B. pertussis* medium, referred to as modified CL was available. P&B with glutamate yielded an OD_{600} of 0.18, P&B with succinate yielded an OD_{600} of 0.28, and modified CL produced a culture with an OD_{600} of 8.52 after 33 hours of growth (see Figure 42). Therefore, original literature CL medium was selected for subsequent experiments.

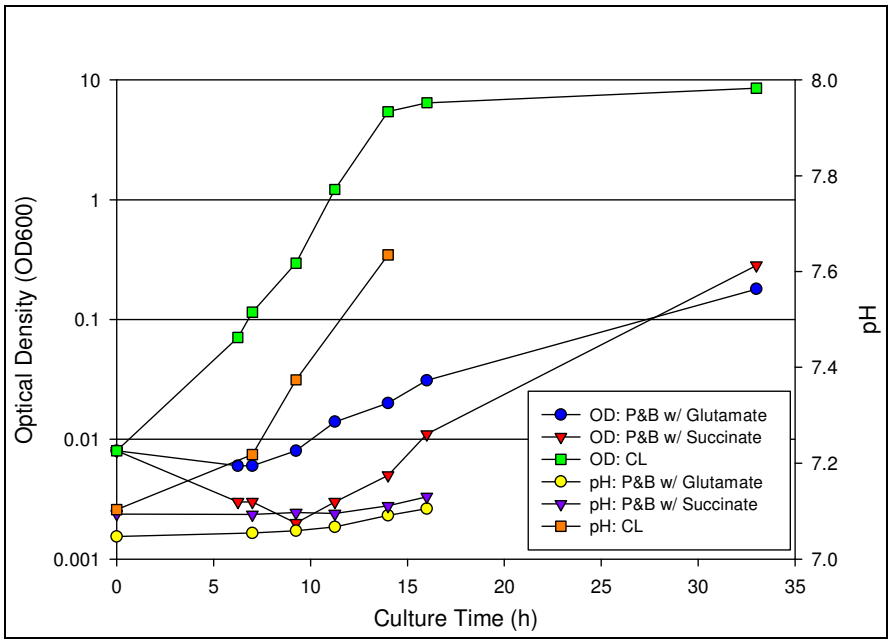

Figure 42: Test media growth curves and pH. Optical Density(black symbols) and pH(white symbols)

Starting with the CL CDM as a basis, the medium was simplified and screened to see the affect of casamino acids, valine, cysteine, lactate, K_2SO_4 on growth. The CDM for screening shake flask experiment is listed in Table 17. RB50 X+6 frozen cell stock, primarily in Bvg^+ phase was used for this investigation. The frozen cell stock (1 mL) was thawed at room

Table 17: Shake flask CDM screening formulation

Component (g/L)	SS	CL	Modified CL	Media A	Media B	Media C	Media D	Media E	Media F
L-Glutamic Acid, monosodium salt monohydrate (Sigma G2834, Lot 06411KE)	10.7	10.7	10.7	10.7	10.7	10.7	10.7	10.7	10.7
L-proline (Sigma P5607-25G Batch 077K0009)	0.24	0.24	0.24	0.24	0.24	0.24	0.24	0.24	0.24
NaCl (Mallinckrodt 7532-20, Lot H50602)	2.5	2.5	2.5	2.5	2.5	2.5	2.5	2.5	2.5
KH_2PO_4 (Mallinckrodt 7096-06, Lot G43581)	0.5	0.5	0.5	0.5	0.5	0.5	0.5	0.5	0.5
$MgCl_2$ * $6H_20$ (Sigma-Aldrich M2670, Batch 028K00222)	0.1	0.1	0.1	0.1	0.1	0.1	0.1	0.1	0.1
KCl (Mallinckrodt 6838-06, Lot E48N94)	0.2	0.2	0.2	0.2	0.2	0.2	0.2	0.2	0.2
$FeSO_4$ * $7H_2O$ (JT Baker 2070-01, Lot C17H24)	0.01	0.01	0.01	0.01	0.01	0.01	0.01	0.01	0.01
$CaCl_2$ (JT Baker 1311-01, Lot V45599)	0.02	0.02	0.02	0.02	0.02	0.02	0.02	0.02	0.02
Nicotinic acid (Sigma N0765, Batch 126K0693)	0.004	0.004	0.004	0.004	0.004	0.004	0.004	0.004	0.004
Casamino Acids (BD 223050 Lot 0221441)	0	10	10	0	0	0	0	0	0
Cysteine HCl*H_2O (Sigma C-7880, Lot 32K0890)	0.04	0.04	0.04	0.04	0.5	0.5	0.5	0.5	0.04
Tris (Sigma-Aldrich 252859, Batch 07705HH)	6.1	6.1	1.52	1.52	1.52	1.52	1.52	1.52	1.52
Glutathione (reduced) (Sigma-Aldrich G4251, Lot 030M1775)	0.10	0.15	0.0013	0.0013	0.0013	0.0013	0.0013	0.0013	0.0013
L-Ascorbic acid (Aldrich A92902, Batch 04308LC)	0.02	0.4	0.02	0.02	0.02	0.02	0.02	0.02	0.02
β-Cyclodextrin (heptakis(2,6-*O*-dimethyl)) (MP 157320, Lot 4318KA)	0	1	1	1	1	1	1	1	0
L-Valine (Sigma-Aldrich V0500, Lot 015K0020)	0	0	0	0	0	0.1	0	0.1	0
Lactic Acid, 85% (JT Baker 0194-01, J11J03)	0	0	0	0	0	0	0.1	0.1	0
K_2SO_4(Sigma P8541, Lot128K00992)	0	0	0	0.1	0.1	0	0	0.1	0

temperature and streaked for Bvg^+ phase colony isolation; plate was incubated at 37°C for 48 hours. A few Bvg^+ phase colonies were selected and restreaked for a lawn of cells, incubated at 37°C for 48 hours. Cells were resuspended in PBS and used to inoculate at a target OD_{600} of 0.05 in 25 mL shake flask CDM in 125 mL vented baffled flasks, which was cultured at 37°C and 150 RPM. OD_{600} with dilutions at 1:10 using 100 µL sample and pH were monitored during growth. The cultures were grown for 22.75 hours. All medium's yielded specific growth rates between 0.60 – 0.75 h^{-1}. It was concluded that casamino acids were not critical for growth. Shake flasks A-F all achieved OD_{600} values greater than 5, with modified CL medium (contains casamino acids) reaching the greatest OD at 7.91. Shake flask C and E, which contained valine, generated a lower specific growth rate than other shake flasks, 0.60 and 0.64 h^{-1} respectively. Therefore, valine was not necessary for growth and may be unfavorable to growth. Based on the screening K_2SO_4 or an increase in cysteine can be substituted for the lost sulfur source in the casamino acids. Lactate and cysteine seemed to facilitate the best growth, µ of shake flask D = 0.75 h^{-1}.

The second phase of this experiment was to further investigate simplified CDM. This experiment investigated if proline was required for growth, if K_2SO_4 could be substituted for cysteine, and if a greater amount of lactate (for a C:N ratio of ~8) had an affect on growth. Cultures were grown in duplicate as previously described using the media composition listed in Table 18. Cultures were monitored for OD_{600}, growth rates, and pH. At end of growth samples were removed and stored at -70°C for FHA ELISA testing. Growth curve for simplified CDM are shown in Figure 43.

CL and modified CL media performed best as expected, but contain casamino acids. The specific growth rates were 0.54 h^{-1} (CL) and 0.58 h^{-1} (modified CL). Medium G, H, and I all

performed similarly with specific growth rates between 0.40 - 0.43 h^{-1}. Based on this study, proline did not seem to be necessary for growth and K_2SO_4 can be substituted for cysteine.

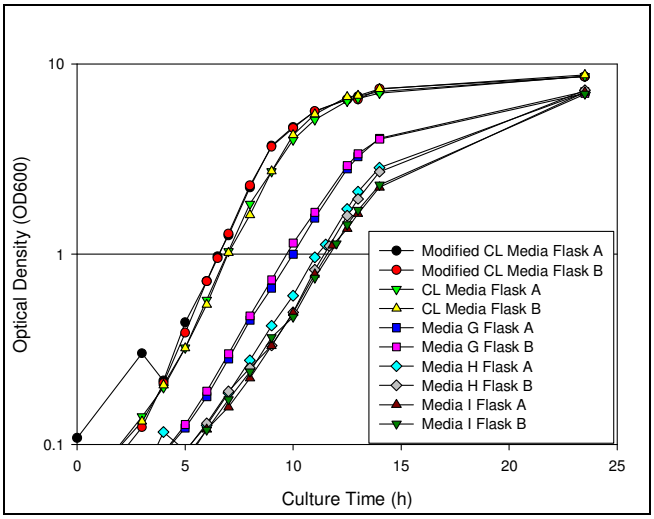

Figure 43: Simplified CDM growth curves during shake flask cultivation

Table 18: Simplified CDM composition (C:N ~8)

Component (g/L)	CL	Modified CL	Media G	Media H	Media I
L-Glutamic Acid, monosodium salt monohydrate (Sigma G2834, Lot 06411KE)	10.7	10.7	10.7	10.7	10.7
L-proline (Sigma P5607-25G Batch 077K0009)	0.24	0.24	0.24	0.24	0
NaCl (Mallinckrodt 7532-20, Lot H50602)	2.5	2.5	2.5	2.5	2.5
KH_2PO_4 (Mallinckrodt 7096-06, Lot G43581)	0.5	0.5	0.5	0.5	0.5
$MgCl_2 \cdot 6H_20$ (Sigma-Aldrich M2670, Batch 028K00222)	0.1	0.1	0.1	0.1	0.1
KCl (Mallinckrodt 6838-06, Lot E48N94)	0.2	0.2	0.2	0.2	0.2
$FeSO_4 \cdot 7H_2O$ (JT Baker 2070-01, Lot C17H24)	0.01	0.01	0.01	0.01	0.01
$CaCl_2$ (JT Baker 1311-01, Lot V45599)	0.02	0.02	0.02	0.02	0.02
Nicotinic acid (Sigma N0765, Batch 126K0693)	0.004	0.004	0.004	0.004	0.004
Casamino Acids (BD 223050 Lot 0221441)	10	10	0	0	0
Cysteine $HCl \cdot H_2O$ (Sigma C-7880, Lot 32K0890)	0.04	0.04	0.04	0.5	0.5
Tris (Sigma-Aldrich 252859, Batch 07705HH)	6.1	1.52	1.52	1.52	1.52
Glutathione (reduced) (Sigma-Aldrich G4251, Lot 030M1775)	0.15	0.001	0.001	0.001	0.001
L-Ascorbic acid (Aldrich A92902, Batch 04308LC)	0.4	0.02	0.02	0.02	0.02
β-Cyclodextrin (heptakis(2,6-*O*-dimethyl)) (MP 157320, Lot 4318KA)	1	1	1	1	1
Lactic Acid, 85% (JT Baker 0194-01, J11J03)	0	0	10	10	10
K_2SO_4(Sigma P8541, Lot128K00992)	0	0	0.4	0	0

*initial pH 6.6

Samples were taken at 23.5 h for FHA ELISA testing. The ELISA results are shown in Table 19. Modified CL media produced the greatest concentration of FHA, as expected. Modified CL media produced nearly 5.5 times the FHA concentration in the unmodified CL media. This may be due to the decreased ionic composition of the media. This was explored in *B. pertussis* for pertussis toxin by Frohlich et al. in 1995. The culture which produced the least amount of FHA was supplemented with 0.4 g/L K_2SO_4 (2.3 mM). This supported the literature which states SO_4 inhibits virulence factor production by switching to the Bvg^- phase. The experiment suggests that either Medium H or Medium I could be used in future experiments. Both of which produced a greater amount of FHA at lower OD_{600} readings than the literature defined CL medium. Medium I was the most simplified medium screened with proline removed. This suggests that balancing the media may improve the concentration of virulence factors.

Table 19: FHA concentrations in simplified CDM based on ELISA

Shake Flask	Sample Average (ng/ml)	Overall Media Average (ng/ml)
CL Flask A	935.6	914.9
CL Flask B	899.4	
Modified CL Flask A	4996.8	5015.6
Modified CL Flask B	5034.5	
Medium G Flask A	175.6	184.5
Medium G Flask B	191.2	
Medium H Flask A	1120.9	1364.7
Medium H Flask B	1689.7	
Medium I Flask A	1120.0	1258.0
Medium I Flask B	1419.1	

It is important to note that a precipitation was observed during the shake flask experimentation in all media. A repeat of the experiment confirmed that the precipitation was formed sometime between 10 and 21 hours of culture growth. The OD and pH data is shown in Table 20. The OD_{600} data for shake flask experimentation must be considered invalid. The precipitation is shown in Figure 44.

Table 20: OD_{600} and pH values for repeated CDM experiment (C:N ~8)

OD_{600}					
Culture time (h)	**CL**	**Modified CL**	**G**	**H**	**I**
0	0.056	0.054	0.052	0.052	0.052
4.5	0.255	0.286	0.171	0.124	0.107
10	2.574	2.989	1.782	0.746	0.597
21	6.560	5.989	6.157	5.664	5.372
pH					
Culture time (h)	**CL**	**Modified CL**	**G**	**H**	**I**
0	6.41	6.48	6.50	6.48	6.49
4.5	6.47	6.69	6.75	6.65	6.59
10	7.12	7.54	7.84	7.46	7.35
21	8.41	8.68	9.15	8.84	8.79

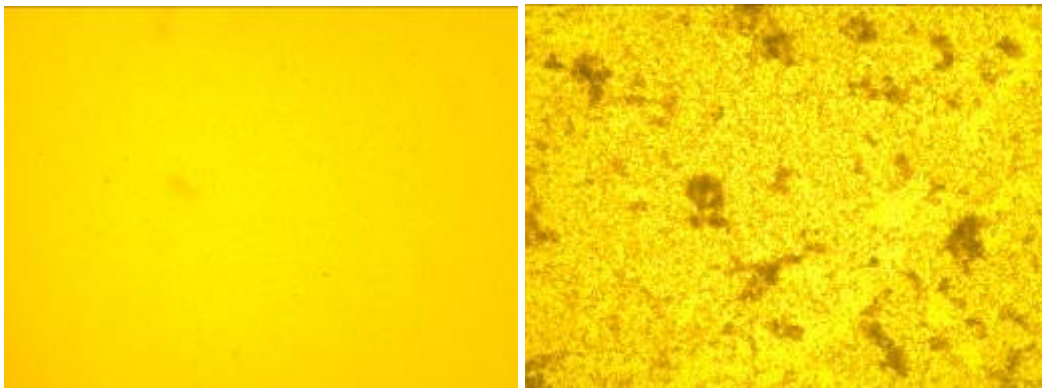

Figure 44: Shake flask CDM-I precipitation at 10 h and 21 h post inoculation: 4X magnification

A subsequent experiment was performed to investigate the formation of precipitate. A small shake flask experiment was performed at 37°C at 150 RPM using medium I at pH 6.6, 7.0, 7.5, 8.0, 7.5 without salts/glutamate, 7.5 without cysteine, 7.5 without ascorbic acid, 7.5 without lactate, and 7.5 without β-Cyclodextrin(heptakis(2,6-*O*-dimethyl)). After 48 hours, no precipitation was formed in any condition tested. It was concluded that the increasing pH of an actively growing culture along with byproduct formation or component reduction caused an irreversible precipitation to occur in shake flask cultures. A trial bioreactor batch fermentation

was performed using CDM-I (1 L working volume, pH 6.9, 37°C, 400 RPM, 400 mL/min sparged air) and inoculated from actively growing plates. No precipitation was observed. All subsequent experiments were therefore performed in bioreactors.

APPENDIX C

EFFECT OF Mg, SO_4, NICOTINIC ACID CONCENTRATIONS ON GROWTH AND FHA GENERATION BY BORDETELLA BRONCHISEPTICA RAW DATA

BioXpert Fermentation Control Charts

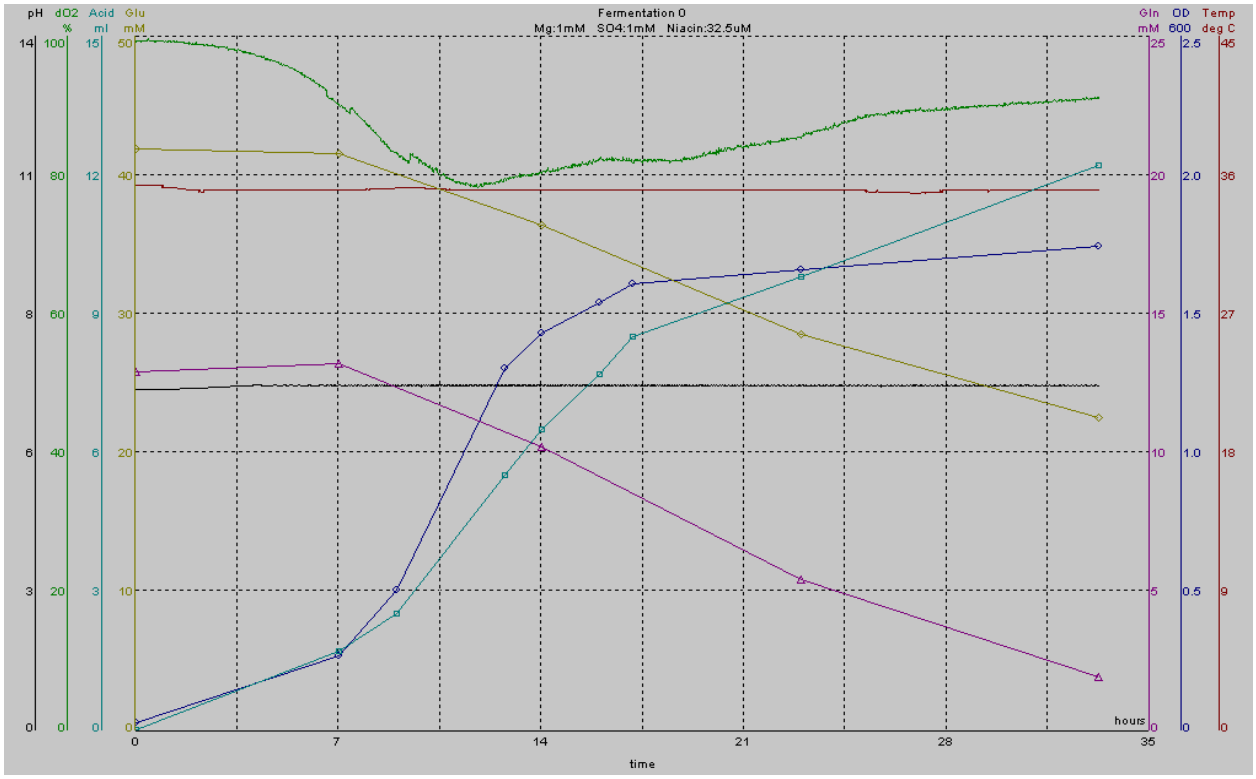

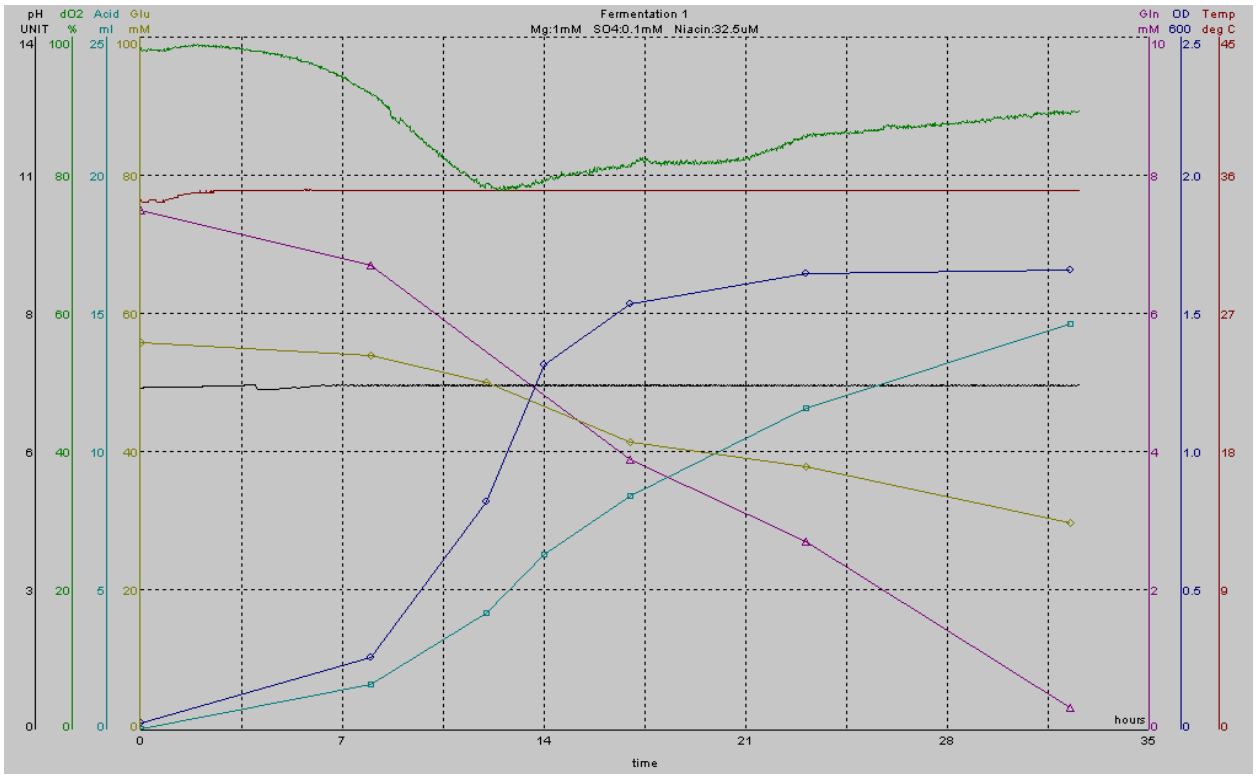
Fermentation 1
Mg:1mM SO4:0.1mM Niacin:32.5uM
pH UNIT
dO2 %
Acid ml
Glu mM
Gln mM
OD 600
Temp deg C
hours
time

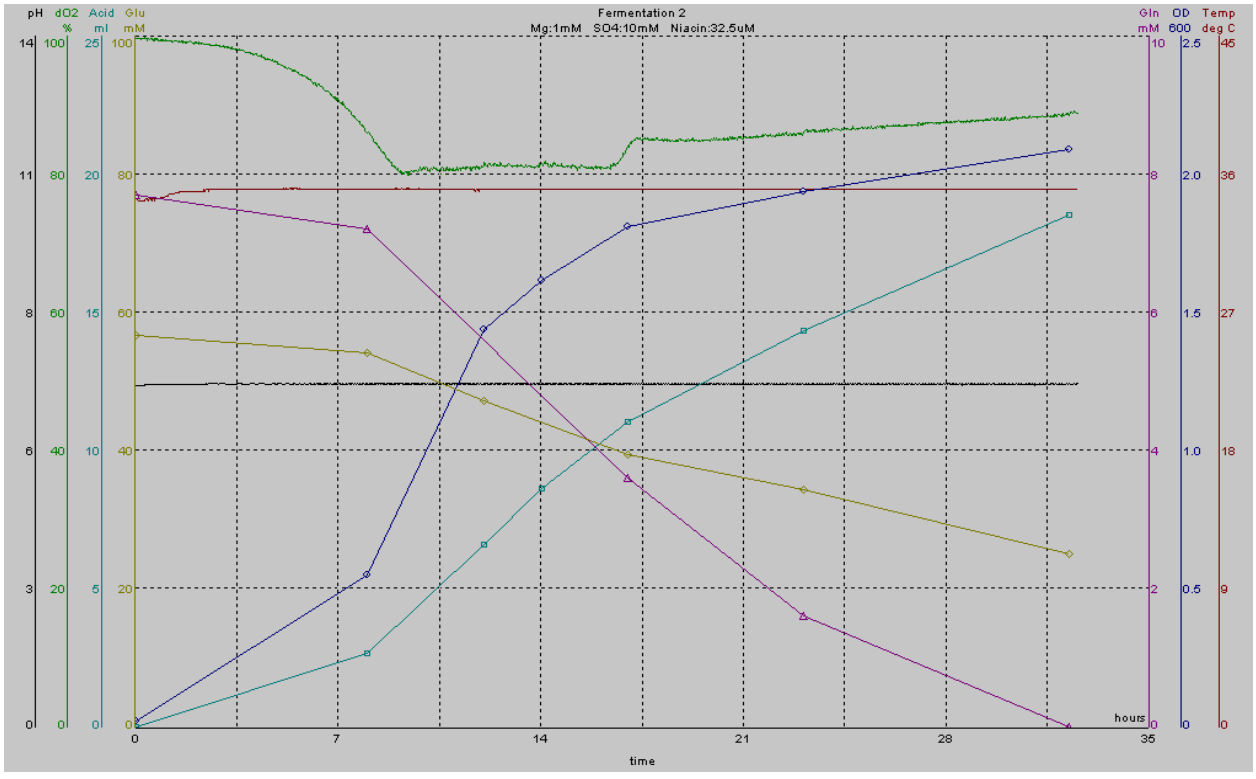
Fermentation 2
Mg:1mM SO4:10mM Niacin:32.5uM
pH UNIT
dO2 %
Acid ml
Glu mM
Gln mM
OD 600
Temp deg C
hours
time

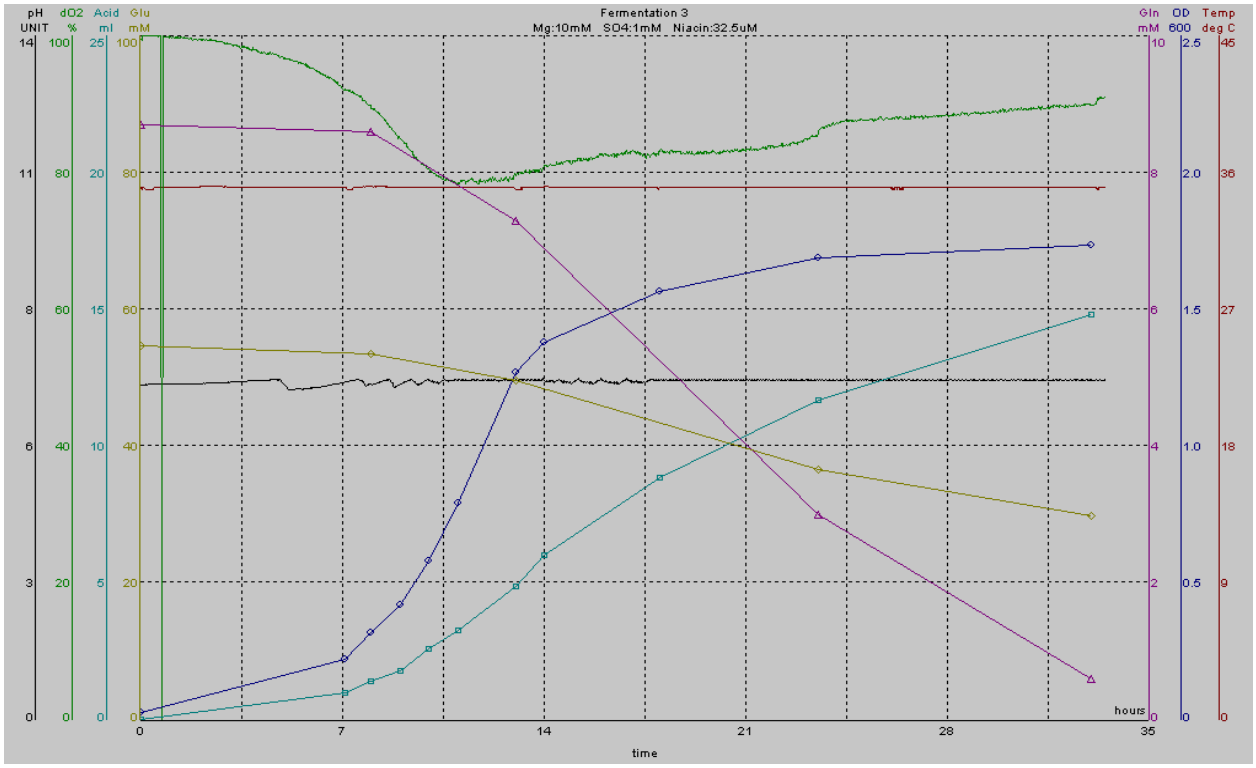
Fermentation 3
Mg:10mM SO4:1mM Niacin:32.5uM
pH UNIT
dO2 %
Acid ml
Glu mM
Gln mM
OD 600
Temp deg C
hours
time

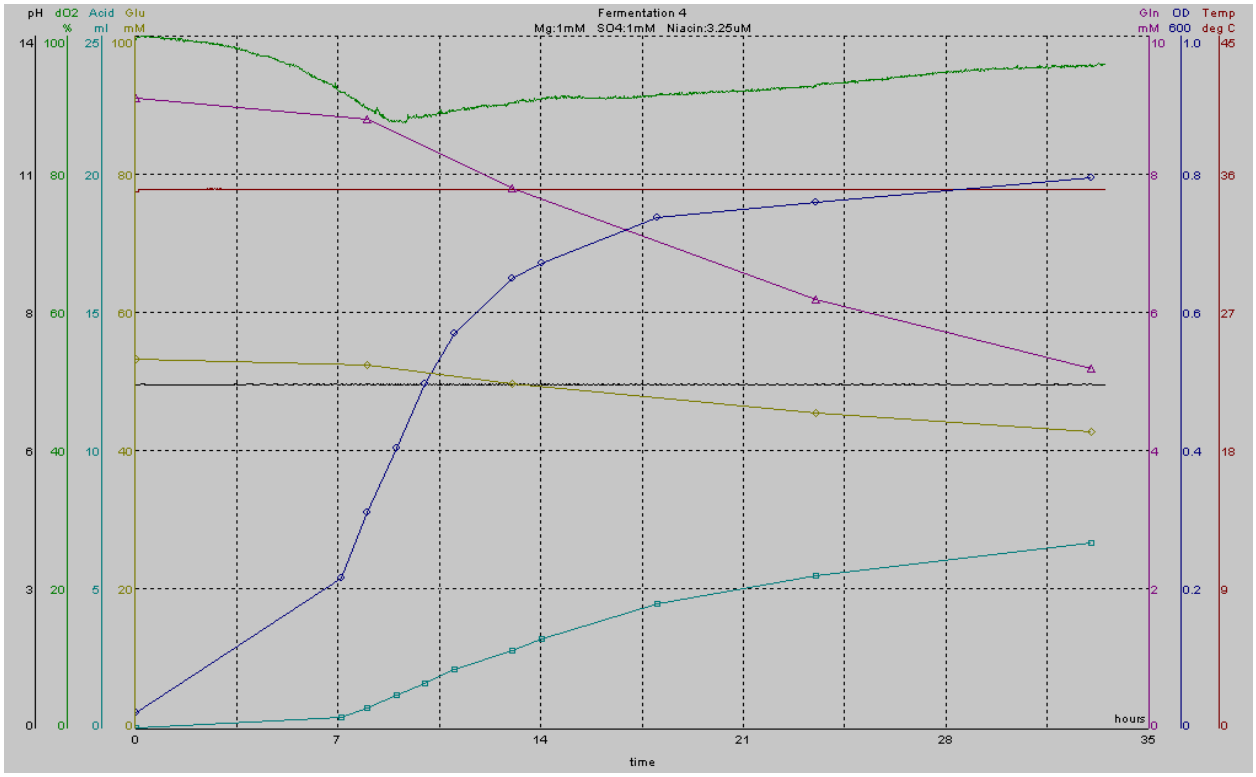
Fermentation 4
Mg:1mM SO4:1mM Niacin:3.25uM
pH UNIT
dO2 %
Acid ml
Glu mM
Gln mM
OD 600
Temp deg C
hours
time

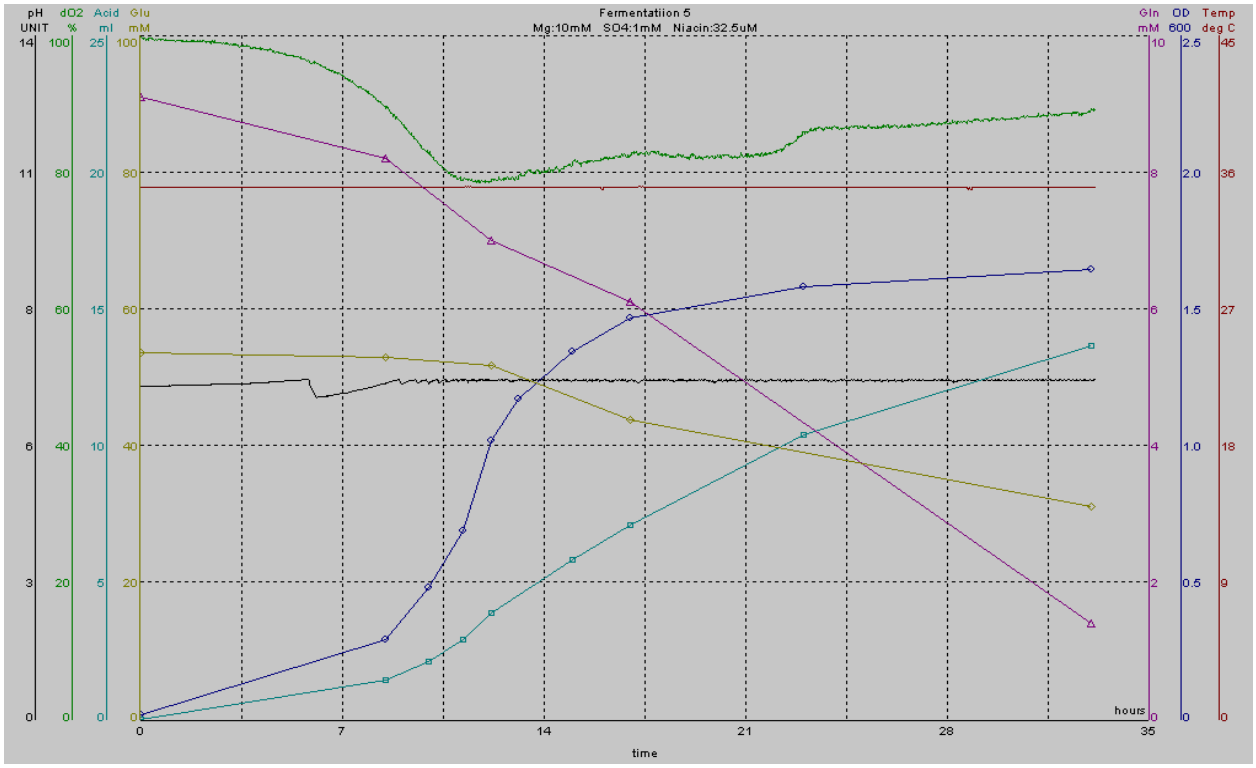
Fermentatiion 5
Mg:10mM SO4:1mM Niacin:32.5uM
pH UNIT
dO2 %
Acid ml
Glu mM
Gln mM
OD 600
Temp deg C
hours
time

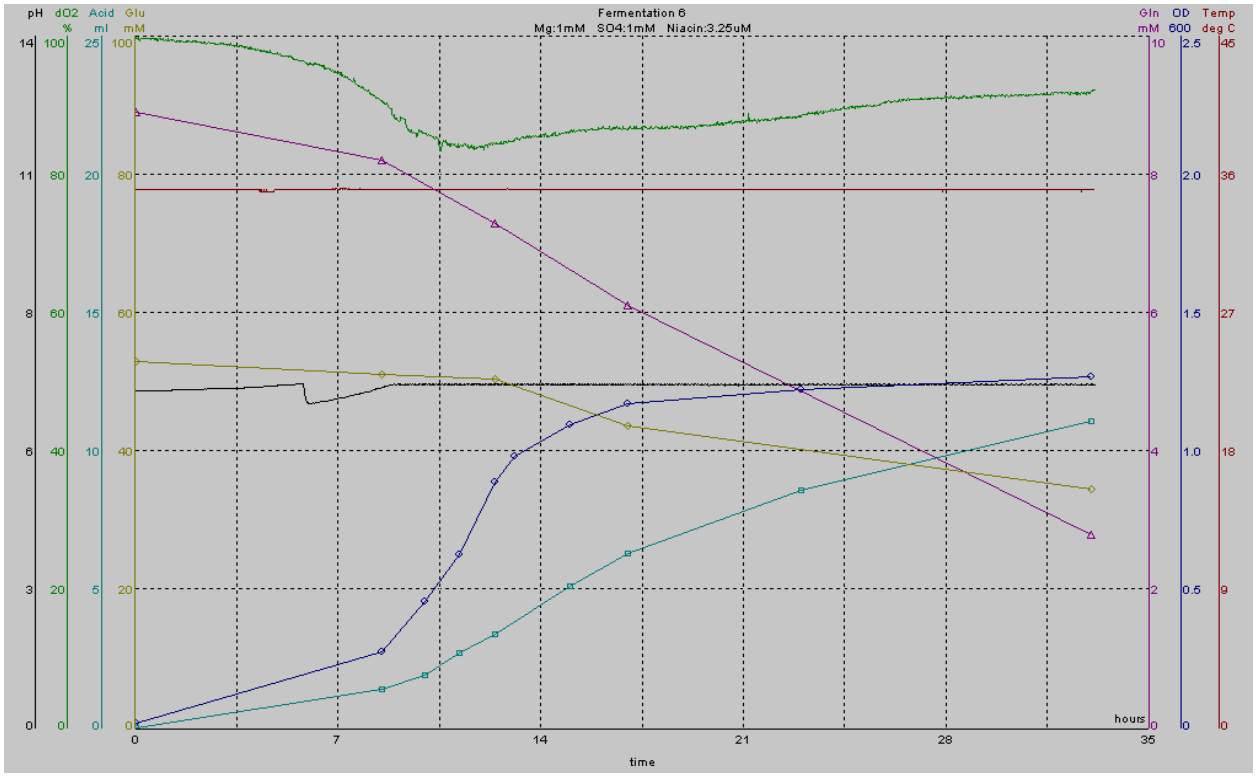
Fermentation 6
Mg:1mM SO4:1mM Niacin:3.25uM
pH
dO2 %
Acid ml
Glu mM
Gln mM
OD 600
Temp deg C
hours
time

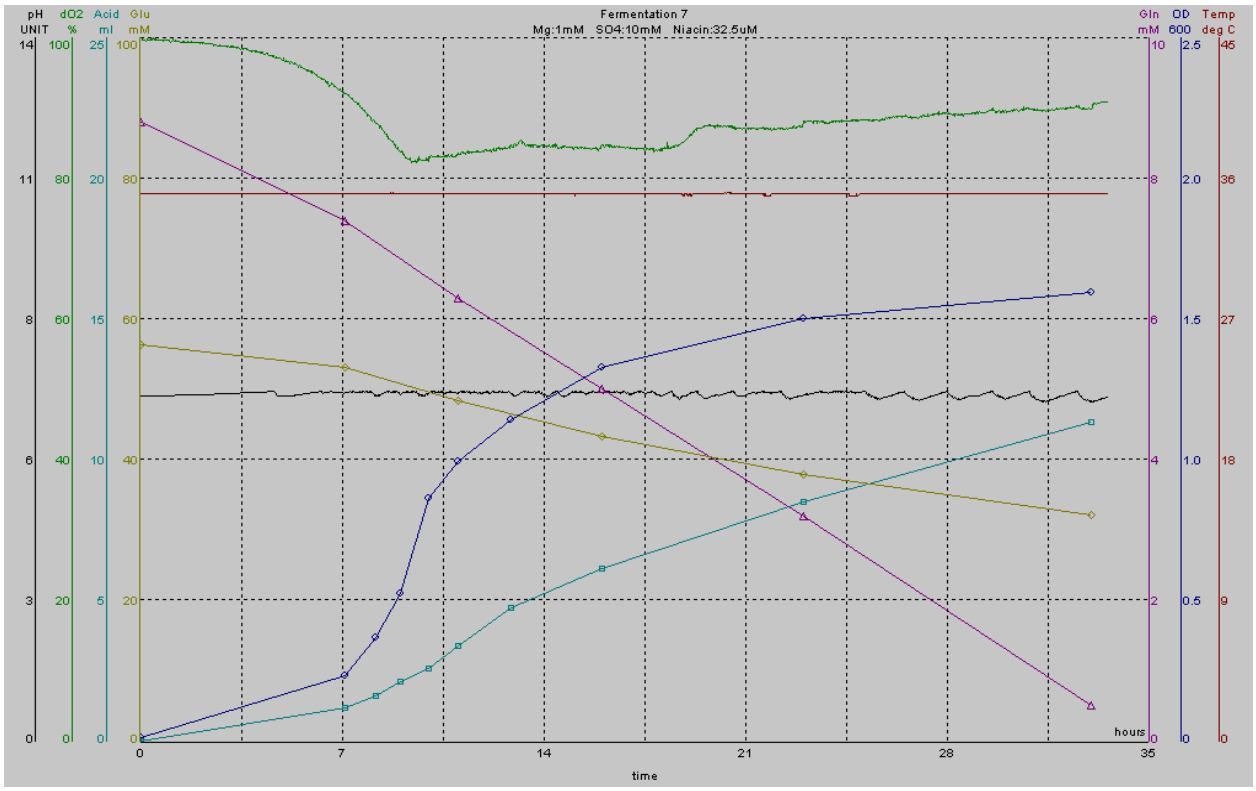
Fermentation 7
Mg:1mM SO4:10mM Niacin:32.5uM
pH UNIT
dO2 %
Acid ml
Glu mM
Gln mM
OD 600
Temp deg C
hours
time

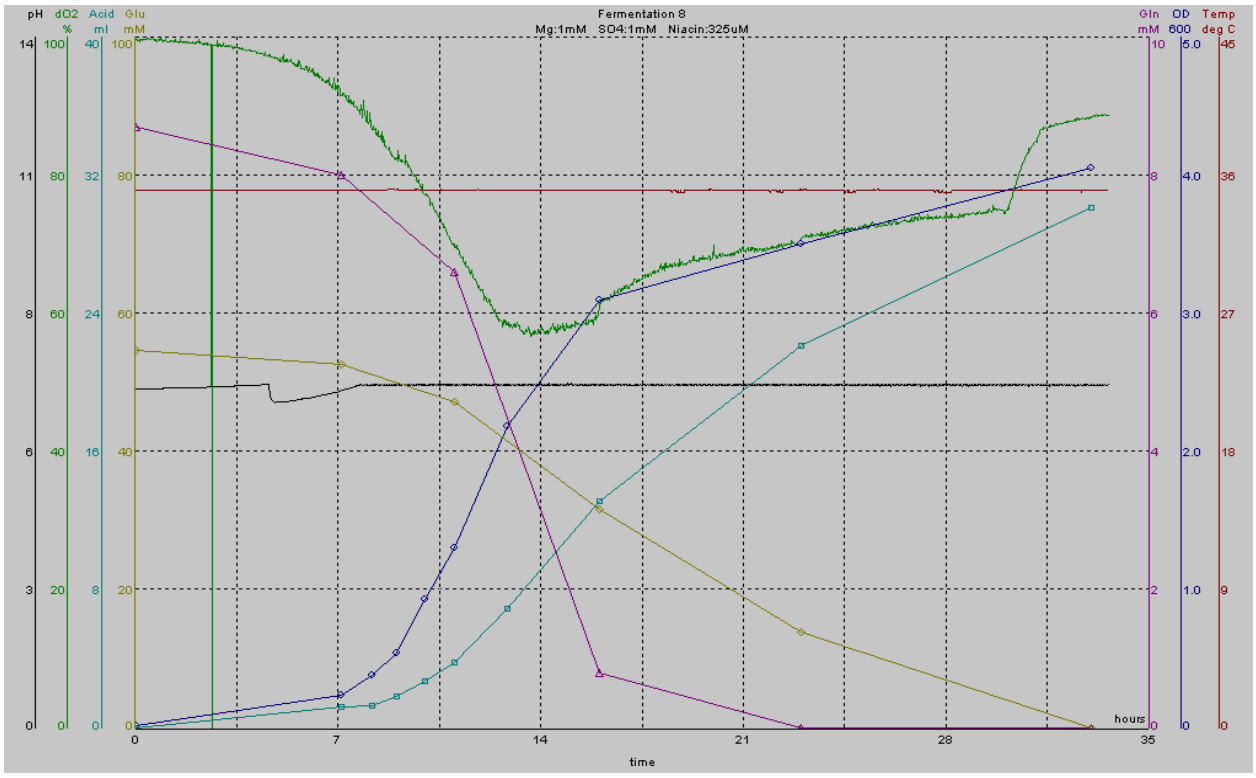
Fermentation 8
Mg:1mM SO4:1mM Niacin:325uM
pH
dO2 %
Acid ml
Glu mM
Gln mM
OD 600
Temp deg C
hours
time

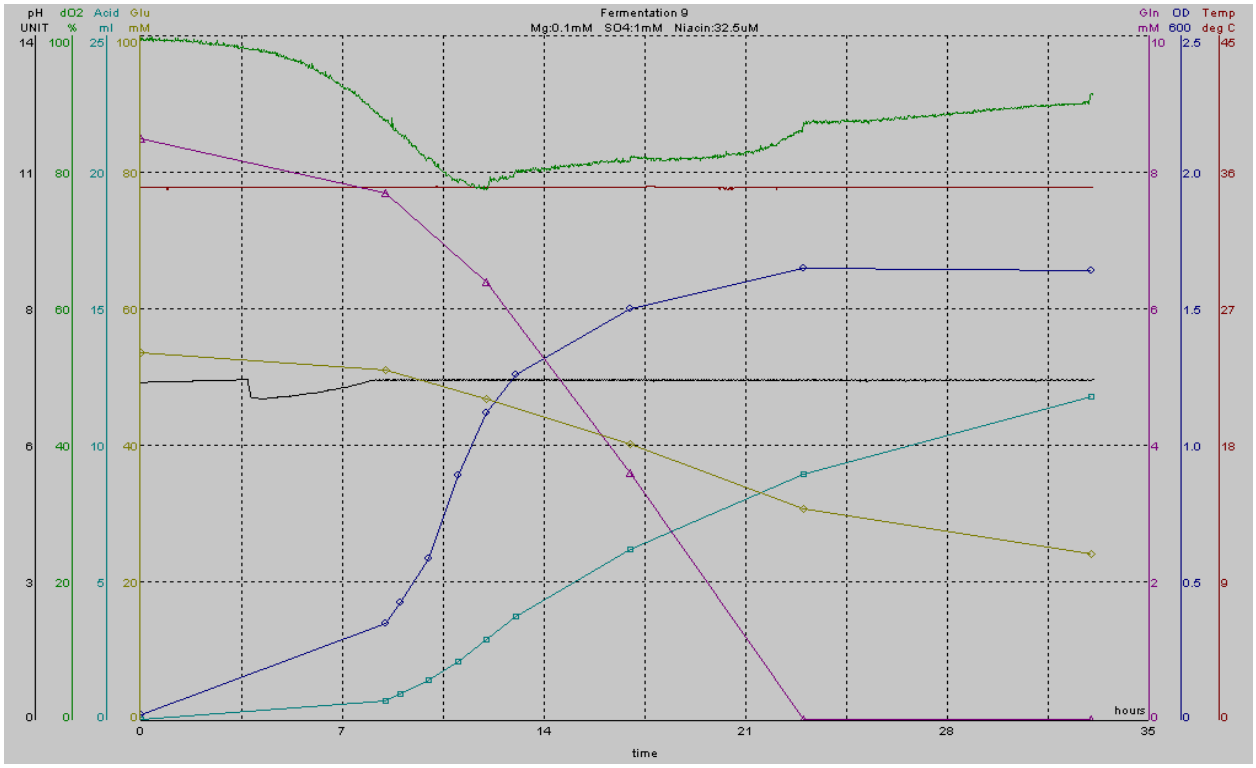
Fermentation 9
Mg:0.1mM SO4:1mM Niacin:32.5uM
pH UNIT
dO2 %
Acid ml
Glu mM
Gln mM
OD 600
Temp deg C
hours
time

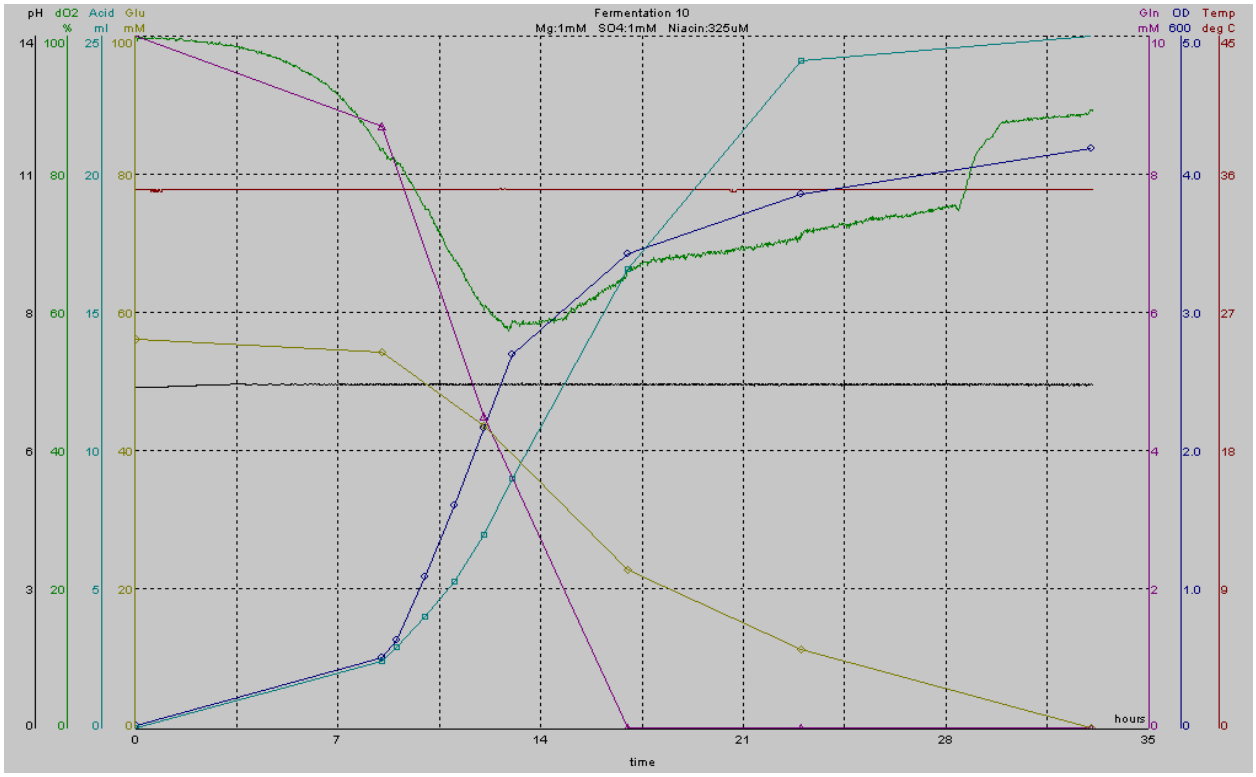
Fermentation 10
Mg:1mM SO4:1mM Niacin:325uM
pH UNIT
dO2 %
Acid ml
Glu mM
Gln mM
OD 600
Temp deg C
hours
time

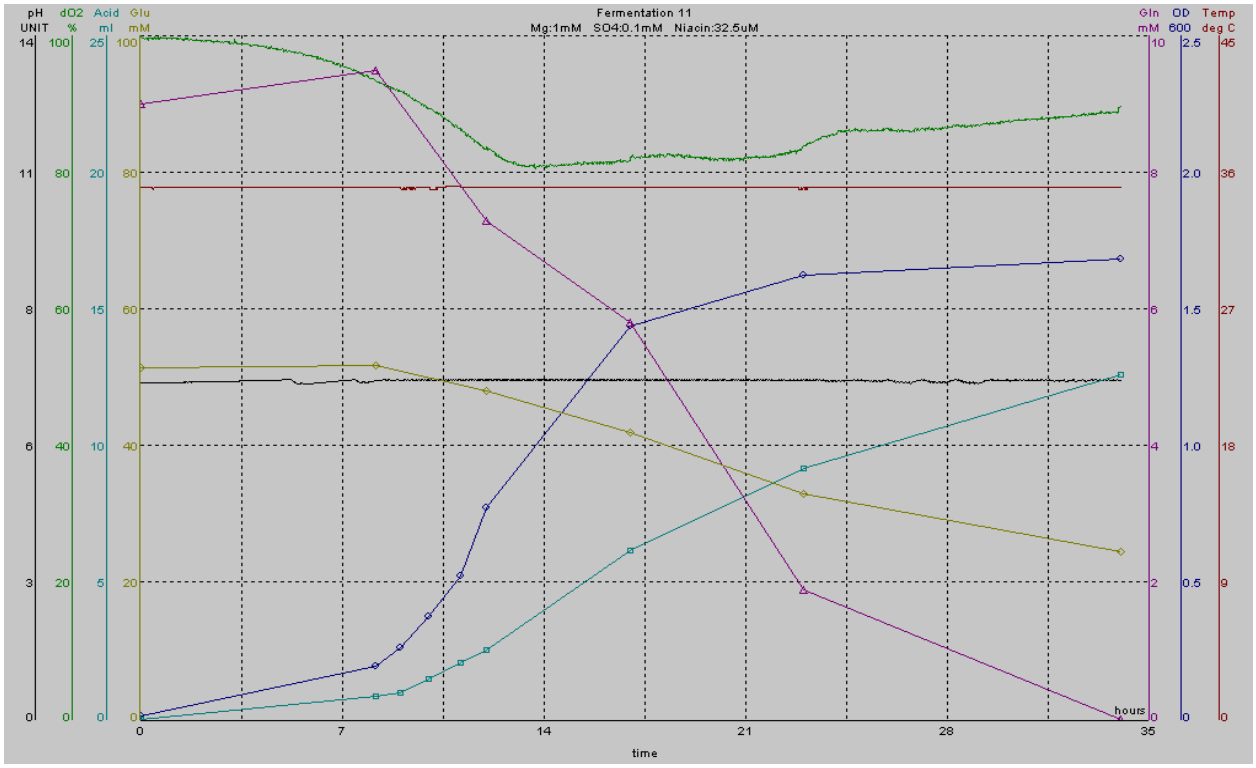
Fermentation 11
Mg:1mM SO4:0.1mM Niacin:32.5uM
pH UNIT
dO2 %
Acid ml
Glu mM
Gln mM
OD 600
Temp deg C
hours
time

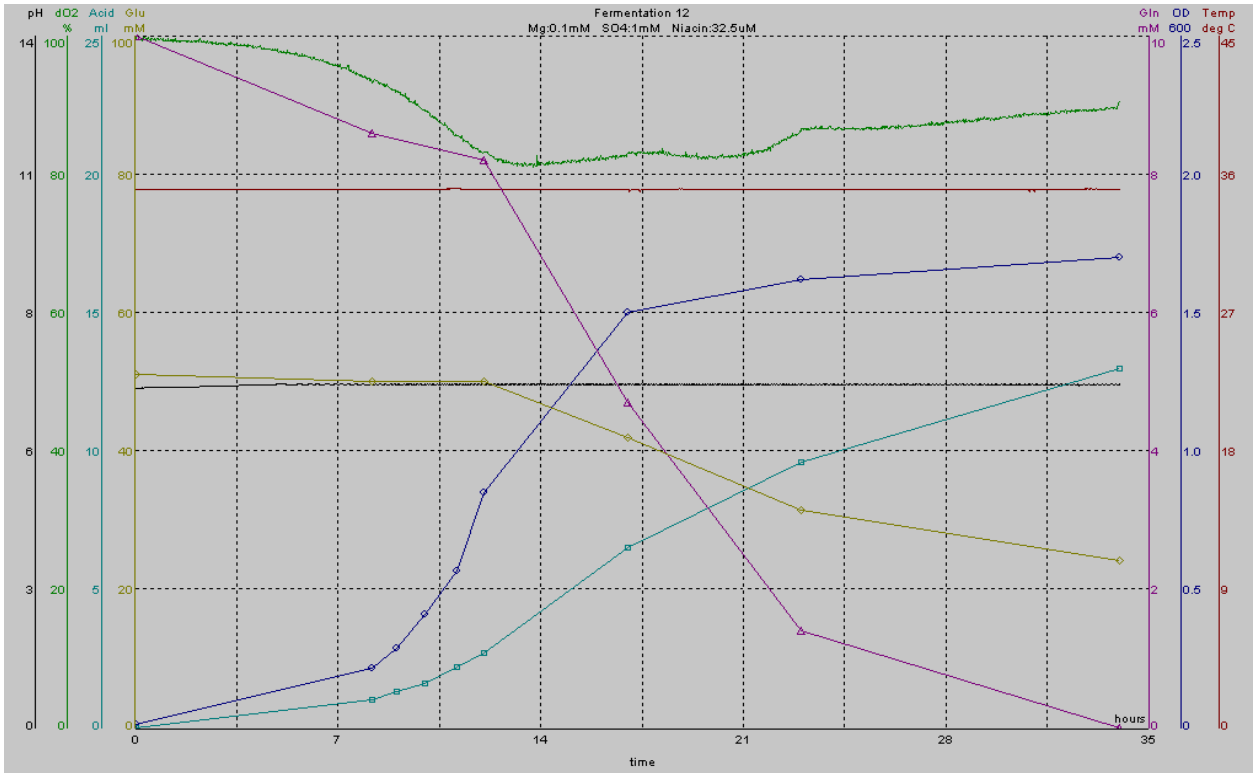
Fermentation 12
Mg:0.1mM SO4:1mM Niacin:32.5uM
pH
dO2 %
Acid ml
Glu mM
Gln mM
OD 600
Temp deg C
hours
time

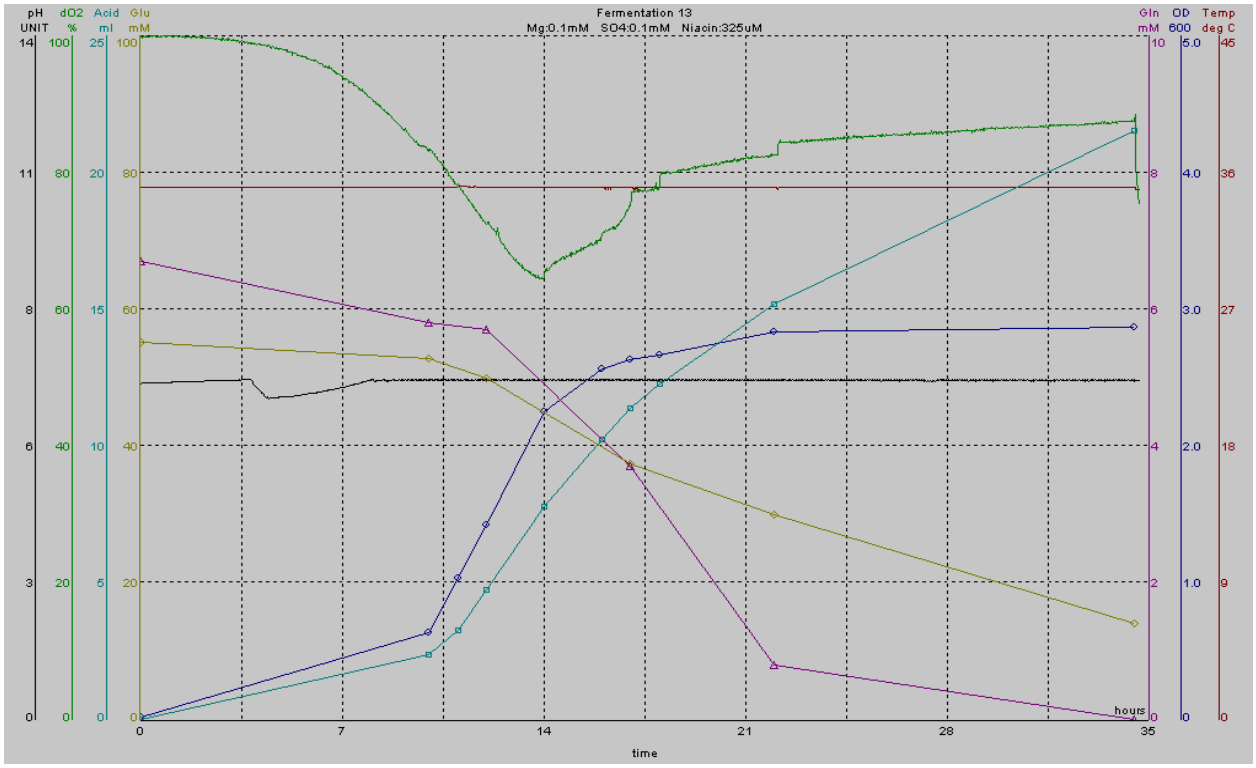
Fermentation 13
Mg:0.1mM SO4:0.1mM Niacin:325uM
pH UNIT
dO2 %
Acid ml
Glu mM
Gln mM
OD 600
Temp deg C
hours
time

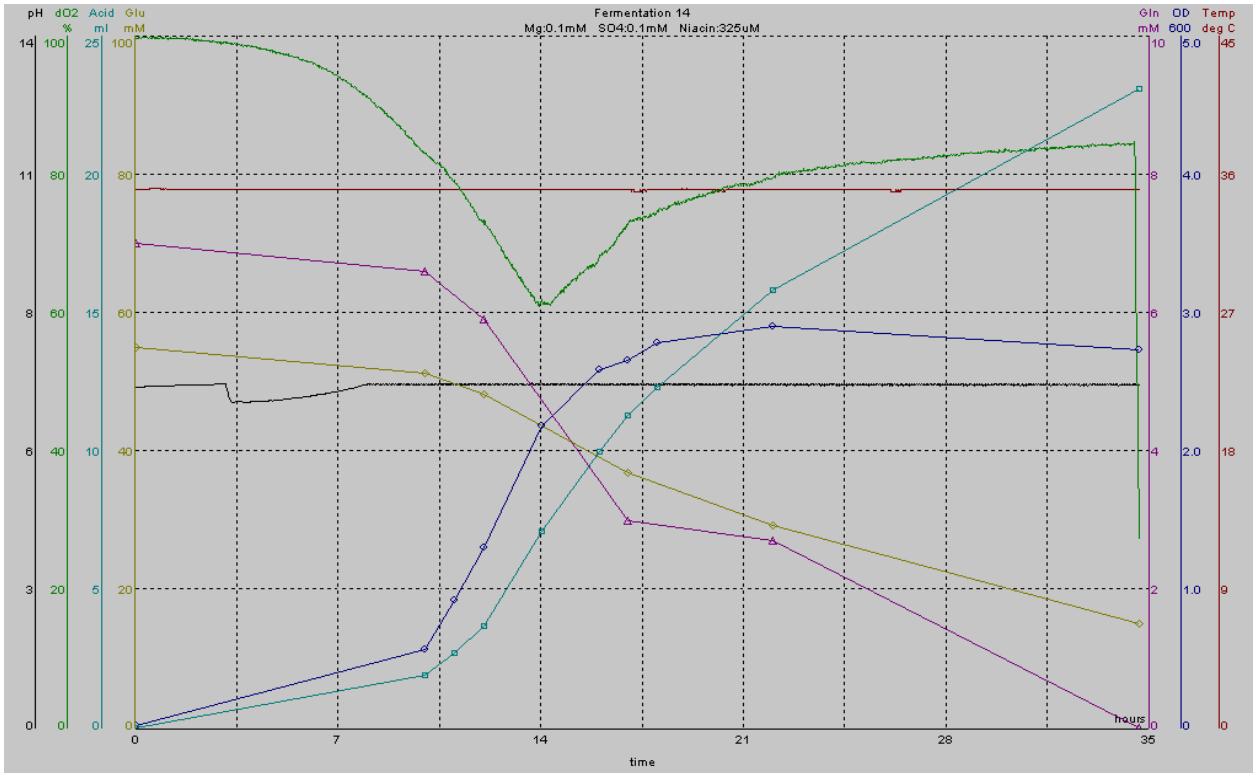
Fermentation 14
Mg:0.1mM SO4:0.1mM Niacin:325uM
pH UNIT
dO2 %
Acid ml
Glu mM
Gln mM
OD 600
Temp deg C
hours
time

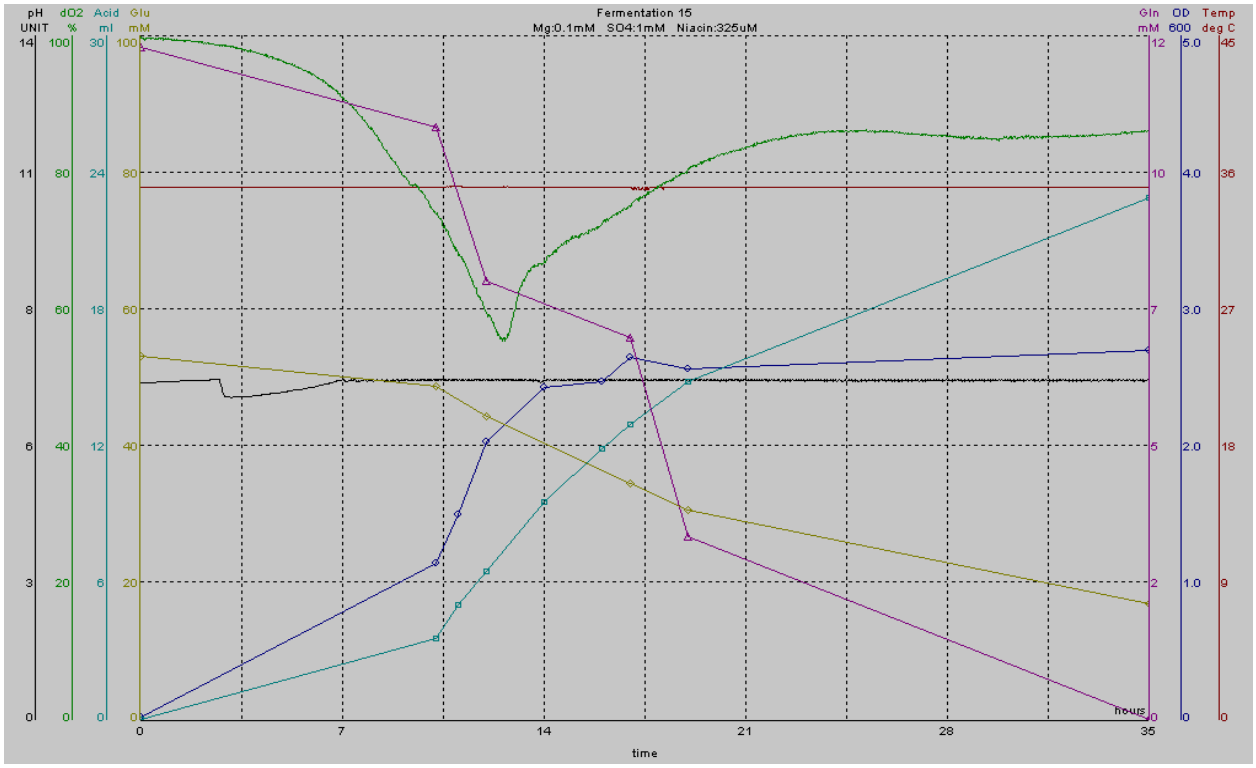
Fermentation 15
Mg:0.1mM SO4:1mM Niacin:325uM
pH UNIT
dO2 %
Acid ml
Glu mM
Gln mM
OD 600
Temp deg C
hours
time

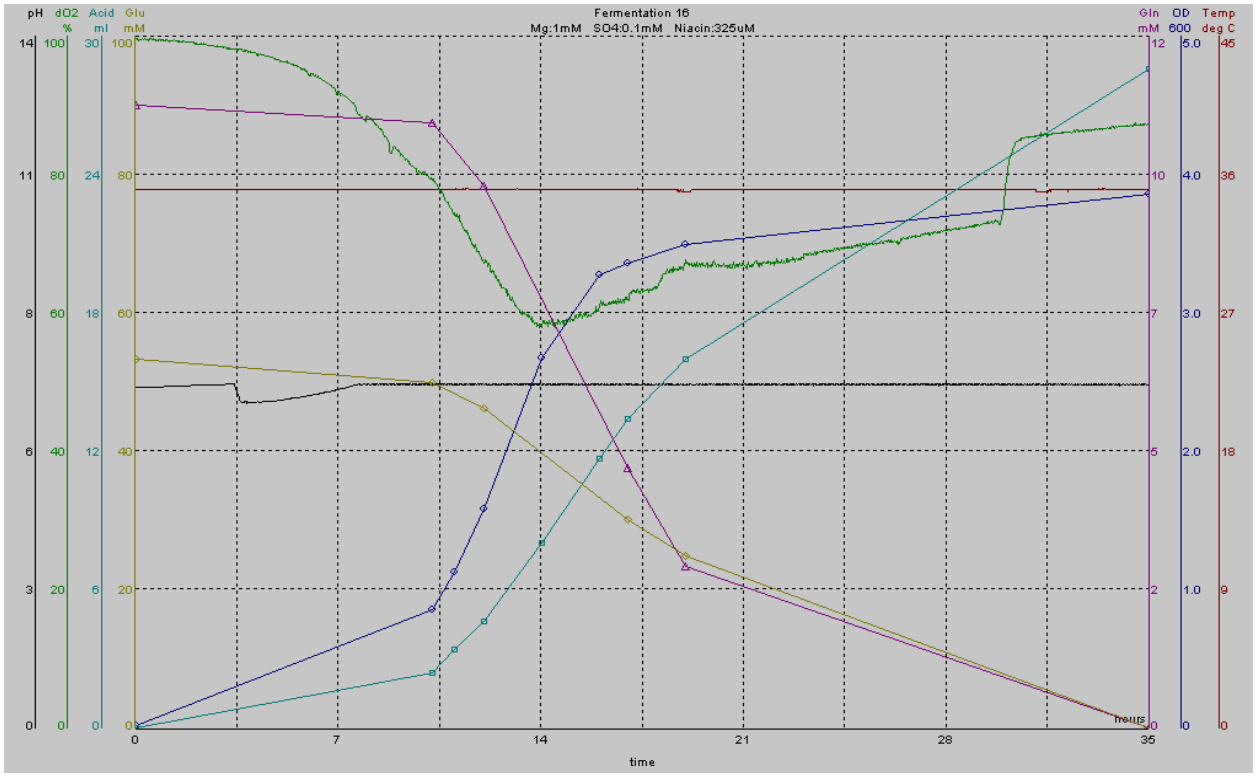
Fermentation 16
Mg:1mM SO4:0.1mM Niacin:325uM
pH UNIT
dO2 %
Acid ml
Glu mM
Gln mM
OD 600
Temp deg C
hours
time

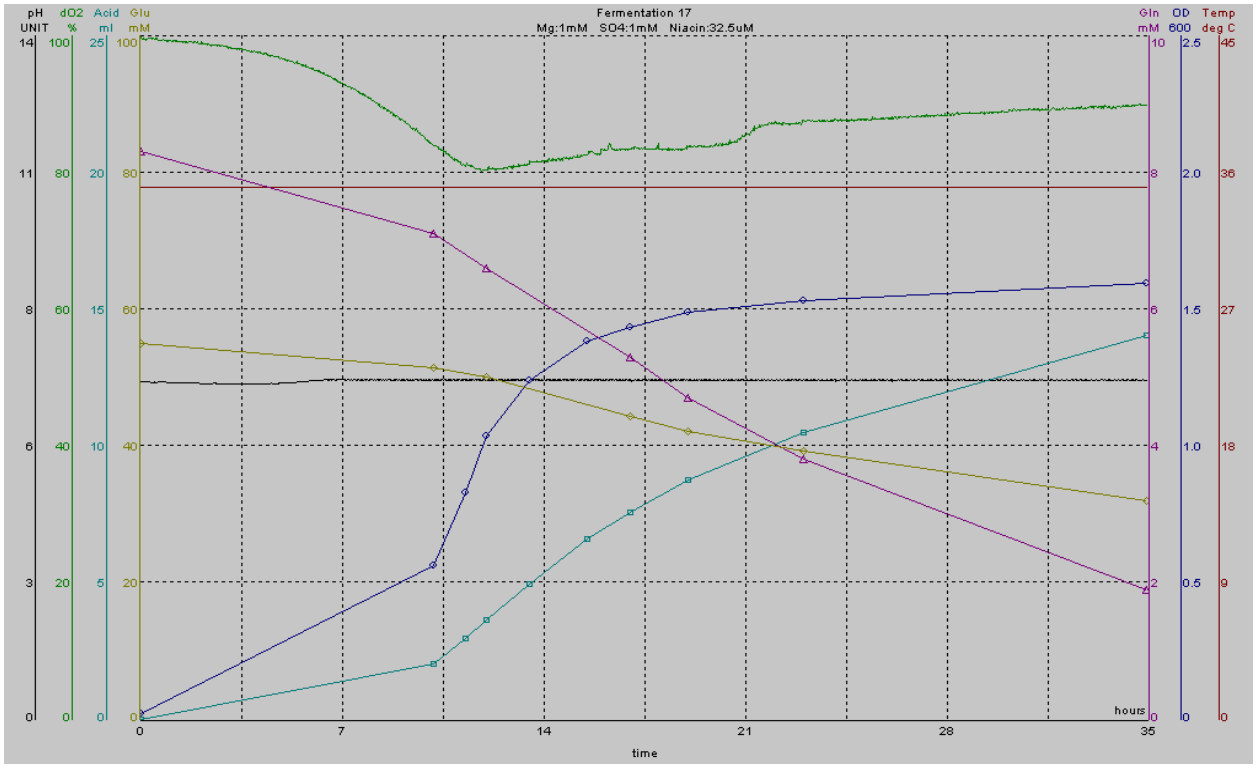
Fermentation 17
Mg:1mM SO4:1mM Niacin:32.5uM
pH UNIT
dO2 %
Acid ml
Glu mM
Gln mM
OD 600
Temp deg C
hours
time

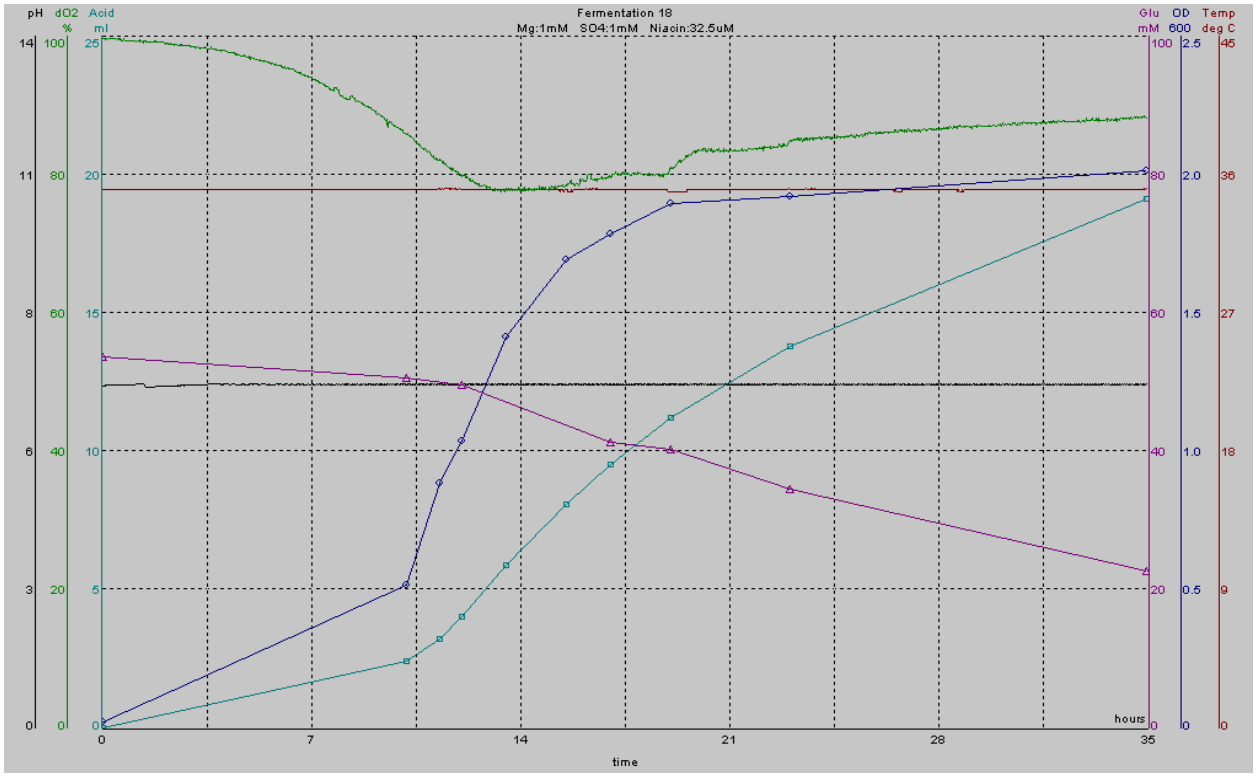
Fermentation 18
Mg:1mM SO4:1mM Niacin:32.5uM
pH
dO2 %
Acid ml
Glu mM
OD 600
Temp deg C
hours
time

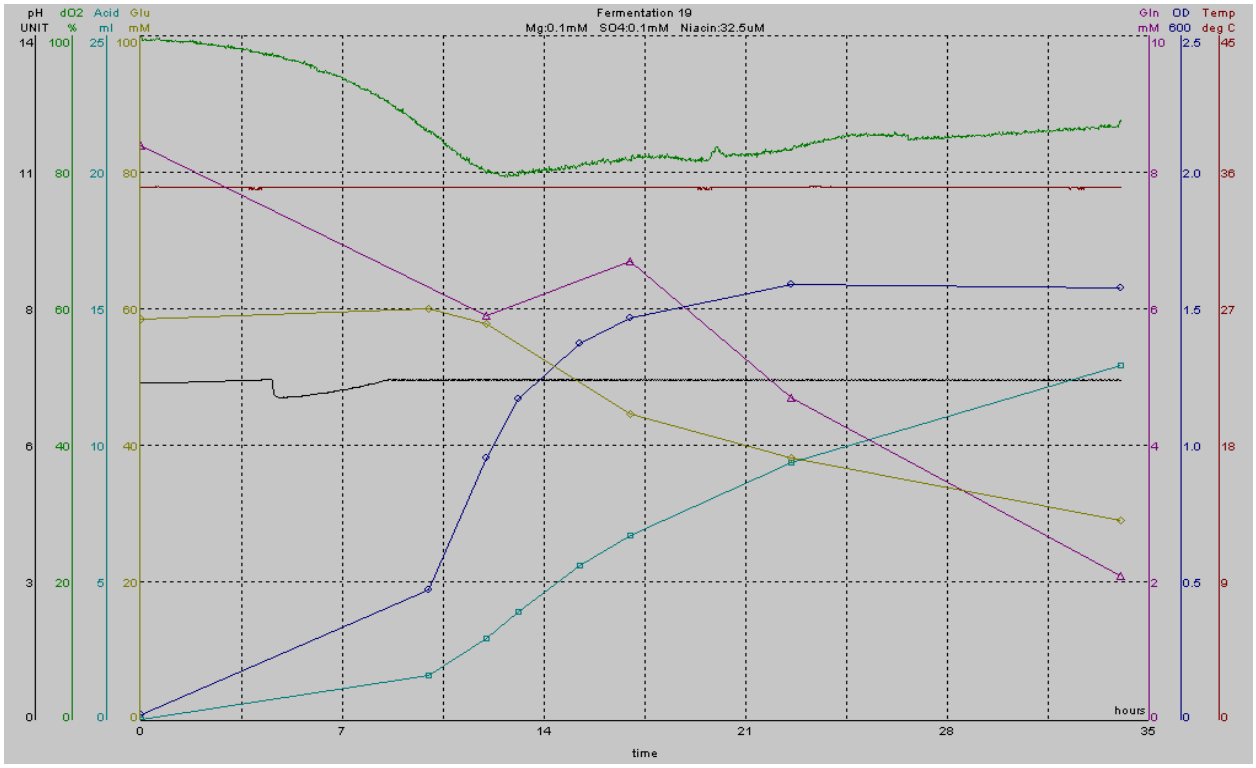
Fermentation 19
Mg:0.1mM SO4:0.1mM Niacin:32.5uM
pH UNIT
dO2 %
Acid ml
Glu mM
Gln mM
OD 600
Temp deg C
hours
time

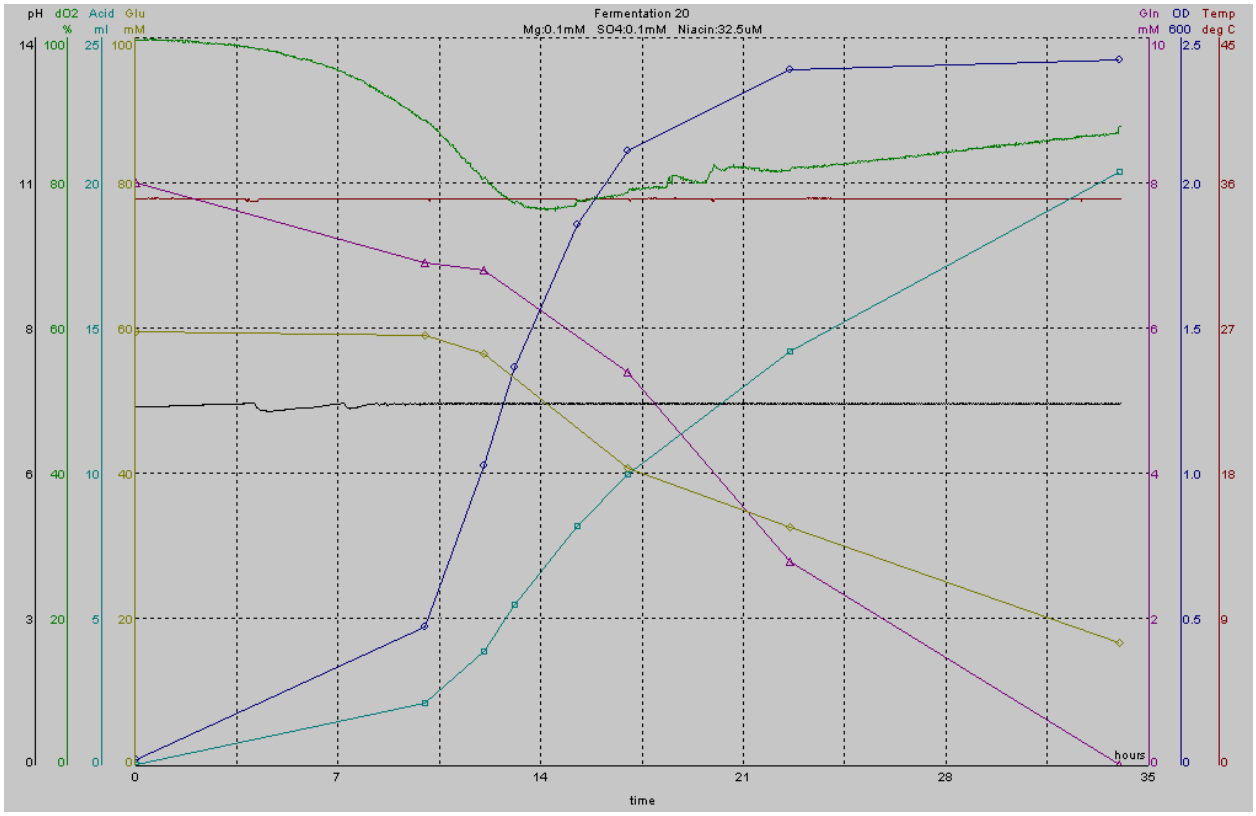
Fermentation 20
Mg:0.1mM SO4:0.1mM Niacin:32.5uM
pH
dO2 %
Acid ml
Glu mM
Gln mM
OD 600
Temp deg C
hours
time

FHA ELISA

Fermentation	11-14 h (ng/ml)	16-18 h (ng/ml)	32-34 h (ng/ml)
0	450.7		211.4
1	396.7	856.0	573.3
2	0.0	0.0	0.0
3	313.6	377.7	355.8
4	84.1	167.4	234.1
5	431.9	347.4	263.5
6	505.4	432.2	480.9
7	-	0.0	0.0
8	329.1	731.0	849.9
9	486.7	885.4	614.3
10	515.8	970.4	1065.2
11	256.6	823.9	1051.1
12	402.1	989.8	1167.2
13	499.2	622.7	325.4
14	476.1	683.8	367.1
15	475.2	801.9	434.1
16	546.9	1014.5	405.8
17	426.3	191.6	193.9
18	416.2	251.4	206.1
19	523.0	396.9	287.2
20	473.3	514.6	332.0

Fermentation	11-14 h (ng/OD_{600} unit)	16-18 h (ng/OD_{600} unit)	32-34 h (ng/OD_{600} unit)
0	315.2	-	121.3
1	482.5	557.3	345.6
2	0.0	0.0	0.0
3	247.2	241.2	205.2
4	137.7	226.8	294.1
5	447.6	236.8	160.3
6	630.9	369.4	379.0
7	-	0.0	0.0
8	252.8	236.1	209.9
9	435.0	589.1	374.6
10	237.9	283.4	254.2
11	331.6	573.3	624.5
12	473.6	658.5	686.2
13	351.8	236.8	113.4
14	365.7	257.5	134.5
15	234.3	303.2	161.1
16	345.2	301.9	105.3
17	411.9	133.6	121.5
18	402.1	140.9	102.4
19	548.2	270.5	182.2
20	461.3	244.0	137.0

Statistical Analysis

Run	Factor 1	Factor 2	Factor 3	Response 1	Response 2
	A: Mg	B: SO_4	C: Nicotinic Acid	ELISA	Spec. ELISA
	mM	mM	μM	ng/mL	ng/OD unit
0	0	0	0	450.7	315.2
1	0	-1	0	856	557.3
2	0	1	0	0	0
3	1	0	0	377.7	247.2
4	0	0	-1	234.1	294.1
5	1	0	0	431.9	447.6
6	0	0	-1	505.4	630.9
7	0	1	0	0	0
8	0	0	1	849.9	252.8

9	-1	0	0	885.4	589.1
10	0	0	1	1065.2	283.4
11	0	-1	0	1051.1	624.5
12	-1	0	0	1167.2	686.2
13	-1	-1	1	622.7	351.8
14	-1	-1	1	683.8	365.7
15	-1	0	1	801.9	303.2
16	0	-1	1	1014.5	345.2
17	0	0	0	426.3	411.9
18	0	0	0	416.2	402.1

Response	**1**	**ELISA**				
ANOVA for Response Surface Reduced Quadratic Model						
Analysis of variance table [Partial sum of squares - Type III]						
Source	**Sum of Squares**	**df**	**Mean Square**	**F Value**	**p-value Prob > F**	
Model	2.05E+06	7	2.93E+05	22.92	< 0.0001	significant
A-Mg	*3.86E+05*	*1*	*3.86E+05*	*30.27*	*0.0002*	
B-SO_4	*9.09E+05*	*1*	*9.09E+05*	*71.26*	*< 0.0001*	
C-Nicotinic Acid	*4.22E+05*	*1*	*4.22E+05*	*33.09*	*0.0001*	
AC	*4.92E+05*	*1*	*4.92E+05*	*38.54*	*< 0.0001*	
BC	*2.73E+05*	*1*	*2.73E+05*	*21.41*	*0.0007*	
A^2	*1.70E+05*	*1*	*1.70E+05*	*13.32*	*0.0038*	
C^2	*1.34E+05*	*1*	*1.34E+05*	*10.53*	*0.0078*	
Residual	1.40E+05	11	12759.38			
Lack of Fit	*17672.03*	*2*	*8836.01*	*0.65*	*0.5458*	*not significant*
Pure Error	*1.23E+05*	*9*	*13631.24*			
Cor Total	2.19E+06	18				

Final Equation in Terms of Actual Factors:	
ELISA	=
+457.2	
-310.8	* Mg
-476.8	* SO_4
+311.0	* Nicotinic Acid
+827.6	* Mg * Nicotinic Acid
+522.6	* SO_4 * Nicotinic Acid
+258.4	* Mg^2

+223.6	* Nicotinic Acid^2

Response	**2**	**Spec. ELISA**				
ANOVA for Response Surface Reduced Quadratic Model						
Analysis of variance table [Partial sum of squares - Type III]						
Source	**Sum of Squares**	**df**	**Mean Square**	**F Value**	**p-value Prob > F**	
Model	5.44E+05	6	90606.74	10.35	0.0004	significant
A-Mg	*84245.06*	*1*	*84245.06*	*9.62*	*0.0092*	
B-SO_4	*3.49E+05*	*1*	*3.49E+05*	*39.88*	*< 0.0001*	
C-Nicotinic Acid	*38207.83*	*1*	*38207.83*	*4.36*	*0.0587*	
AC	*54859.37*	*1*	*54859.37*	*6.27*	*0.0278*	
BC	*49021.61*	*1*	*49021.61*	*5.6*	*0.0356*	
A^2	*64973.16*	*1*	*64973.16*	*7.42*	*0.0185*	
Residual	1.05E+05	12	8754.93			
Lack of Fit	*15058.87*	*3*	*5019.62*	*0.5*	*0.6903*	*not significant*
Pure Error	*90000.29*	*9*	*10000.03*			
Cor Total	6.49E+05	18				

Final Equation in Terms of Actual Factors:	
Spec. ELISA	=
+344.3	
-145.1	* Mg
-295.5	* SO_4
-93.3	* Nicotinic Acid
+256.6	* Mg * Nicotinic Acid
+216.7	* SO_4 * Nicotinic Acid
+148.2	* Mg^2

Supplemental Statistical Analysis (Fermentations 20 and 21 included)

Run	Factor 1	Factor 2	Factor 3	Response 1	Response 2
	A:Mg	B:SO_4	C:Nicotinic Acid	ELISA	Spec. ELISA
	mM	mM	µM	ng/mL	ng/OD unit
0	0	0	0	450.7	315.2
1	0	-1	0	856	557.3
2	0	1	0	0	0
3	1	0	0	377.7	247.2
4	0	0	-1	234.1	294.1

5	1	0	0	431.9	447.6
6	0	0	-1	505.4	630.9
7	0	1	0	0	0
8	0	0	1	849.9	252.8
9	-1	0	0	885.4	589.1
10	0	0	1	1065.2	283.4
11	0	-1	0	1051.1	624.5
12	-1	0	0	1167.2	686.2
13	-1	-1	1	622.7	351.8
14	-1	-1	1	683.8	365.7
15	-1	0	1	801.9	303.2
16	0	-1	1	1014.5	345.2
17	0	0	0	426.3	411.9
18	0	0	0	416.2	402.1
19	-1	-1	0	523	548.2
20	-1	-1	0	514.6	461.3

Response	**1**	**ELISA**				
ANOVA for Response Surface Reduced Quadratic Model						
Analysis of variance table [Partial sum of squares - Type III]						
Source	**Sum of Squares**	**df**	**Mean Square**	**F Value**	**p-value Prob > F**	
Model	1.87E+06	6	3.12E+05	12.88	< 0.0001	significant
A-Mg	*3.36E+05*	*1*	*3.36E+05*	*13.88*	*0.0023*	
B-SO_4	*8.83E+05*	*1*	*8.83E+05*	*36.53*	*< 0.0001*	
C-Nicotinic Acid	*2.93E+05*	*1*	*2.93E+05*	*12.12*	*0.0037*	
AB	*7.80E+05*	*1*	*7.80E+05*	*32.27*	*< 0.0001*	
AC	*81891.61*	*1*	*81891.61*	*3.39*	*0.0871*	
A^2	*86438.98*	*1*	*86438.98*	*3.57*	*0.0796*	
Residual	3.39E+05	14	24186.35			
Lack of Fit	*2.16E+05*	*4*	*53973.11*	*4.4*	*0.0262*	*significant*
Pure Error	*1.23E+05*	*10*	*12271.64*			
Cor Total	2.21E+06	20				

Final Equation in Terms of Actual Factors:	
ELISA	=
+515.8	
-274.9	* Mg

-431.4	* SO4
248.6	* Nicotinic Acid
-795.4	* Mg * SO_4
+257.7	* Mg * Nicotinic Acid
+163.9	* Mg^2

Response	**2**	**Spec. ELISA**				
ANOVA for Response Surface Reduced Quadratic Model						
Analysis of variance table [Partial sum of squares - Type III]						
Source	**Sum of Squares**	**df**	**Mean Square**	**F Value**	**p-value Prob > F**	
Model	5.55E+05	6	92532.89	10.11	0.0002	significant
A-Mg	*78265.81*	*1*	*78265.81*	*8.55*	*0.0111*	
B-SO_4	*3.82E+05*	*1*	*3.82E+05*	*41.77*	*< 0.0001*	
C-Nicotinic Acid	*64869.82*	*1*	*64869.82*	*7.09*	*0.0186*	
AB	*37794.24*	*1*	*37794.24*	*4.13*	*0.0616*	
B^2	*74313.71*	*1*	*74313.71*	*8.12*	*0.0129*	
C^2	*28933.39*	*1*	*28933.39*	*3.16*	*0.0972*	
Residual	1.28E+05	14	9154.15			
Lack of Fit	*34382.05*	*4*	*8595.51*	*0.92*	*0.4911*	*not significant*
Pure Error	*93776.09*	*10*	*9377.61*			
Cor Total	6.83E+05	20				

Final Equation in Terms of Actual Factors:	
Spec. ELISA	=
+440.1	
-128.1	* Mg
-287.3	* SO_4
-109.6	* Nicotinic Acid
-172.5	* Mg * SO_4
-152.8	* SO_4^2
-87.3	* Nicotinic $Acid^2$

APPENDIX D

EFFECT OF CARBON SOURCE ON GROWTH AND FHA GENERATION BY BORDETELLA BRONCHISEPTICA RAW DATA

BioXpert Fermentation Control Charts

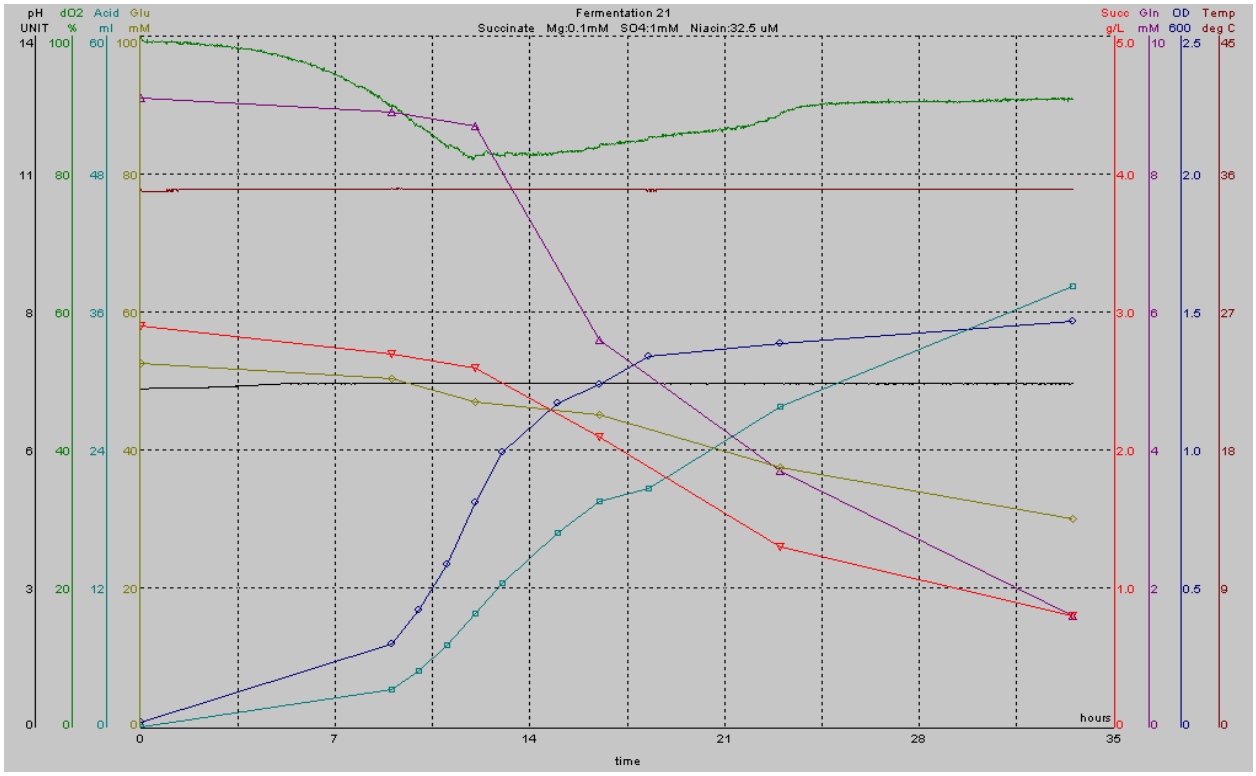

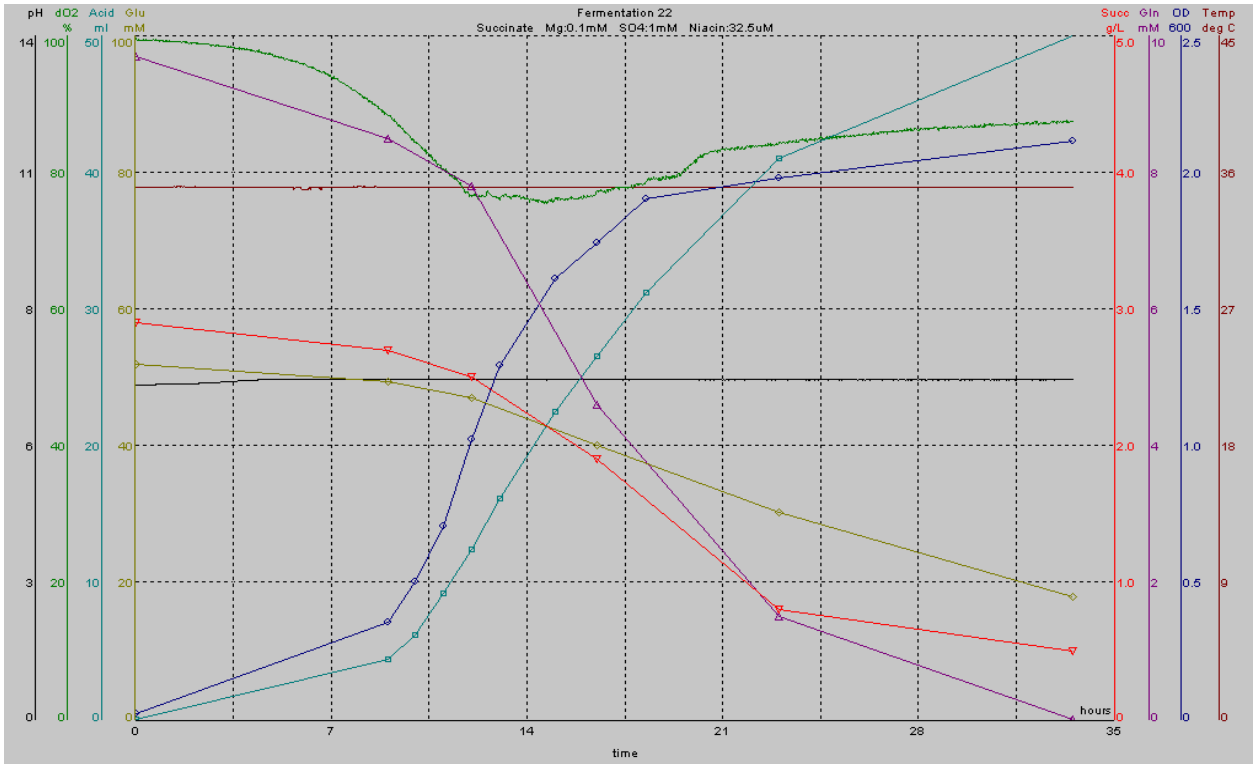
Fermentation 22
Succinate Mg:0.1mM SO4:1mM Niacin:32.5uM
pH
dO2 %
Acid ml
Glu mM
Succ g/L
Gln mM
OD 600
Temp deg C
hours
time

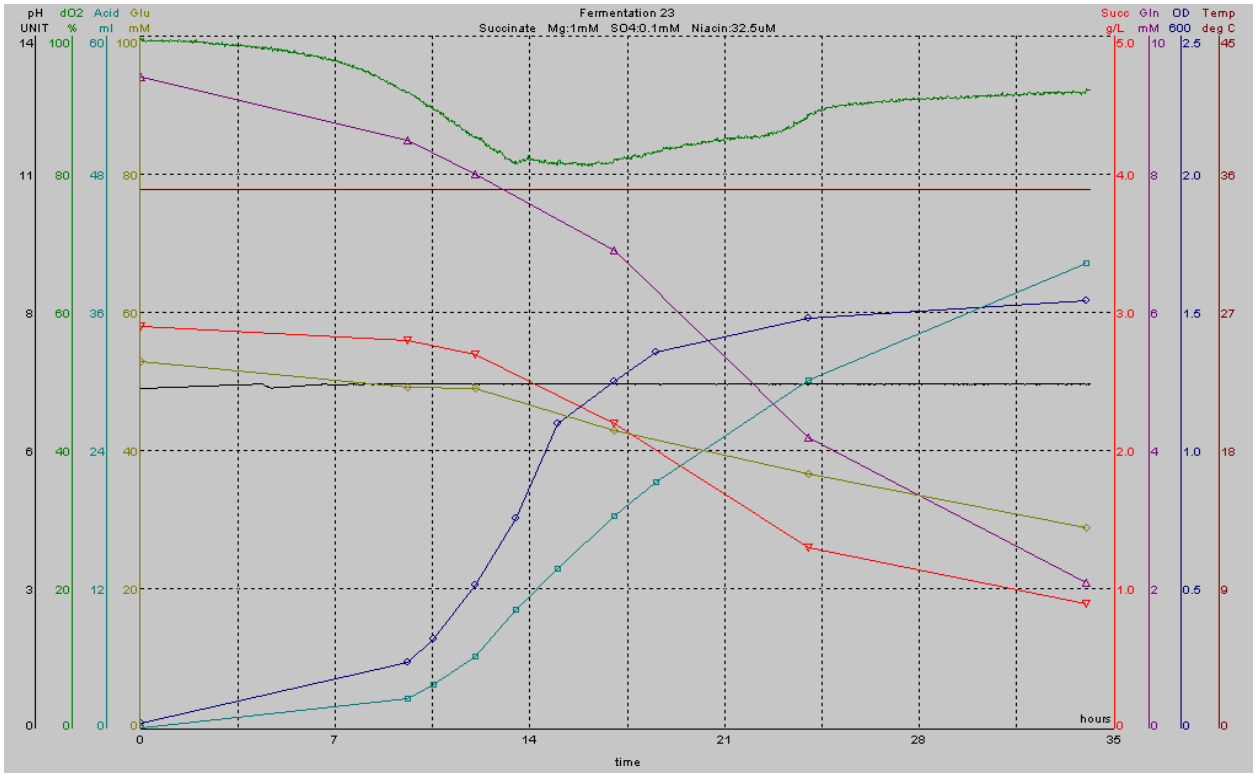
Fermentation 23
Succinate Mg:1mM SO4:0.1mM Niacin:32.5uM
pH UNIT
dO2 %
Acid ml
Glu mM
Succ g/L
Gln mM
OD 600
Temp deg C
hours
time

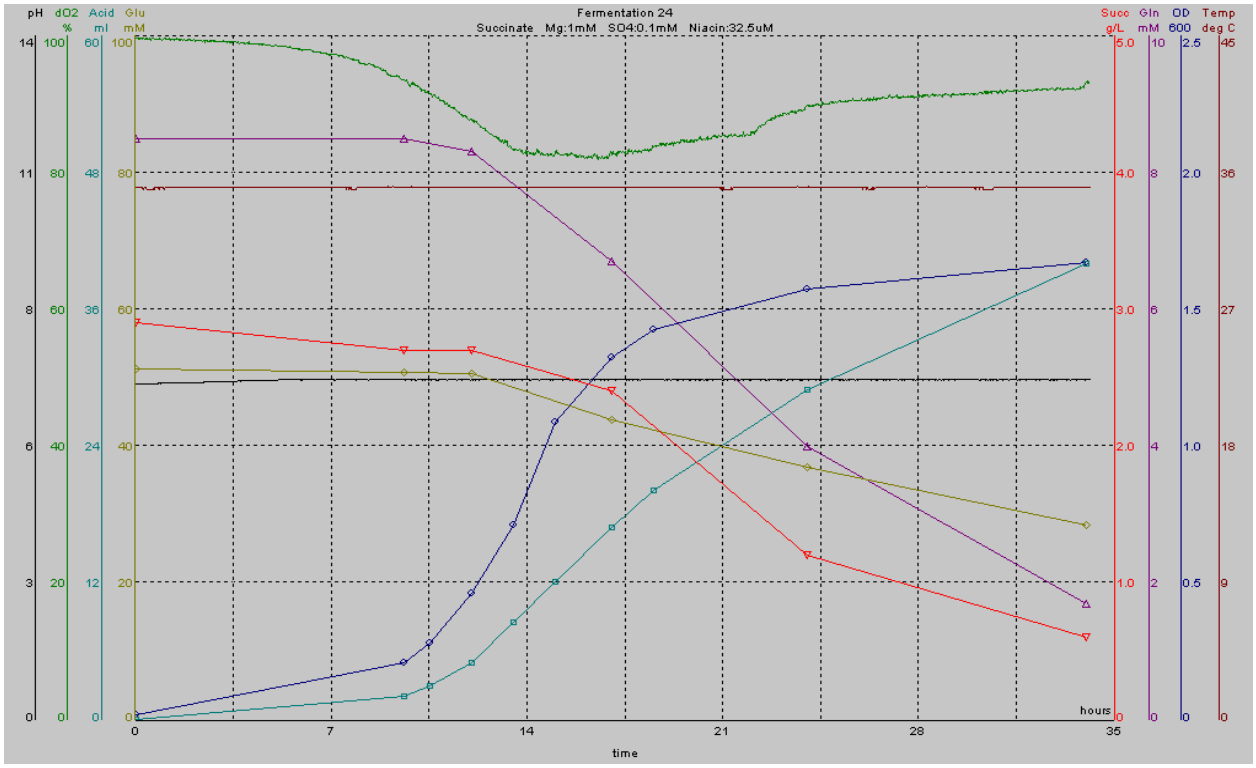
Fermentation 24
Succinate Mg:1mM SO4:0.1mM Niacin:32.5uM
pH
dO2 %
Acid ml
Glu mM
Succ g/L
Gln mM
OD 600
Temp deg C
hours
time

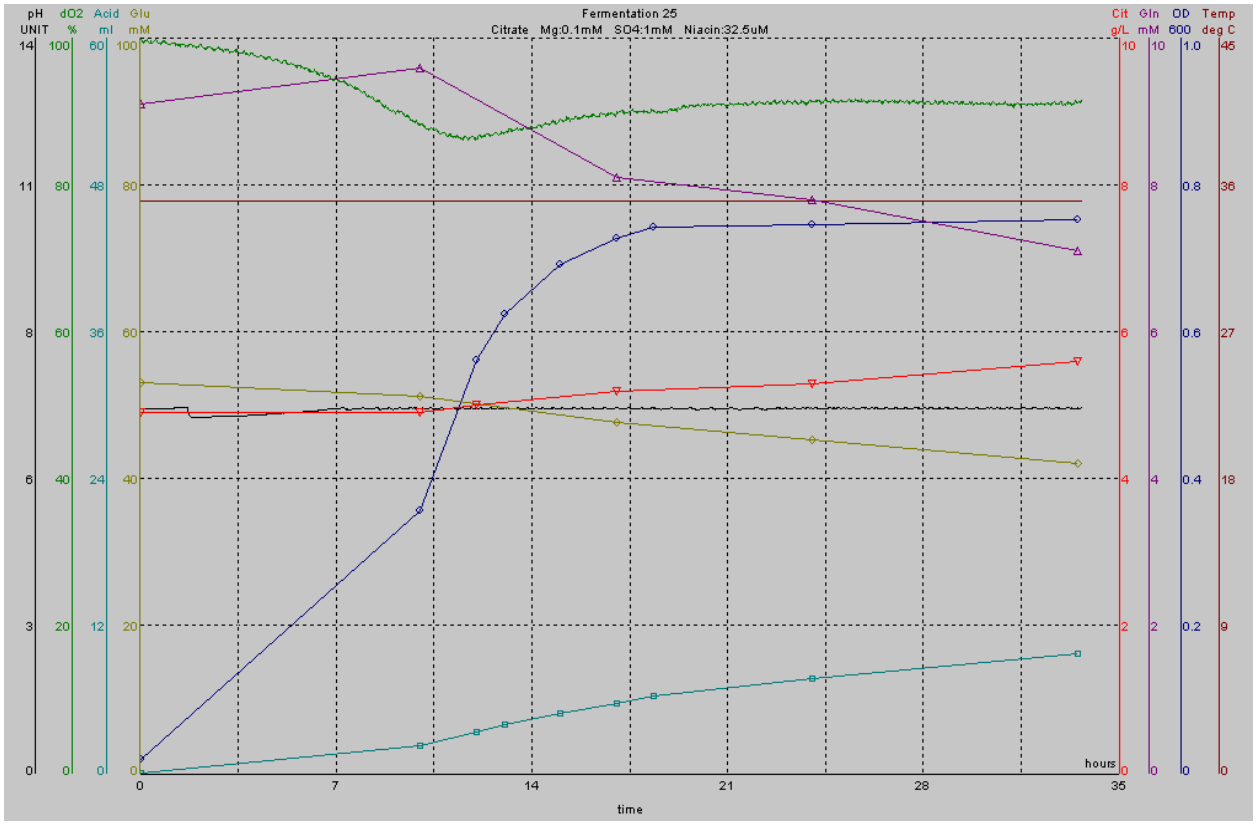
Fermentation 25
Citrate Mg:0.1mM SO4:1mM Niacin:32.5uM
pH UNIT
dO2 %
Acid ml
Glu mM
Cit g/L
Gln mM
OD 600
Temp deg C
hours
time

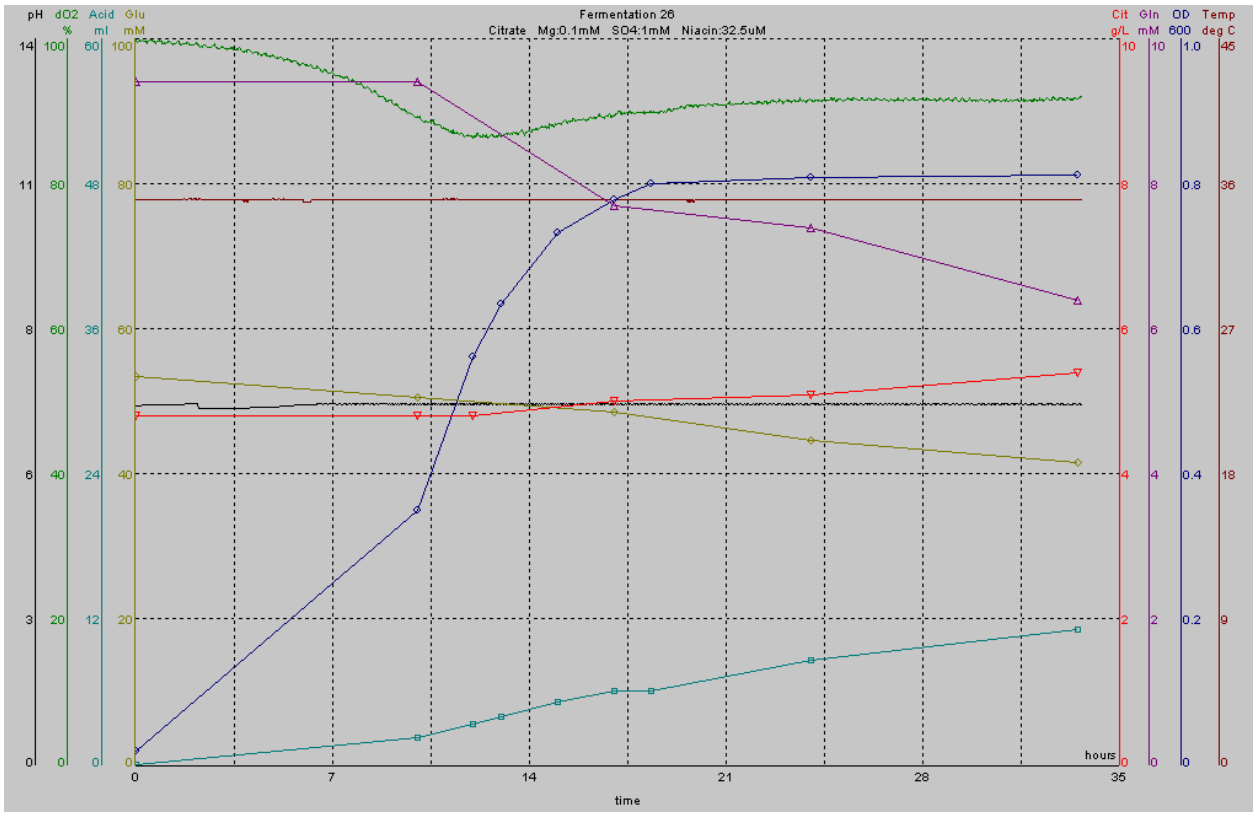
Fermentation 26
Citrate Mg:0.1mM SO4:1mM Niacin:32.5uM
pH
dO2 %
Acid ml
Glu mM
Cit g/L
Gln mM
OD 600
Temp deg C
hours
time

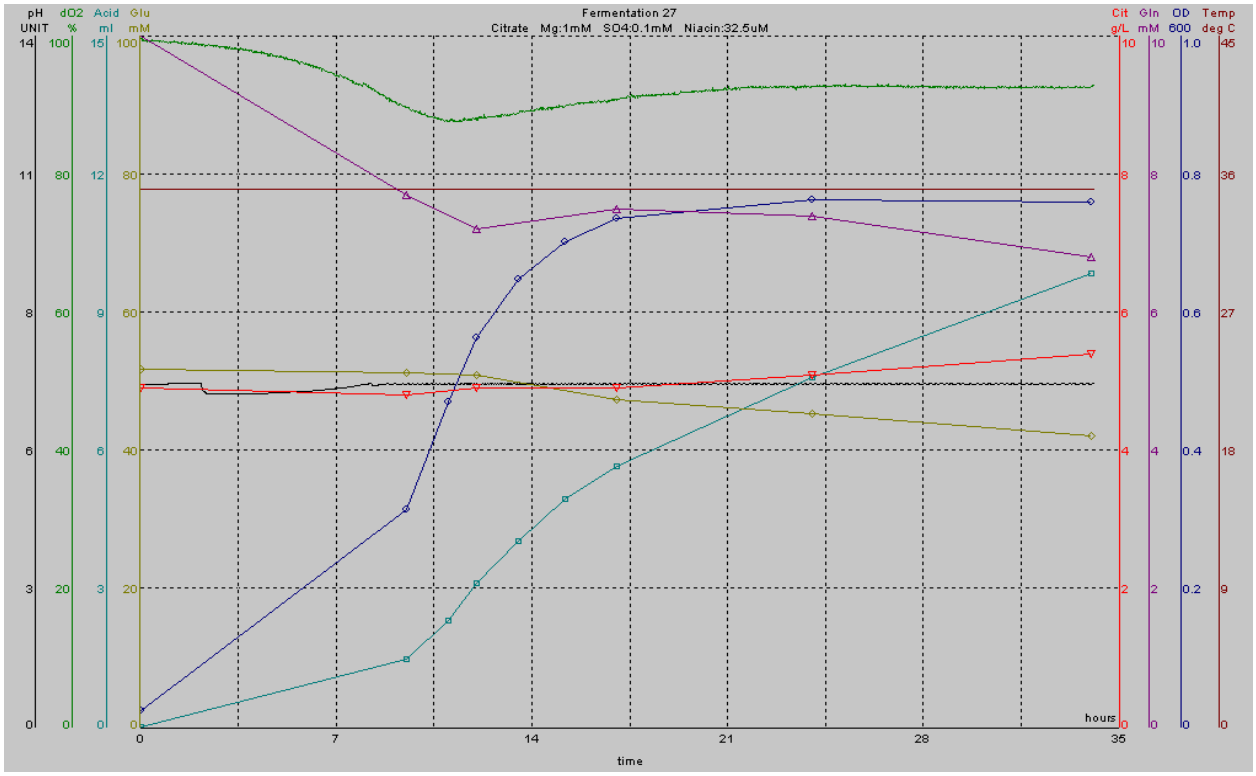
Fermentation 27
Citrate Mg:1mM SO4:0.1mM Niacin:32.5uM
pH UNIT
dO2 %
Acid ml
Glu mM
Cit g/L
Gln mM
OD 600
Temp deg C
hours
time

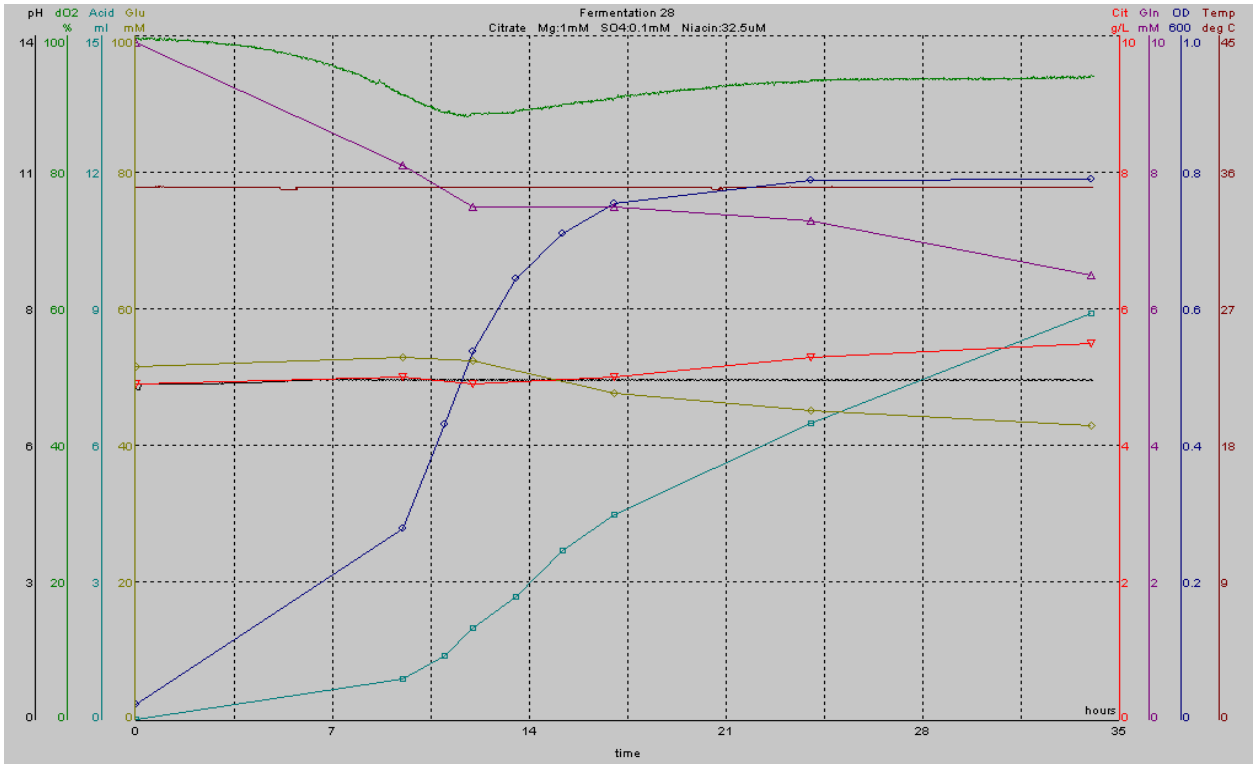
Fermentation 28
Citrate Mg:1mM SO4:0.1mM Niacin:32.5uM
pH dO2 % Acid ml Glu mM
Cit g/L Gln mM OD 600 Temp deg C
hours
time

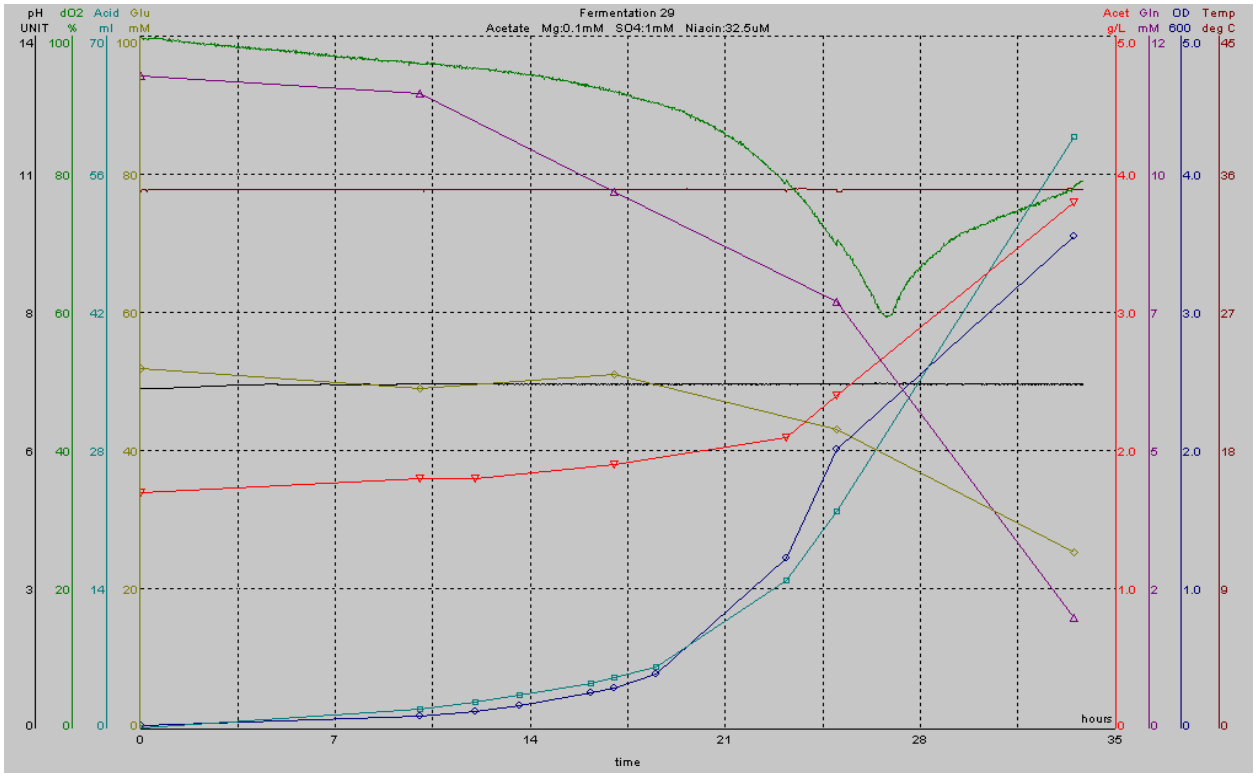
Fermentation 29
Acetate Mg:0.1mM SO4:1mM Niacin:32.5uM
pH UNIT dO2 % Acid ml Glu mM
Acet g/L Gln mM OD 600 Temp deg C
hours
time

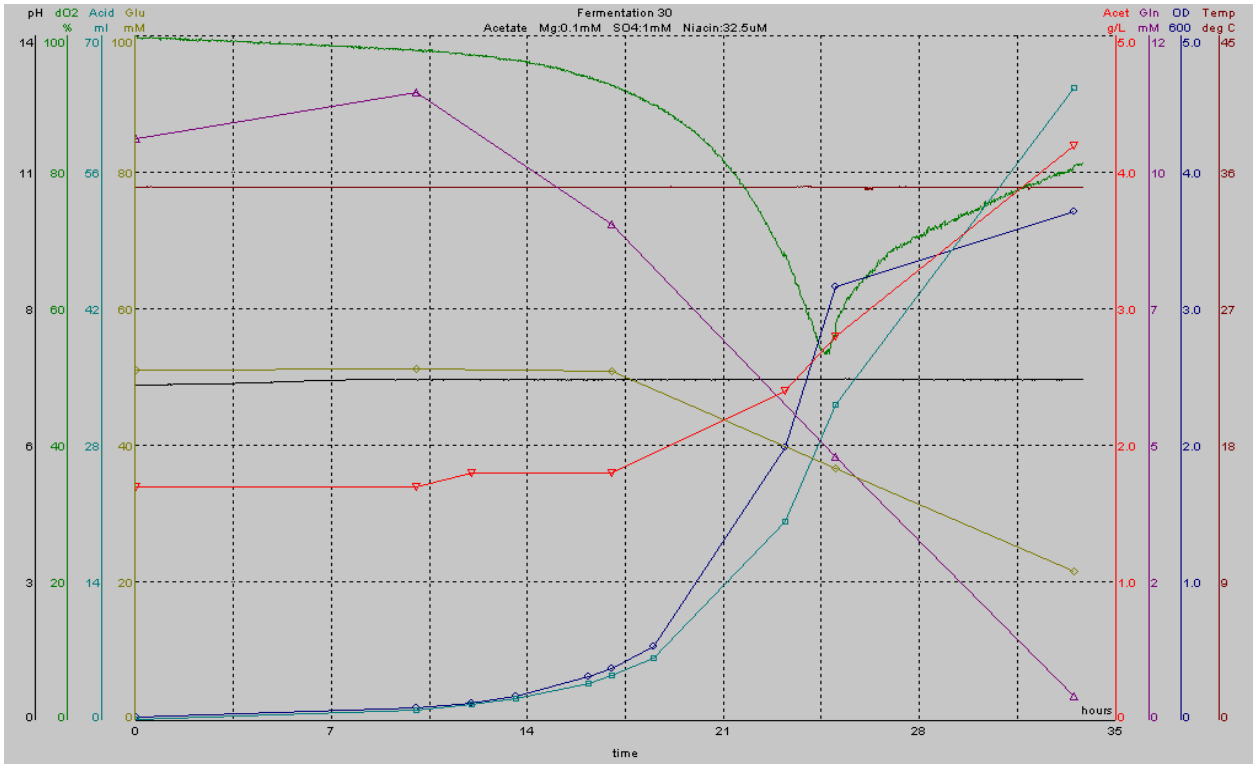
Fermentation 30
Acetate Mg:0.1mM SO4:1mM Niacin:32.5uM
pH
dO2 %
Acid ml
Glu mM
Acet g/L
Gln mM
OD 600
Temp deg C
hours
time

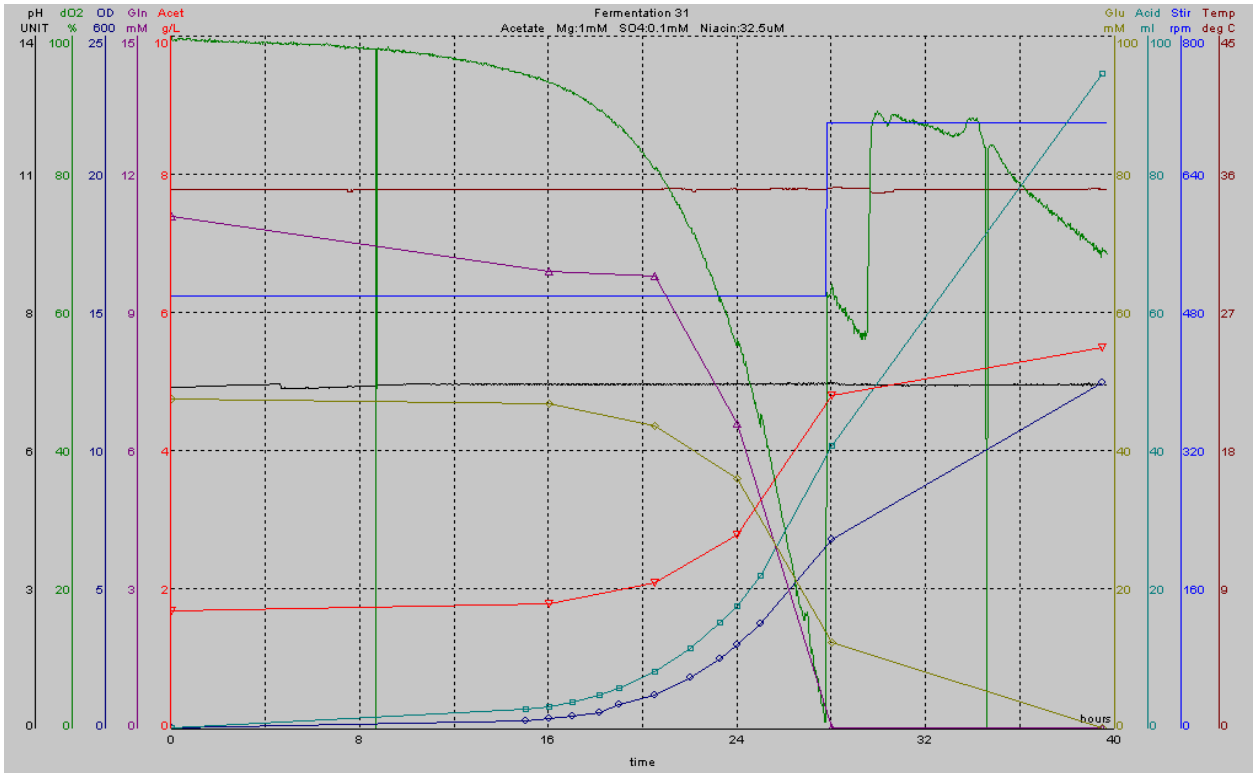
Fermentation 31
Acetate Mg:1mM SO4:0.1mM Niacin:32.5uM
pH UNIT
dO2 %
OD 600
Gln mM
Acet g/L
Glu mM
Acid ml
Stir rpm
Temp deg C
hours
time

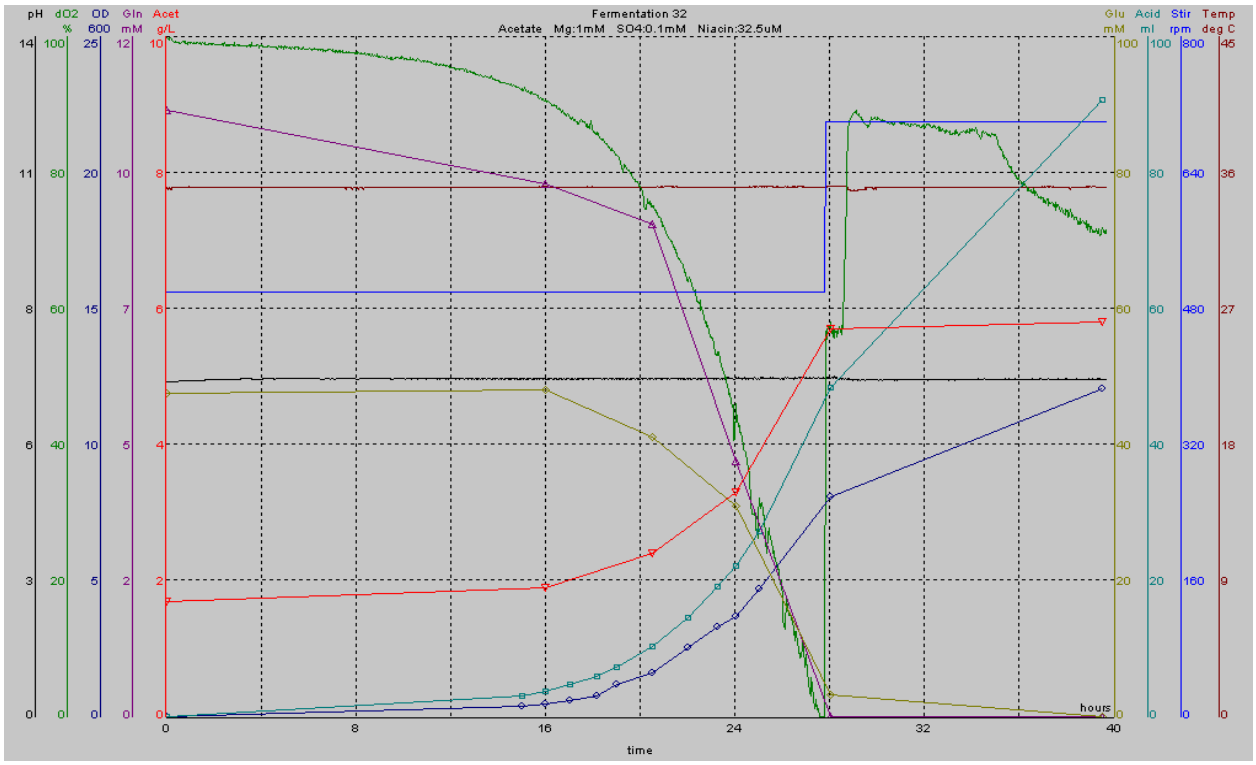

FHA ELISA

Fermentation	8-10 h (ng/mL)	12 h (ng/mL)	16-17 h (ng/mL)	23-24 h (ng/mL)	32-34 h (ng/mL)
9	219.2	525.9	838.3	691.7	427.1
12	179.5	484.3	553.2	575.1	360.8
1	316.7	693.2	625.3	698.7	470.6
11	184.1	453.4	569.5	604.9	471.9
21	277.0	529.5	474.1	424.4	353.3
22	388.6	721.4	958.8	576.7	359.0
23	257.3	441.3	627.7	351.2	254.7
24	173.6	373.7	557.3	424.7	252.4
25	207.3	270.7	112.1	121.5	80.4
26	314.1	408.5	252.5	156.5	122.3
27	317.6	357.9	185.8	159.3	143.1
28	274.1	462.4	228.3	180.6	177.9
	12 h (ng/mL)	**17 h (ng/mL)**	**23 h (ng/mL)**	**25 h (ng/mL)**	**33.5 h (ng/mL)**
29	67.9	194.4	683.8	864.9	770.7
30	120.6	369.9	989.9	1153.3	879.7
	16 h (ng/mL)	**20.5 h (ng/mL)**	**24 h (ng/mL)**	**28 h (ng/mL)**	**39.5 h (ng/mL)**
31	310.4	841.5	1090.1	943.7	1079.0
32	444.1	788.1	1252.0	1054.6	1122.4

Condition	8-10 h (ng/mL)	12 h (ng/mL)	16-17 h (ng/mL)	23-24 h (ng/mL)	32-34 h (ng/mL)
Lactate 0.1mM Mg;1 mM SO4;32.5μM Nicotinic acid	199.4	505.1	695.7	633.4	394.0
Lactate 1mM Mg;0.1mM SO4;32.5μM Nicotinic acid	250.4	573.3	597.4	651.8	471.3
Succinate Low Mg;1mM SO4;32.5μM Nicotinic acid	332.8	625.4	716.5	500.6	356.1
Succinate 1mM Mg;0.1mM SO4;32.5μM Nicotinic acid	215.4	407.5	592.5	387.9	253.6
Citrate 0.1mM Mg;1mM SO4;32.5μM Nicotinic acid	260.7	339.6	182.3	139.0	101.4
Citrate 1mM Mg;0.1mM SO4;32.5μM Nicotinic acid	295.8	410.2	207.0	170.0	160.5
	12 h (ng/mL)	**17 h (ng/mL)**	**23 h (ng/mL)**	**25 h (ng/mL)**	**33.5 h (ng/mL)**
Acetate 0.1mM Mg;1mM SO4;32.5 μM Nicotinic acid	94.3	282.2	836.9	1009.1	825.2
	16 h (ng/mL)	**20.5 h (ng/mL)**	**24 h (ng/mL)**	**28 h (ng/mL)**	**39.5 h (ng/mL)**
Acetate 1mM Mg;0.1mM SO4;32.5 μM Nicotinic acid	377.2	814.8	1171.1	999.2	1100.7

Fermentation	8-10 h (ng/OD_{600}Unit)	12 h (ng/OD_{600}Unit)	16-17 h (ng/OD_{600}Unit)	23-24 h (ng/OD_{600}Unit)	32-34 h (ng/OD_{600}Unit)
9	622.7	469.9	557.7	419.7	260.4
12	850.9	570.4	368.1	355.0	212.1
1	1237.1	843.4	407.1	425.3	283.7
11	958.9	585.8	396.3	372.7	280.4
21	926.5	651.3	382.6	305.5	240.8
22	1097.8	705.2	550.1	291.3	169.7
23	1090.1	857.0	500.6	237.0	165.2
24	846.8	810.7	421.2	269.7	151.1
25	580.7	481.7	154.1	162.6	106.8
26	897.5	728.1	324.1	193.7	150.7
27	1008.1	635.7	252.4	208.8	188.3
28	979.0	859.5	302.7	229.0	225.2
	12 h (ng/OD_{600}Unit)	**17 h (ng/OD_{600}Unit)**	**23 h (ng/OD_{600}Unit)**	**25 h (ng/OD_{600}Unit)**	**33.5 h (ng/OD_{600}Unit)**
29	556.6	668.1	569.9	429.9	217.1
30	996.8	994.4	510.3	364.5	237.1
	16 h (ng/OD_{600}Unit)	**20.5 h (ng/OD_{600}Unit)**	**24 h (ng/OD_{600}Unit)**	**28 h (ng/OD_{600}Unit)**	**39.5 h (ng/OD_{600}Unit)**
31	926.6	711.9	362.2	138.8	86.6
32	976.0	488.3	340.2	130.5	93.1

Condition	8-10 h (ng/OD_{600}Unit)	12 h (ng/OD_{600}Unit)	16-17 h (ng/OD_{600}Unit)	23-24 h (ng/OD_{600}Unit)	32-34 h (ng/OD_{600}Unit)
Lactate 0.1mM Mg;1 mM SO4;32.5μM Nicotinic acid	736.8	520.2	462.9	387.4	236.3
Lactate 1mM Mg;0.1mM SO4;32.5μM Nicotinic acid	1098.0	714.6	401.7	399.0	282.0
Succinate 0.1mM Mg;1mM SO4;32.5μM Nicotinic acid	1012.1	678.2	466.4	298.4	205.3
Succinate 1mM Mg;0.1mM SO4;32.5μM Nicotinic acid	968.4	833.8	460.9	253.3	158.1
Citrate 0.1mM Mg;1mM SO4;32.5μM Nicotinic acid	739.1	604.9	239.1	178.2	128.7
Citrate 1mM Mg;0.1mM SO4;32.5μM Nicotinic acid	993.6	747.6	277.6	218.9	206.7
	12 h (ng/OD_{600}Unit)	**17 h (ng/OD_{600}Unit)**	**23 h (ng/OD_{600}Unit)**	**25 h (ng/OD_{600}Unit)**	**33.5 h (ng/OD_{600}Unit)**
Acetate 0.1mM Mg;1mM SO4;32.5 μM Nicotinic acid	776.7	831.2	540.1	397.2	227.1
	16 h (ng/OD_{600}Unit)	**20.5 h (ng/OD_{600}Unit)**	**24 h (ng/OD_{600}Unit)**	**28 h (ng/OD_{600}Unit)**	**39.5 h (ng/OD_{600}Unit)**
Acetate 1mM Mg;0.1mM SO4;32.5 μM Nicotinic acid	951.3	600.1	351.2	134.7	89.8

APPENDIX E

STEADY-STATE CONTINUOUS CULTURE BY BORDETELLA BRONCHISEPTICA RAW DATA

Chemostat Type		**Mg-Limited**	**S-Limited**	**Mg-Limited**	**Modified S-Limited**	**Fe-Limited**	**Comments**
		Lactate	**Lactate**	**Acetate**	**Lactate**	**Licari et al. (1991)**	
Target D (h^{-1})	h^{-1}	0.1	0.1	0.1	0.1	0.075	Chemostat Calculations
Date of Steady-State	date	6/17/2011	6/21/2011	6/25/2011	6/28/2011	8/19/2011	LAC = Lactate
Flowrate	L/h	0.102	0.102	0.102	0.102	0.078	ACE = Acetate
Final Volume	L	1.00	1.00	1.00	1.00	1.00	X = Cells
Dilution Rate	h^{-1}	0.102	0.102	0.102	0.102	0.078	GLT = Glutamate
Qgas (STP)	L/min	0.4	0.4	0.4	0.4	0.4	GLN = Glutamine
CELL MASS							
Sample volume	L	0.040	0.040	0.040	0.040	0.040	
Boat 1 Wt. before	g	0.71	0.71	0.72	0.72	0.5623	
Boat 1 Wt. after	g	0.74	0.77	0.79	0.78	0.6329	
Cell Wt. 1	g	0.0253	0.0594	0.0677	0.0693	0.0706	
Boat 2 Wt. before	g	0.70	0.71	0.71	0.71	0.5642	
Boat 2 Wt. after	g	0.72	0.77	0.78	0.78	0.6356	
Cell Wt. 2	g	0.0253	0.0618	0.0686	0.0697	0.0715	
Ave. Cell Wt.	g	0.0253	0.0606	0.0681	0.0695	0.0710	
DCW	g/L	0.63	1.52	1.70	1.74	1.78	DCW = cell wt. / sample volume
CONCENTRATIONS							
$MgCl_2 \cdot 6H_2O$ in feed (intended)	mg/L	8.00	203.30	8.00	203.30	100.00	
Mg in feed (intended)	mM	0.04	1.00	0.04	1.00	0.49	
S in feed (intended)	mM	3.84	0.40	3.84	0.14	0.72	
Lactate in Feed (measured)	mM	42.63	40.52	0.00	40.96		
Lactate in Effluent (measured)	mM	35.41	29.42	0.00	18.43		
Acetate in Feed	mM	0.00	0.00	61.28	0.00		
Acetate in Effluent	mM	0.00	1.33	6.33	0.00		

Glutamate in Feed	mM	54.50	52.60	56.50	56.35	65.70	
Glutamate in Effluent	mM	47.05	32.35	39.10	30.55	43.45	
Glutamine in Feed	mM	11.50	8.45	9.00	7.30	7.40	
Glutamine in Effluent	mM	6.45	1.20	0.55	0.85	5.15	
FHA in Feed	U	0.00	0.00	0.00	0.00	0.00	
FHA in Effluent	U	0.00	0.00	0.00	0.00	0.00	

Chemostat Type		**Mg-Limited**	**S-Limited**	**Mg-Limited**	**Modified S-Limited**	**Fe-Limited**	**Comments**
		Lactate	**Lactate**	**Acetate**	**Lactate**	**Licari et al. (1991)**	
YIELDS							
$Y_{X/LAC}$	g/g	0.972	1.515	N/A	0.856	N/A	$Y_{X/L} = DCW/((LAC_{in}-LAC_{out})*M_{LAC})$
$Y_{X/ACE}$	g/g	N/A	-18.938	0.516	N/A	N/A	$Y_{X/L} = DCW/((ACE_{in}-ACE_{out})*M_{ACE})$
RATES							
Q_{LAC}	mmol/Lh	0.736	1.132	0.000	2.299	0.000	$Q_{LAC} = (LAC_{IN}-LAC_{OUT})*D$
q_{LAC}	mmol/gh	1.165	0.747	0.000	1.323	0.000	$q_{LAC} = Q_{LAC}/X$
Q_{ACE}	mmol/Lh	0.000	-0.136	5.605	0.000	0.000	$Q_{ACE} = (ACE_{IN}-ACE_{OUT})*D$
q_{ACE}	mmol/gh	0.000	-0.090	3.292	0.000	0.000	$q_{ACE} = Q_{ACE}/X$
Q_{GLT}	mmol/Lh	0.760	2.066	1.775	2.632	1.736	$Q_{GLT} = (GLT_{IN}-GLT_{OUT})*D$
q_{GLT}	mmol/gh	1.203	1.363	1.042	1.514	0.977	$q_{GLT} = Q_{GLT}/X$
Q_{GLN}	mmol/Lh	0.515	0.740	0.862	0.658	0.176	$Q_{GLN} = (GLN_{IN}-GLN_{OUT})*D$
q_{GLN}	mmol/gh	0.816	0.488	0.506	0.379	0.099	$q_{GLN} = Q_{GLN}/X$
Q_{FHA}	U/Lh	0.000	0.000	0.000	0.000	0.000	$Q_{FHA} = (FHA_{OUT}-FHA_{IN})*D$
q_{FHA}	U/gh	0.000	0.000	0.000	0.000	0.000	$q_{FHA} = Q_{FHA}/X$
OXYGEN							
O_2 initially	%	20.93	20.93	20.93	20.94	21.1	
O_2 at steady state	%	20.58	19.95	19.750	19.94	19.94	
Density of O_2 at 0°C	g/L	1.43	1.43	1.43	1.43	1.43	
OUR	g O_2/min	0.0020	0.0056	0.0067	0.0057	0.0066	$OUR = (O_{2,ini}-O_{2,steady})*Qgas*\rho$
OUR	mmol O_2/h	2.73	7.64	9.20	7.80	9.05	
q_{O2}	mmol O_2/g DCW h	4.32	5.05	5.41	4.49	5.09	$q_O = OUR/(V*DCW)$
CARBON DIOXIDE							
CO_2 initially	%	0	0	0	0	0	
CO_2 at steady state	%	0.3	0.78	0.920	0.83	0.93	
Density of CO_2 at 0°C	g/L	1.98	1.98	1.98	1.98	1.98	
CER	g CO_2/min	0.0024	0.0062	0.0073	0.0066	0.0074	$CER = (CO_{2,steady}-$

							$CO_{2,ini}$)*Qgas*ρ
CER	mmol CO_2/h	3.24	8.41	9.94	8.96	10.04	
q_{CO2}	mmol CO_2/g DCW h	5.12	5.55	5.84	5.16	5.66	q_{CO2} = CER/(V*X)
RQ	mol/mol	1.19	1.10	1.08	1.15	1.11	

FHA ELISA Fe-Limitation in Licari et al. (1991) Medium

Chemostat Phase	End of Batch Growth	Dilution 1	Dilution 2	Dilution 3	Steady State
ng/mL	485.4	732.8	0.0	0.0	0.0

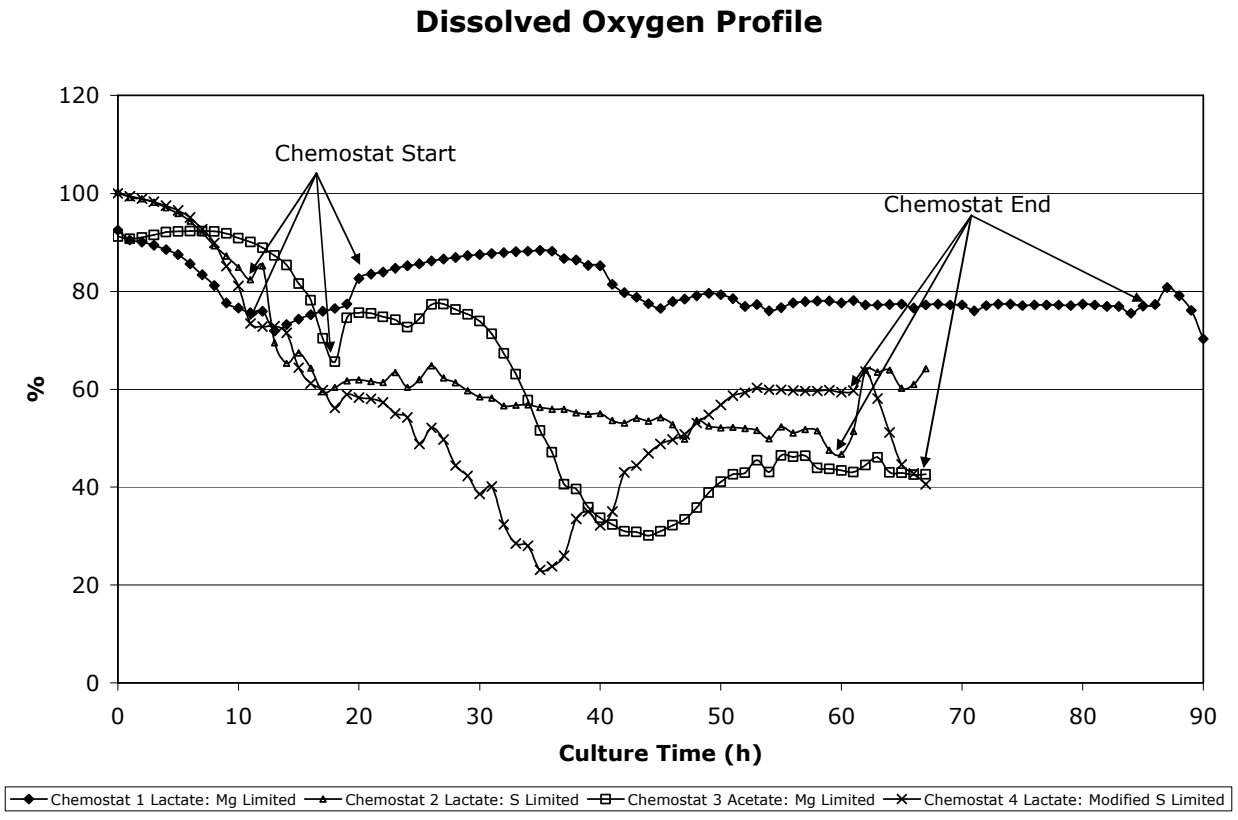

APPENDIX F

FED-BATCH FERMENTATION RAW DATA

BioXpert Fermentation Control Charts

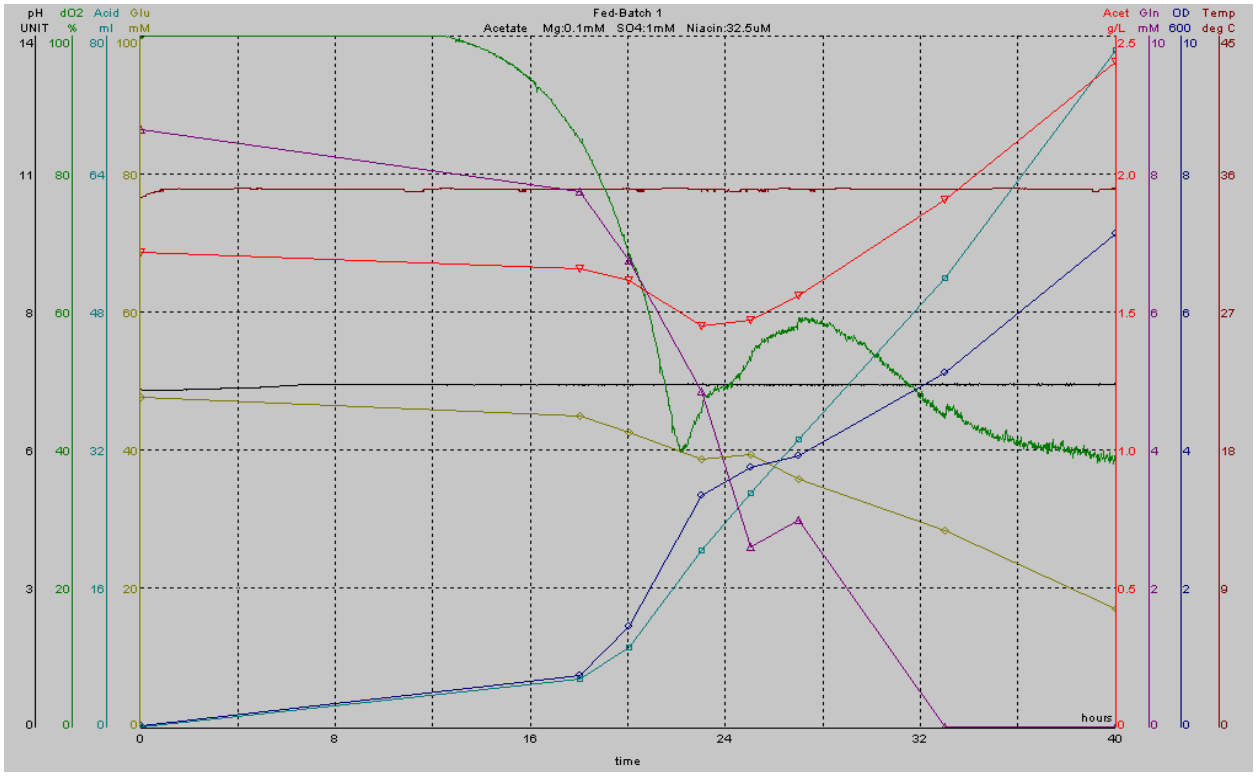

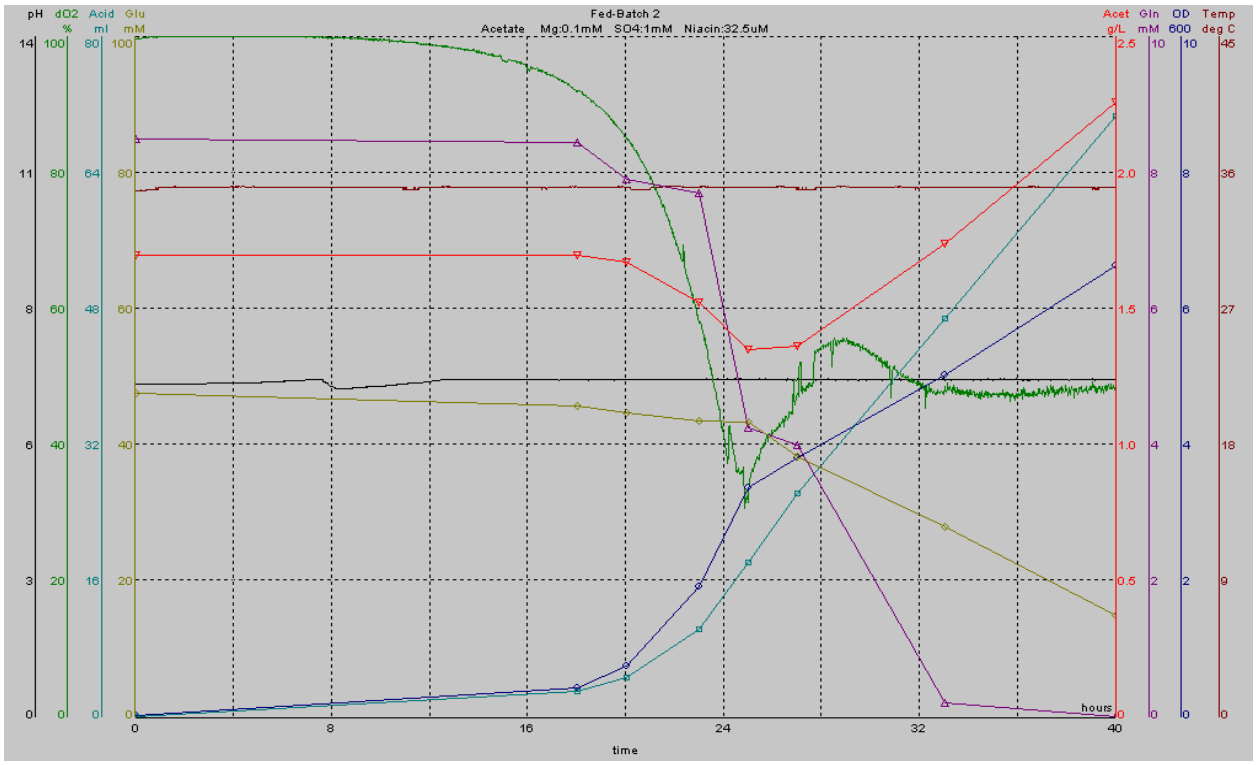
Fed-Batch 2
Acetate Mg:0.1mM SO4:1mM Niacin:32.5uM
pH
dO2 %
Acid ml
Glu mM
Acet g/L
Gln mM
OD 600
Temp deg C
hours
time

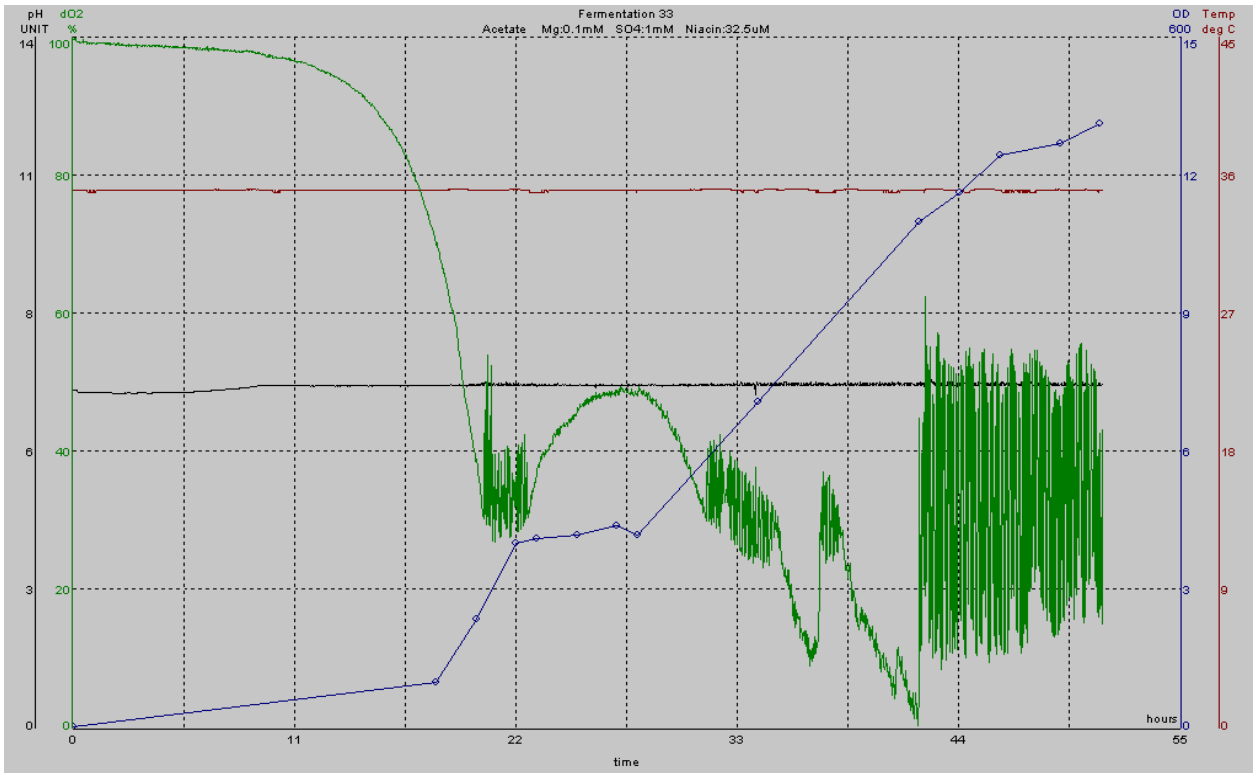
Fermentation 33
Acetate Mg:0.1mM SO4:1mM Niacin:32.5uM
pH UNIT
dO2 %
OD 600
Temp deg C
hours
time

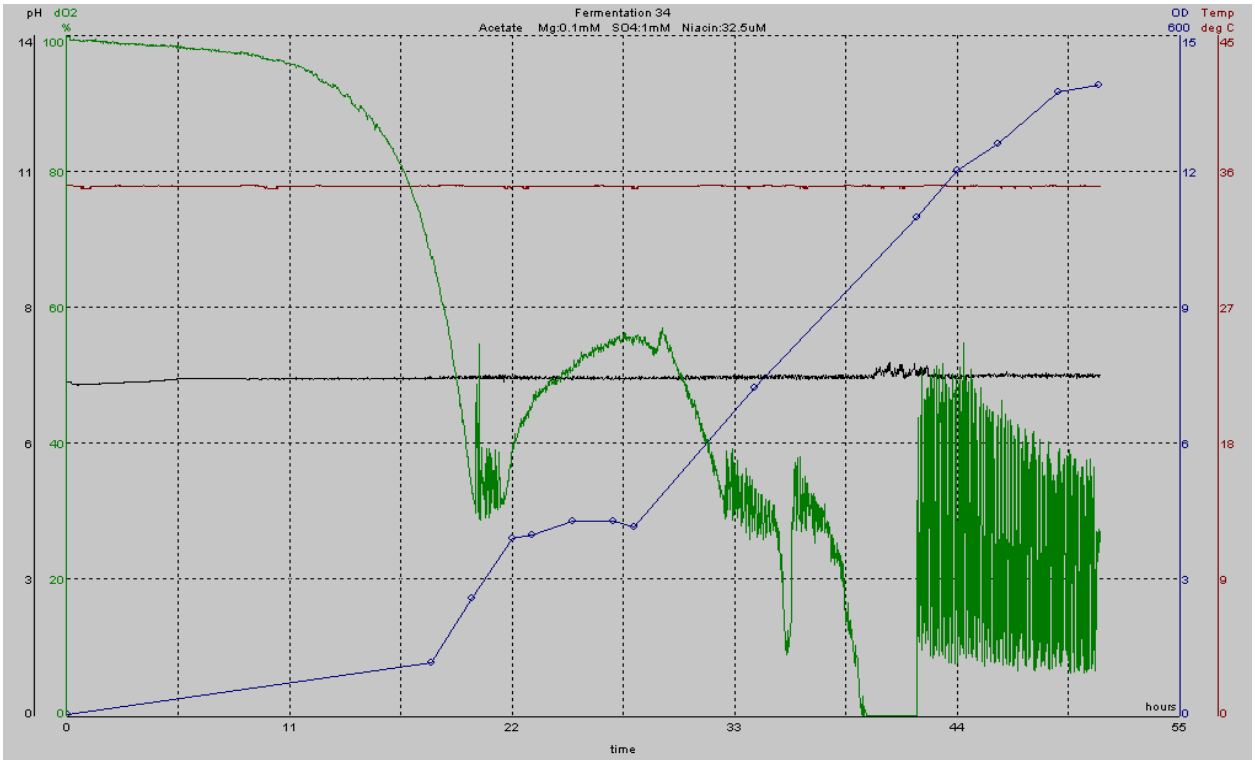

FHA ELISA

Condition	20 h (ng/mL)	23 h (ng/mL)	27 h (ng/mL)	33 h (ng/mL)	40 h (ng/mL)
Fed-Batch 1 Acetate 0.1mM Mg;1mM SO4;32.5µM Nicotinic acid	566.2	762.0	561.3	719.6	706.7
Fed-Batch 2 Acetate 0.1mM Mg;1mM SO4;32.5µM Nicotinic acid	300.8	632.5	590.4	736.5	676.1

Condition	22 h (ng/mL)	28 h (ng/mL)	34 h (ng/mL)	42 h (ng/mL)	51 h (ng/mL)
Fermentation 33 Acetate 0.1mM Mg;1mM SO4;32.5µM Nicotinic acid	286.8	209.2	148.5	124.3	95.4
Fermentation 34 Acetate 0.1mM Mg;1mM SO4;32.5µM Nicotinic acid	480.8	371.2	230.1	202.3	147.0